

# Millimeter-Wave Properties of the Atmosphere: Laboratory Studies and Propagation Modeling

Hans J. Liebe  
Donald H. Layton



**U.S. DEPARTMENT OF COMMERCE**  
**Clarence J. Brown, Acting Secretary**

Alfred C. Sikes, Assistant Secretary  
for Communications and Information

October 1987



## CONTENTS

	Page
ABSTRACT.....	1
1. INTRODUCTION.....	1
2. LABORATORY STUDIES OF MOIST AIR ABSORPTION AT 138 GHz.....	3
2.1 Experimental Arrangement.....	4
2.2 Moist Air Attenuation Measurements .....	9
2.3 Water Vapor and Moist Air Attenuation Results .....	13
3. ATMOSPHERIC PROPAGATION MODEL MPM.....	16
3.1 Features of the Program .....	16
3.2 MPM Calibration.....	19
3.3 Interpretation of H <sub>2</sub> O Continuum Absorption.....	19
3.4 MPM Predictions.....	21
4. EXPERIMENTAL-VERSUS-MODEL (MPM) DATA.....	28
4.1 Laboratory Measurements.....	32
4.2 Field Measurements.....	32
5. CONCLUSIONS.....	39
6. ACKNOWLEDGMENTS.....	42
7. REFERENCES.....	43
APPENDIX A: THE REFRACTIVE INDEX OF THE NEUTRAL ATMOSPHERE FOR FREQUENCIES UP TO 1000 GHz.....	45
APPENDIX B: PRINTOUT OF MPM-N PROGRAM FOR VERSION A (FREQUENCY PROFILES).....	61

## LIST OF FIGURES

	Page
Figure 1. Millimeter wave spectrometer for controlled moist air studies (a) schematic and (b) cell design.....	6
Figure 2. Photograph of millimeter-wave spectrometer.....	7
Figure 3. Mm-wave spectrometer operational data (five temperatures $T_i$ ;) peak values of reference and reflected signals $a_k$ , and $a$ ; and relative attenuation $\alpha_r$ ) for a 1-hour measurement period with an evacuated cell ( $f_R = 137.8$ GHz): (a) automatic calibration to $\alpha_r = 0$ dB for changes, $\Delta a_k = 0-1$ dB; (b) detection stability and sensitivity ( $\alpha_{\min}^k \approx 0.006/0.13 \leq 0.05$ dB/km). ....	10
Figure 4. Temperature responses inside the spectrometer cell: (a) time-response test of gas temperature ( $T_g$ ) sensors, (b) temperature-vs.-pressure behavior for a typical dry air case.....	12
Figure 5. Mixing effects of $H_2O + Air$ from time series of 138 GHz attenuation: (a) piston effect and diffusion mixing; (b) decompression condensation during pump-down over open vapor source.....	12
Figure 6. Typical raw data plots of relative attenuation $\alpha(P)$ for pressure scans at 137.8 GHz introducing (a) water vapor, $P = e$ , and (b) $P = e_1 + p$ .....	17
Figure 7. MPM-predicted specific values of attenuation $\alpha$ and dispersive delay $\beta$ at sea level height $h = 0$ km ( $P=101.3$ kPa, $T=25^\circ$ , $RH=0$ to 100%) over the frequency range, $f = 1$ to 350 GHz. Window ranges are marked W1 to W5.....	22
Figure 8. Water vapor absorption in window ranges for constant relative humidity increments ( $\Delta RH = 12.5\%$ ) at sea level.....	24
Figure 9. Pressure broadening (Air) example of the 183 GHz $H_2O$ line.....	24
Figure 10. Attenuation $\alpha$ and delay rate $\beta$ for three rain events ( $R=10, 50,$ and $100$ mm/h) added to moist air ( $RH=95\%$ ), sea level condition. Also shown are dry air (0% RH) and moist air (50% RH) characteristics.....	25

- Figure 11. Attenuation  $\alpha$  and delay  $\beta$  rates for three fog events ( $w=0.10, 0.125, \text{ and } 0.5 \text{ g/m}^3$ ) added to saturated air (RH=100%) sea level condition. Also shown are dry air (0% RH) and moist air (50% RH) characteristics:  
 (a)  $f = 1-1000 \text{ GHz}$  ..... 26  
 (b)  $f = 1-350 \text{ GHz}$  ..... 27
- Figure 12. Absolute ( $v$ ) and relative (RH) humidity dependence of attenuation  $\alpha$  and delay  $\beta$  at  $f = 94 \text{ GHz}$  for various sea level conditions ( $P = 101.3 \text{ kPa}$  and  $T = -20 \text{ to } 40^\circ\text{C}$ )... 29
- Figure 13. Two haze cases (A:  $1 \text{ mg/m}^3$  and C:  $1 \text{ mg/m}^3$ ) for prefog (RH=99-99.9%) and fog ( $w=0.1$  and  $0.2 \text{ g/m}^3$ ) conditions at three temperatures (0, 10,  $20^\circ\text{C}$ ) displaying the associated attenuation  $\alpha$  and delay  $\beta$  rates at  $f = 220 \text{ GHz}$  ..... 30
- Figure 14. Pressure profiles at  $f = 138 \text{ GHz}$  simulating the laboratory attenuation measurements presented in Section 2.3 ..... 31
- Figure 15. Moist air attenuation  $\alpha$  across the atmospheric window ranges W5 and W6 (320 to 430 GHz) at temperatures 8.5, 25.5 and  $32.9^\circ\text{C}$ : data points [21], [22]; solid lines MPM ..... 35
- Figure 16. Moist air attenuation  $\alpha(v)$  measured at 96.1 GHz over a 21.4 km line-of-sight path located in Huntsville, AL ( $h \approx 0.3 \text{ km}$ ) for six temperature groups between 2.5 and  $37.5^\circ\text{C}$  [19]: data points are 5-min averages for 4.5 days (5/4-6, 8/15-16/1986); solid lines, MPM ..... 36
- Figure 17. Water vapor attenuation rates  $\alpha(v)$  across the atmospheric window range W4 at four temperatures, 5, -7, -10,  $-18^\circ\text{C}$ : data points [20]; solid lines, MPM ..... 37
- Figure 18. Terrestrial path attenuation at 94 GHz and  $0.65 \mu\text{m}$  (visible light) under nonprecipitating conditions as a function of absolute ( $v$ ) and relative (RH) humidity [3]:  
 (a) data points, 5-min averages taken every 30 min during a period of 4 months [23]; (b) MPM simulation of (a) for absolute humidity; (c) MPM simulation of (a) over the range, RH=95 to 100%, including haze model C ..... 38
- Figure 19. Correlated vertical atmospheric noise temperatures  $T_A$  at the frequency pairs 10/33, 10/90, and 33/90 GHz. Path-integrated water vapor is  $V = \int v dh, \text{ mm}$ . The measurements were conducted from two sites located at height levels  $h_0=0.25$  and  $3.30 \text{ km}$ : data points [24]; solid lines, MPM with a mean July height profile (0-30 km) of  $P, T,$  and RH for San Francisco, CA [3]..... 40

- Figure A-1. Moist air refractivity  $\bar{N} = N' - jN''$  for sea level condition (P,T) and various relative humidities (RH) over the frequency range from 0 to 1000 GHz ..... 58
- Figure A-2. Moist air attenuation ( $\alpha$ ) and delay ( $\beta$ ) rates for a sea level condition (P,T) and various relative humidities (RH) over the frequency range from 1 to 1000 GHz ..... 60

LIST OF TABLES

	Page
Table 1. Comparison between Measured (X) and Model-Predicted (M=MPM, see Section 3) Coefficients $k_{S,f}$ of (5). Experimental conditions: $f = 137.8$ GHz, $T = 282-316$ K, $P = e_1 + p$ , $p = 0-110$ kPa .....	14
Table 2. Attenuation Measurements of Water-Vapor/Air-Constituent Mixtures ( $f=137.8$ GHz, $T=303$ K, $e_1=3.80$ and $p=0-100$ kPa) Expressed with $k_x$ -Coefficients of (5), and Corresponding Broadening Efficiencies $m_x$ (6). Included are Line-Core Measurements $m_l$ and their Predictions $m_l$ and $k_l$ Transposed to 138 GHz .....	15
Table 3. Summary Data of H <sub>2</sub> O line Spectrum and H <sub>2</sub> O Excess Attenuation at 137.8 GHz, $T = 300$ K .....	20
Table 4. Reported Data on (H <sub>2</sub> O) <sub>2</sub> Dimer Concentration $e_D/e$ over the Temperature Range for 300 to 386 K .....	20
Table 5. Measured (EXP) and Predicted (MPM) Dispersion in Dry Air at 300 K (Interference Coefficients from Rosenkranz [10])....	33
Table 6. Comparison between MPM-Predicted and Experimental Attenuation for Water Vapor (e) and Moist Air ( $P = e_1 + p$ ) in the Wing Region of the H <sub>2</sub> O Line Centered at $\nu_0 = 183.310$ GHz .....	34
Table A1. Frequency Profiles of Atmospheric Complex Refractivity .....	57
Table A2. Frequency Profiles of Attenuation and Delay Rates .....	59





# MILLIMETER-WAVE PROPERTIES OF THE ATMOSPHERE LABORATORY STUDIES AND PROPAGATION MODELING

Hans J. Liebe and Donald H. Layton\*

Laboratory measurements have been performed at 138 GHz of water vapor attenuation  $\alpha_x$  for pure vapor ( $H_2O$ ) and its mixtures with air, nitrogen ( $N_2$ ), oxygen ( $O_2$ ), and Argon (Ar). Temperatures ranged from 8 to 43 °C, relative humidities from 0 to 95% and total pressures reached 1.5 atm. A computer-controlled resonance spectrometer was employed. The results are interpreted in terms of underlying absorption mechanisms. Broadening efficiencies  $m$  of mixtures  $H_2O + N_2$ ,  $O_2$ , Ar agree among themselves with those measured within cores of the 22 and 183 GHz  $H_2O$  absorption lines. The  $m$ -factors are applied to predict what share  $\alpha_0$  of the total  $\alpha_x$  results from the complete pressure-broadened  $H_2O$  spectrum. A substantial amount of the self-broadening term proportional to the square of vapor pressure is left unaccounted. The negative temperature coefficient of the excess absorption is consistent with a dimer  $(H_2O)_2$  model. An empirical formulation of the experimental findings is incorporated into the parametric propagation model MPM that utilizes a local (30x  $H_2O$ , 48x  $O_2$ ) line base to address frequencies up to 1000 GHz. Details of MPM are given in two Appendixes. Predictions of moist air attenuation and delay by means of the revised MPM program generally compare favorably with reported (10 - 430 GHz) data from both field and laboratory experiments.

Key Words: atmospheric attenuation and delay; laboratory studies of moist air attenuation; millimeter/submillimeter-wave spectral range; propagation program MPM; radio path data

## 1. INTRODUCTION

Extending the radio spectrum into the near-millimeter region (NMMW: 0.1-1 THz) is an active area for research. Possible applications lie in short-range communications, radar, radiometry, and radio astronomy. Atmospheric effects of transmission and emission are described by the complex refractivity  $N$  that provides a measure of the interactions between radiation and the atmospheric propagation medium. A reliable  $N$ -model allows calculation of frequency-dependent rates for delay (real part) and attenuation (imaginary part) based on measurable meteorological variables. Dry air and atmospheric water vapor are major millimeter-wave absorbers; so are suspended droplets (haze, fog, cloud) and precipitating water drops that emanate from the vapor

---

\*The authors are with the Institute for Telecommunication Sciences, National Telecommunications and Information Administration, U. S. Department of Commerce, Boulder, CO 80303-3328.

phase. Laboratory research and analytical studies have been conducted with the primary purpose of understanding power attenuation  $\alpha$  (dB/km) and group delay  $\beta$  (ps/km). Emphasis was placed on the fundamental concepts that support an N formulation.

Refractivity  $N$  for moist air can be obtained, in principle, by a line-by-line summation over all molecular absorption lines. In practice, various approximations are employed to reduce labor and computer time, since the number of contributing spectral lines by the dominant absorbers (water vapor and oxygen) and by various trace gases (e.g.,  $O_3$ ) exceeds 10,000. A practical propagation model, indexed MPM (and described in Appendix A and B), consists of local  $H_2O$  (30x) and  $O_2$  (48x) lines below 1 THz and an approximation to the contributions by  $H_2O$  lines above 1 THz [1] - [3].

The experiments have been performed at 138 GHz to measure absolute attenuation rates by dry air, moist air, water vapor, and water-vapor mixtures with nitrogen ( $N_2$ ), oxygen ( $O_2$ ), and argon (Ar) at temperatures between 8 and 43°C, total pressures up to 1.5 atm, and relative humidities between 0 and 95 percent. The experimentally observed absorption is not described by standard line shape models. Such failure reveals difficulties in modeling frequency, temperature, and pressure dependences for moist air attenuation. An unexplained excess is identified for which the name "water-vapor continuum" was coined since it appears to increase smoothly with frequency within the NMMW range.

Experimental studies are compared with model calculations. The MPM program is a user-friendly, PC-operated code that generates numerical values of  $\alpha(f)$  and  $\beta(f)$  for frequencies  $f$  up to 1000 GHz. Input parameters are five measurable atmospheric quantities: barometric pressure  $P$ , ambient temperature  $T$ , relative humidity  $RH$  (absolute humidity  $v$ ), suspended droplet water content  $w$ , and rainfall rate  $R$ . Controlled laboratory measurements were limited to moist air studies ( $P$ ,  $T$ ,  $RH$ ), and the data obtained at 138 GHz are reasonably complete and accurate to assess water vapor pressure and temperature dependences for the water-vapor continuum. Both variabilities point to the distinct possibility of an absorption mechanism related to water vapor that is not accounted for by molecular theory of  $H_2O$ .

This report is organized in three parts. The first part (Section 2) gives details of the experimental setup, its achieved performance, and a summary of reduced data. After many improvements, a detection sensitivity of

$\alpha_{\min} = 0.05 \text{ dB/km}$  or  $1.2 \times 10^{-7} \text{ cm}^{-1}$  was realized. In the second part (Section 3), results from the laboratory experiments are applied (a) to calibrate the MPM program with an empirical continuum term, (b) to demonstrate the parametric flexibility of the code (i.e.,  $f$ ,  $v(\text{RH})$ , and  $P$  can be selected as variables), and (c) to conjecture on the physical basis for a water vapor continuum that is defined by the limited  $\text{H}_2\text{O}$  line base of MPM. Finally Section 4 contains examples of recently reported data from laboratory and field experiments on water vapor absorption (10-430 GHz) and their comparison with MPM predictions.

## 2. LABORATORY STUDIES OF MOIST AIR ABSORPTION AT 138 GHZ

Controlled experiments that simulate atmospheric conditions provide test cases for studying specific contributions to  $\underline{N}$ . Assessments of basic physical principles underlying the attenuation rate  $\alpha$  are difficult to make from measurements in the actual atmosphere. The objective of this study was to measure water vapor (continuum) absorption. A test frequency of 138 GHz was selected because of its remoteness from local  $\text{H}_2\text{O}$  lines. The expected window attenuation falls in the range 0.1 to 5 dB/km and the required detection sensitivity calls for a long ( $>0.1 \text{ km}$ ) effective path length, which can be attained with a resonant absorption cell.

The response curve  $A(f)$  of an isolated, high  $Q$ -value resonance is detected with a power (square-law) detector. Both, the peak value  $a_0$  at center frequency  $f_R$  and the bandwidth  $b_0$  spread over a range  $f_R \pm b_0/2$  at the level  $a_0/2$  might be used to detect the relative attenuation,

$$\alpha_r = 8.686(\sqrt{a_0/a} - 1) = 8.686(b/b_0 - 1) \quad \text{dB}, \quad (1)$$

of an absorbing gas that changes the corresponding quantities to  $a$  and  $b$  when introduced into the resonator. Around 138 GHz it is possible to design a compact (20 cm mirror spacing) Fabry-Perot resonator with a loaded  $Q$ -value on the order of  $4 \times 10^5$ , which defines ( $Q = f_R/b_0$ ) a resonance bandwidth,  $b_0 = 350 \text{ kHz}$ .

A crucial question to be resolved is whether amplitude ( $a_0/a$ ) or frequency ( $b/b_0$ ) detection schemes provide the optimum sensitivity for the spectrometer. After extensive testing it was found that digital averaging of  $A(f)$ , displayed over a frequency span  $\Delta f_M = f_R \pm 6b_0$ , was capable of resolving

$a_0/a = 1.002$  (512 pts)--but only  $b/b_0 = 1.015$  even with 1024 pts. Amplitude peak-value detection provided optimum sensitivity for absorption studies. The frequency span  $\Delta f_M$  is needed to establish the baseline  $A(f) = 0$  of the resonance response. In addition, a detection at  $f_R$  avoids corrections for dispersive distortions of  $A(f)$  [4].

Absolute calibration of absorption is accomplished by defining an equivalent path length ( $b_0$  in kHz),

$$L_E = 47.71/b_0 \quad \text{km}, \quad (2)$$

for the resonance spectrometer operating at  $f_R$ . From (1) and (2) follows that the absolute power attenuation rate of an absorbing gas is given by

$$\alpha = 0.1820 b_0 (\sqrt{a_0/a} - 1) \quad \text{dB/km}. \quad (3)$$

If the estimations ( $a_0/a = 1.002$ ,  $b_0 = 350$  kHz) can be achieved, then the projected detection sensitivity,  $\alpha_{\min} = 0.064$  dB/km, is adequate for the planned water vapor studies.

## 2.1 Experimental Arrangement

The measuring system consists of the millimeter-wave resonance spectrometer and a humidity simulator. An insulated box contains a high-vacuum stainless steel vessel that houses a temperature-controlled mini-lake (10 cm across) and the resonator. Temperatures are controlled to better than 1/100 of a degree Celsius, pressure ranges over seven orders of magnitude ( $10^3$  to  $10^{-4}$  torr), and relative humidity is varied between 0 and 99.5 percent.

Schematic diagrams of physical and electronic (Figure 1) arrangements and a photograph of the equipment (Figure 2) convey an overview of the experiment. A temperature-controlled water reservoir serves as the vapor source. Electropolished stainless steel was used exclusively as construction material. Various hydrophobic coatings were studied as possible means for neutralizing the absorption/desorption cycle of surfaces exposed to water vapor [5], but were abandoned in favor of slightly heating the mirrors of the resonator. Four fast-responding ( $\tau < 1s$ ) temperature sensors inside the cell signaled any disturbance of isothermal conditions. Data acquisition was computer controlled.

The resonator inside a vacuum chamber (Figure 1b) is the heart of the absorption spectrometer. A key-word summary of its specifications reads as follows: Fabry-Pérot reflection-type, semiconfocal arrangement, 10 cm mirror diameter, 40 cm curvature radius, mirror heating: 1°C/0.3 W, Fresnel number: 6; pinhole coupling: circular, 0.65 mm diameter, 0.075 mm double Mylar vacuum/pressure seal, coupling factor  $k = 0.0550$ ; resonance frequency, selected for optimum performance of the available klystron,  $f_R = 137.80$  GHz, temperature compensated ( $\Delta f/f_R = 0.9 \times 10^{-6}/^\circ\text{C}$ ) and insensitive to pressure loads from 0 to 2 atm; resonance bandwidth:  $b_0 = 334$  kHz yielding an effective path length,  $L_E = 0.141$  km (Eq. 2), mirror spacing:  $x_R = 182 \lambda/2 = 198.0$  mm; micrometer tuning:  $0.3175$  mm/rev  $\equiv 2500$  SU/rev (SU = scale unit on micrometer) with a resolution,  $\Delta x_R = 0.127$   $\mu\text{m}/\text{SU}$ , which converts into a frequency change,

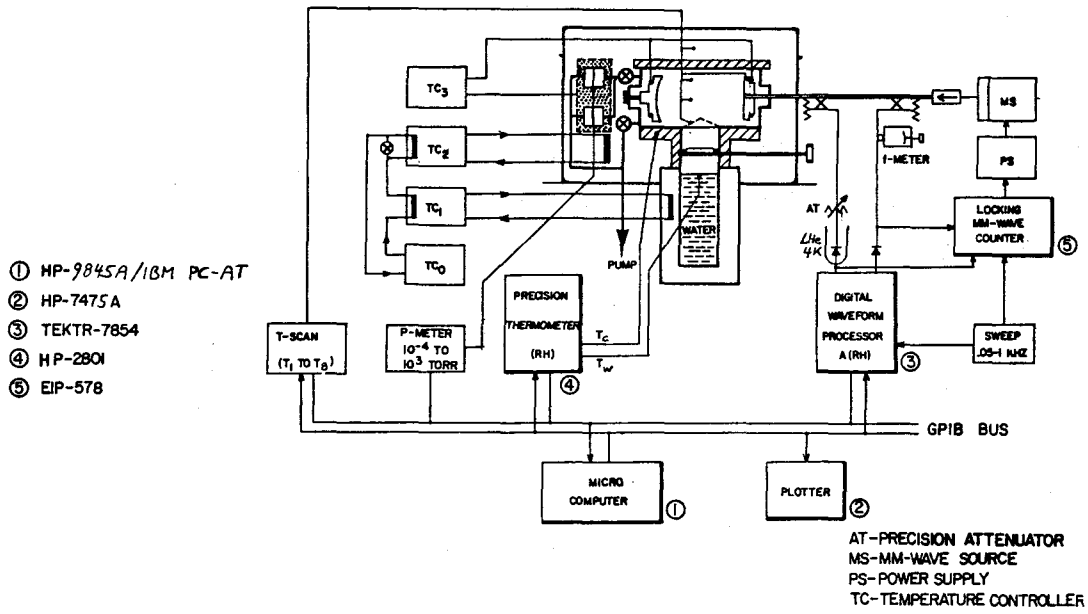
$$\Delta f_R = -f_R(\Delta x/x)_R = -88.4 \text{ kHz/SU}. \quad (4)$$

Over a 2.5 cm tuning range of the micrometer, the resonance at  $x_R$  was the "best" out of 52 choices with respect to other-mode interferences and Q-values.

The detector of the resonance pulse  $A(t)$  was an InSb bolometer, cooled to 4.2 K-LHe, and connected by a WR-12 waveguide mount. The maximum voltage output of the preamplifier was 10 V. A power-linear response of 4.2 V/mW was measured up to 1.0 V. With a 50-kHz detection bandwidth, the noise power was about 5 nW. The bolometer bias (92 mV) served as cryogenic thermometer ( $T_D$ ).

The power source was a 138 GHz klystron (20 mW) that was frequency-modulated by a sawtooth voltage generator to provide frequency-to-time domain conversion. The modulation frequency was exactly 500 Hz derived from a 10 MHz frequency standard. The linear sawtooth ramp was gated at exactly 1925  $\mu\text{s}$ , the fly-back time took only 2  $\mu\text{s}$ , which eliminated  $A(t)$  from the retrace. The modulation sensitivity of the klystron was determined to be 12.56(13) MHz/V by using the resonance peak  $a_0$  as frequency marker, tuned with the resonator micrometer to the end points of the ramp and checked for linearity over a modulation voltage range from 0.500 to 3.000 V. A tuning uncertainty of 1 SU introduced about 1 percent error in determining the frequency-to-voltage conversion factor.

(a)



(b)

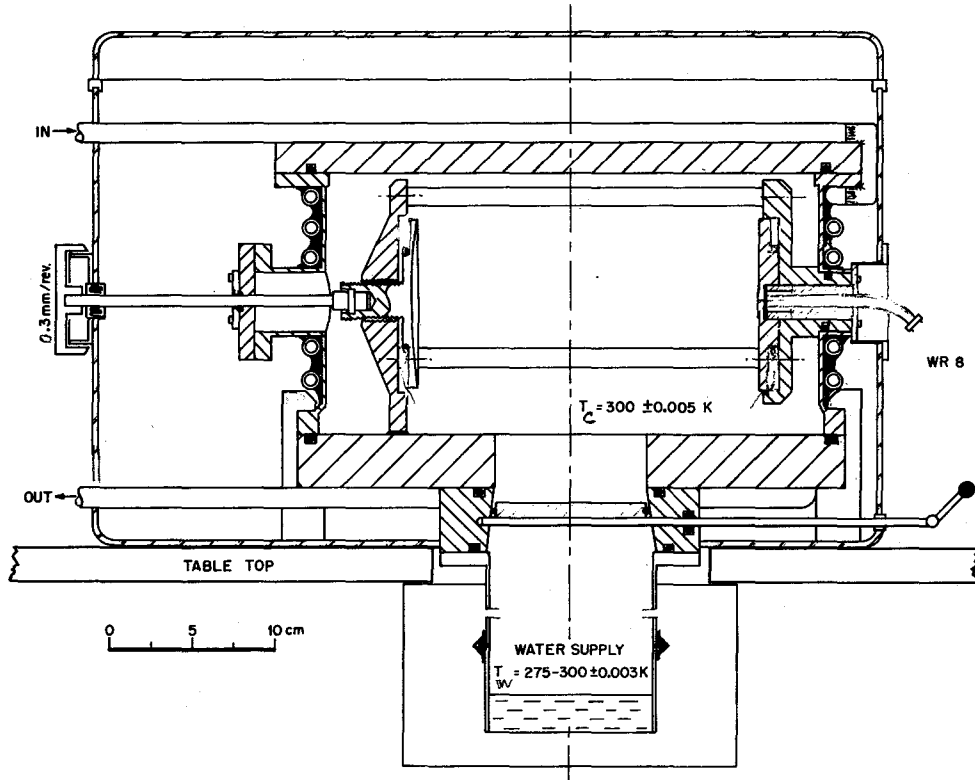


Figure 1. Millimeter-wave spectrometer for controlled moist air studies:  
(a) schematic and (b) cell design.

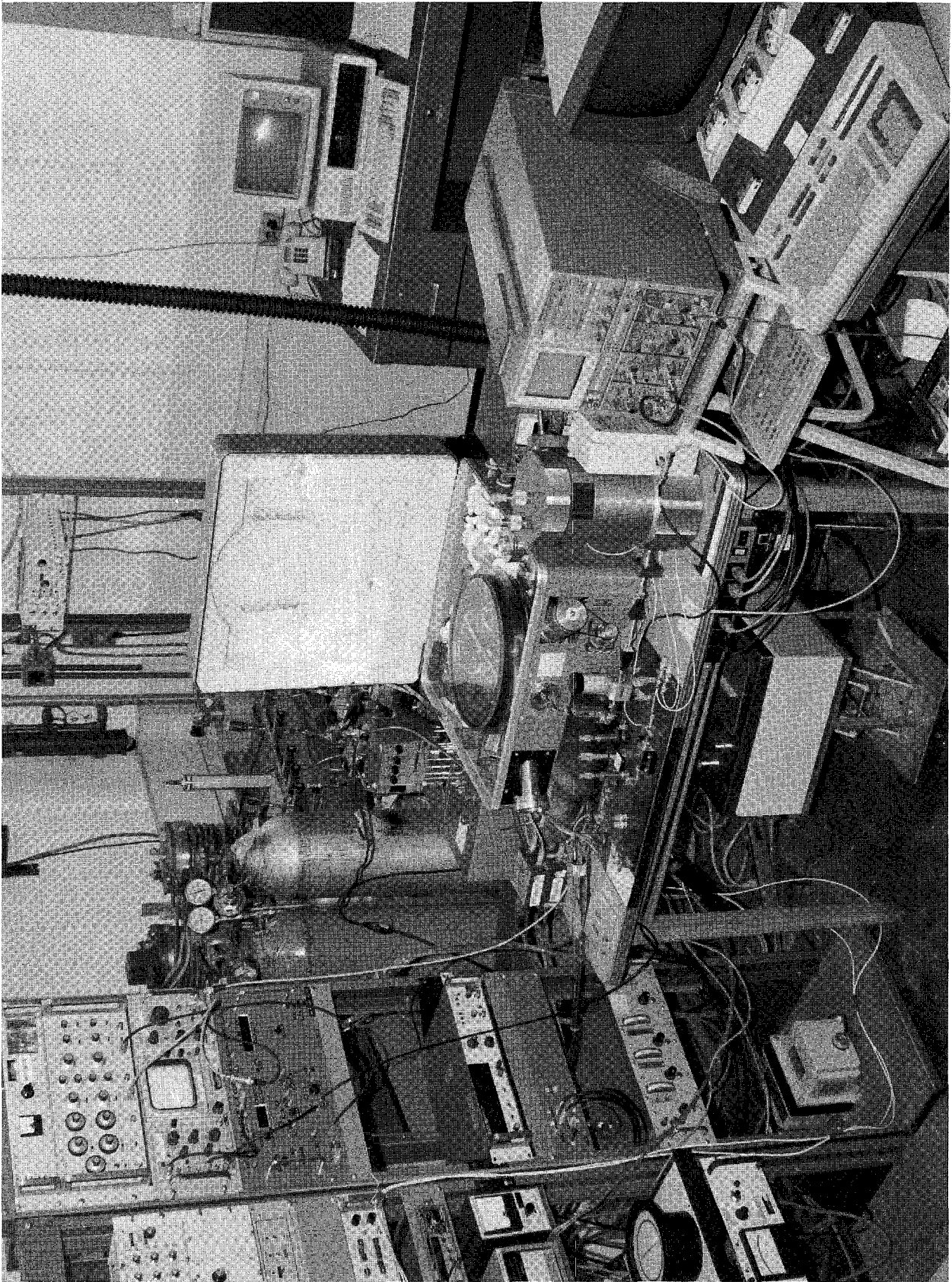


Figure 2. Photograph of millimeter-wave spectrometer.

The reference power  $a_0 = k \cdot a_K$  for (1) was measured by periodically (30s) switching on computer command to a 36 V modulation voltage, which displayed the power mode  $A_K(t)$  with a peak value,  $a_K = 909$  mV and a bandwidth,  $b_K = 186$  MHz. This feature provided an automatic calibration of  $\alpha_r$  (1) when the power level changed during a data run (e.g., refractive-tuning reduces  $f_R$  and the peak value  $a_K$  can change when the klystron is readjusted).

An electronic lock-on circuit centered the resonance  $f_R$  within one time frame; that is, the klystron center frequency  $f_K(a_K)$  was prevented from drifting with reference to  $f_R$ . A flat baseline  $A(t) = 0$  was established by adjusting  $f_K$  in such a way that two adjacent  $A(t)$  frames were displayed on a control scope and kept level. The reflected resonance signal  $A(t)$  could be eliminated by injecting a steel rod into the resonance volume. This measure provided baseline reference data in the "low" (0.36 V) and more accurate peak readings  $a_K$  in the "high" (36 V) mode of the modulator.

The waveform processor for  $A(t)$  was a digital storage oscilloscope, synchronized with the sawtooth modulator and capable of resolving 512/1024 pts per 2000  $\mu$ s. Operational resolution was typically 3.91  $\mu$ s/pt. The modulator voltage for  $A(t)$ -detection was 0.360 V resulting in a frequency resolution of 9.2 kHz/pt, which is an improvement over (4). Extensive averaging of the repetitive waveforms  $A(t)$  100 times, and  $A_K(t)$  50-times, was performed in real time to improve the signal-to-noise ratio of the a and b results.

For a measurement of the resonance bandwidth  $b_0$ , the digitizing increments were doubled (1024 pts) and the modulation voltage was varied in the 0.150 to 0.400 V range, allowing the resolution uncertainty to be reduced to  $\pm 5$  kHz. The resultant error in an absolute calibration of  $\alpha$  (3) was less than 3 percent.

The computer of the spectrometer had a control-program that was designed to be flexible in order to allow changes in data collection procedures. It is written in BASIC with about 500 lines of code to control the readings of eight temperatures, two pressures, and a/b values from the waveform processor and to store the data on a magnetic medium for future processing. The program is time controlled. The fastest acquisition time for a complete measurement cycle was 30 seconds.

Measurements begin by starting the internal program of the waveform-processor, which does 100 averages on the output  $A(t)$  from the InSb detector. Since averaging takes about 14 seconds, the computer program con-



tinues data recovery from the temperature sensors which measure chamber ( $T_c$ ), water bath ( $T_w$ ), room ( $T_r$ ), gas ( $T_{1,2,3}$ ), mirror ( $T_m$ ) temperatures, and data from the total pressure meter (P). By this time the oscilloscope is nearly ready with its data so the computer program returns to wait for the final steps in the scope program. After the scope completes 100 averages on  $A(t)$  it normalizes (by setting cursors at 0.1 and 0.9 of the time base) the trace to remove any baseline slope, then stores the waveform. Next, an auxiliary output from the scope switches the sweep generator voltage from low (0.36 V) to high (36 V). The scope input changes to the power envelope of the klystron with the lock-on disabled. The scope program performs 50 averages on the power curve and stores the waveform  $A_k$ . The next computer step is to call for the  $a/b$  and  $a_k/b_k$  values of the stored waveforms.

All of the measured data were temporarily stored in computer memory and transferred along with time-of-day to magnetic tape or disk storage for safe keeping and later recovery and processing.

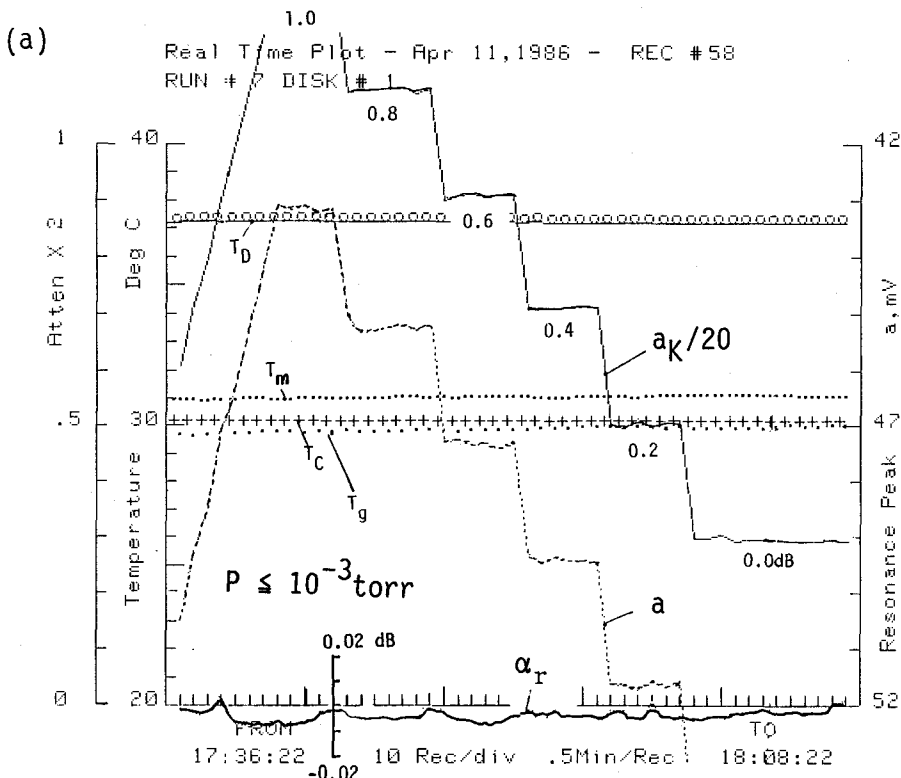
Real-time data were plotted on the CRT of the computer to follow the progress of an experiment. The selection of what was displayed is part of the program configuration. Two typical examples of 1-hour operating periods are shown in Figure 3. Figure 3a demonstrates the automatic calibration to  $\alpha_r = 0$  dB for input power variations of 1 dB. The reference power trace  $a_k$  was reduced by a factor 0.05 for display, but the correct coupling factor  $k = 0.0550$  was applied for the relative attenuation trace (1)  $\alpha_r = 8.686 (\sqrt{k \cdot a_k / a} - 1) = 0$  dB. Each 1-hour frame represents averages of about  $10^7$  actually acquired data points. Detection sensitivity and long-term stability are displayed in Figure 3b.

Program configuration is stored in a separate file on disk. An auto-start function is available for studies that are conducted unattended. In the event of a power failure the program will automatically restart.

Post processing of data repeats calibrated signal corrections as done in the real-time mode. Scatter plots of  $\alpha_r$  are made versus pressure in a point-mode (e.g., Figure 6).

## 2.2 Moist Air Attenuation Measurements

The objective of the experiments was to perform pressure scans of the attenuation rate  $\alpha$  due to water vapor absorption in moist air. An extensive series of controlled measurements was performed at 137.8 GHz to determine



Temperature Readings

$T_D = 92\text{mV}$ , bias of InSb detector ( $\approx 4.2\text{K}$ )

$T_m$  = mirror

$T_g$  = gas

$T_c$  = cell wall

$T_w$  = water (vapor source)

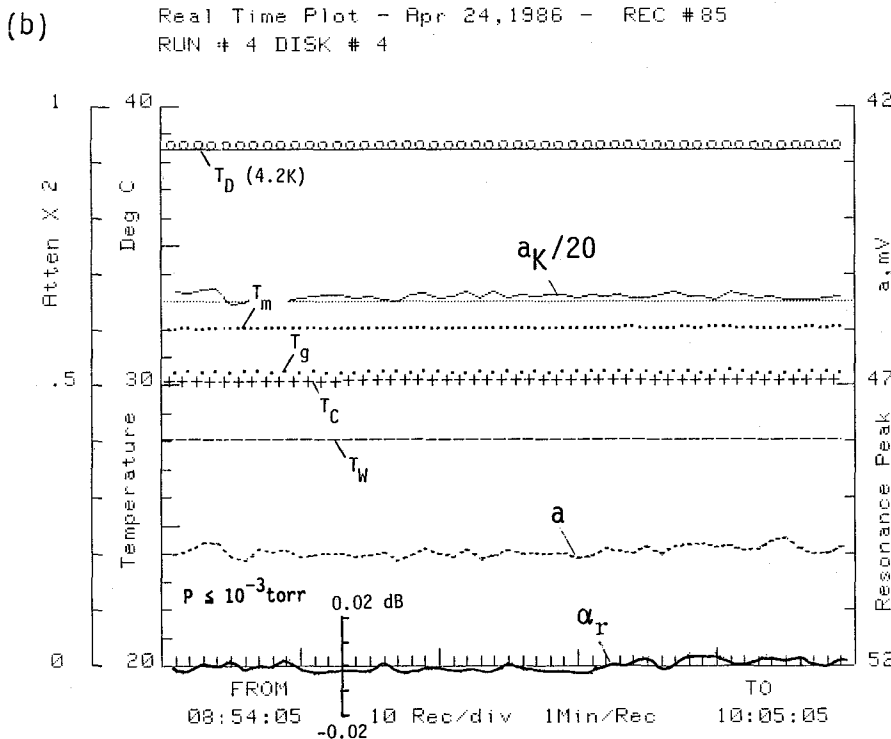


Figure 3. Mm-wave spectrometer operational data (five temperatures  $T_i$ ;) peak values of reference and reflected signals  $a_k$ , and  $a$ ; and relative attenuation ( $\alpha_r$ ) for a 1-hour measurement period with an evacuated cell ( $f_R = 137.8$  GHz):

(a) automatic calibration to  $\alpha_r = 0$  dB for changes,  $\Delta a_k = 0-1$  dB;

(b) detection stability and sensitivity

( $\alpha_{\min} \approx 0.006/0.13 \leq 0.05$  dB/km).

$\alpha(P = e+p)$ . Data  $\alpha(T, e, p)$  were taken covering the following range of parameters:

temperature	$T = 316$ to $282$ K;
vapor pressure	$e = 0$ to $e_1$ (RH < 95%); and
total pressure	$P = e_1 + p$ , where $p = 0$ to 1200 torr (capacitance manometer), $p = 0$ to 3 atm (aneroid manometer)*.

Maximum vapor pressure  $e_1$  was determined by the temperature  $T_W$  of the water reservoir.

With the spectrometer performance optimized at  $P = 0$  (see Figure 3b), an additional set of problems appeared when the gas pressure was varied. Introducing and removing gas from an enclosure changes the temperature  $T_g$  of a sample (Figure 4). Only pressure scan rates below  $\pm 100$  torr/min ensured quasi-static gas conditions,  $T_g = T_C$ . Typically, the pressure was varied in steps. While the gas settled, the klystron frequency  $f_K$  was retuned to balance the baseline of  $A(t)$ .

Working with water vapor often brought disappointing results with respect to reproductibility. Condensation effects on both mirrors and pinhole coupling were avoided (see p. 5). One source was the "piston" effect where local compression condenses part of the vapor; another error source was the slow diffusion-mixing of water vapor with stagnant air. We calculated the diffusion time constant for vapor molecules to travel 30 cm inside the cell against 1 atm of dry air to be

$T$	(K)		315	300	285
$\tau_D$	(min)		5.4	6.0	6.7 .

It takes a period longer than  $5 \cdot \tau_D$  for a homogeneous moist air mixture  $P = e_1 + p$  to develop. A measurement of  $a(P)$  shown in Figure 5a indicates even longer time periods. Water pressure  $e_1(T_W)$  settled with no delay when the  $H_2O$ -valve was opened. Dry air injection first reduced  $e_1$  (piston effect) and then it took up to 1 hour to obtain a stable value  $a(e_1+p)$ . Mixing was accelerated to less than 5 minutes by installing a fan, driven by a magnetically coupled rotary vacuum feed-through.

\*Experimental pressure scale is measured in torr; the prediction model MPM uses the pressure unit  $1 \text{ kPa} = 10 \text{ mb} = 7.5006 \text{ torr}$ .

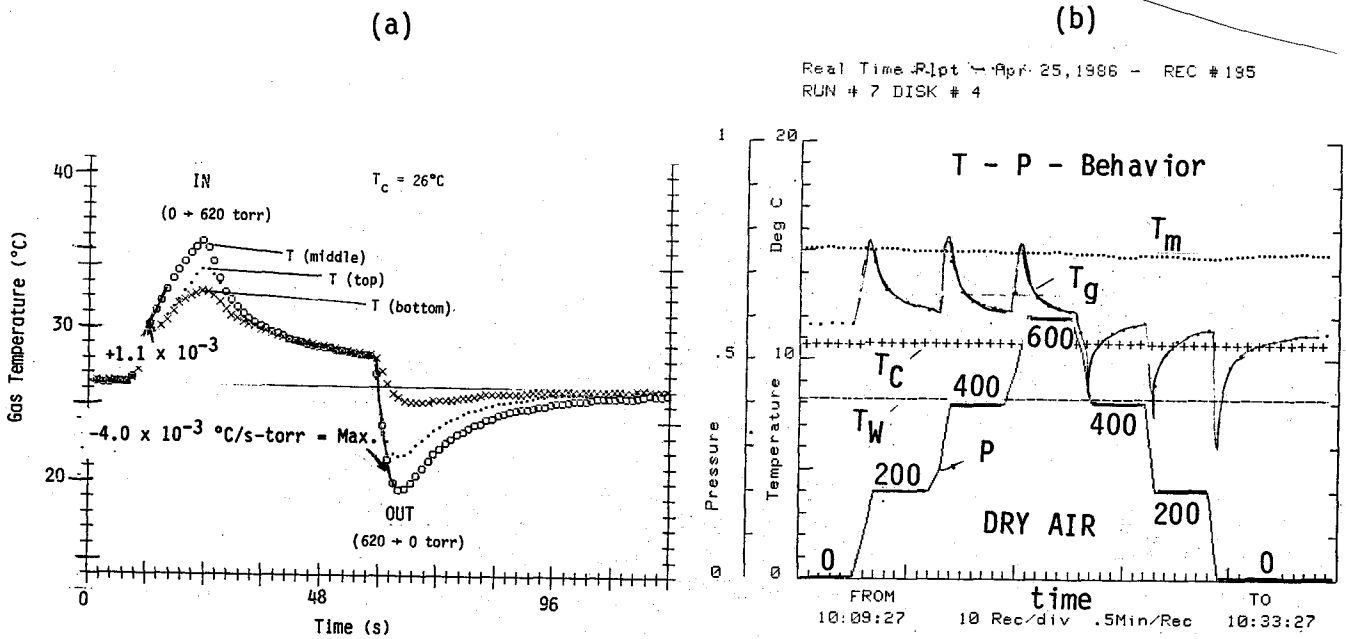


Figure 4. Temperature responses inside the spectrometer cell:  
 (a) time-response test of gas temperature ( $T_g$ ) sensors,  
 (b) temperature-vs.-pressure behavior for a typical dry air case.

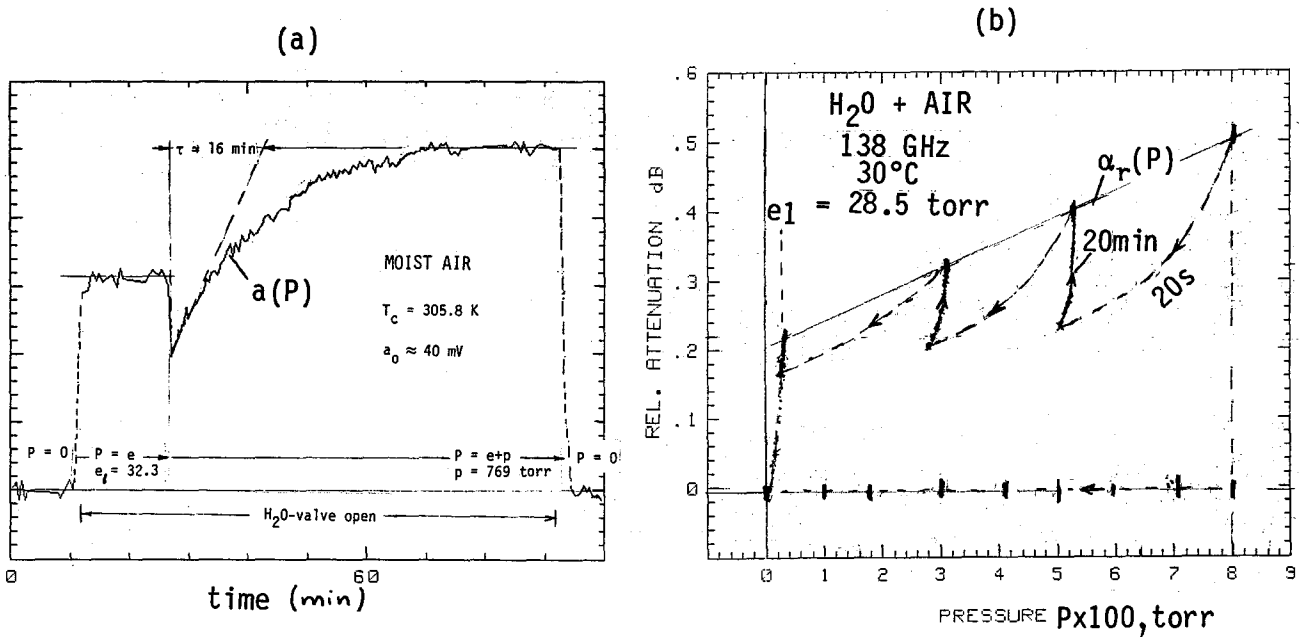


Figure 5. Mixing effects of H<sub>2</sub>O + AIR from time series of 138 GHz attenuation:  
 (a) piston effect and diffusion mixing;  
 (b) decompression condensation during pump-down over open vapor source.

One other effect was observed when dealing with moist air inside a vessel: reducing the total pressure  $P$  caused the water vapor to condense by decompression cooling. Even with the water vapor supply fully exposed to the air mixture, it took a long time (20 min) to reestablish the initial vapor pressure  $e_1$  as indicated by  $\alpha_r(P)$  in Figure 5b (mixing fan was off).

### 2.3 Water Vapor and Moist Air Attenuation Results

Moist air attenuation  $\alpha$  at a frequency  $f$  that falls within the millimeter-wave window range centered at 140 GHz, can be expressed by [6], [7]

$$\alpha = k_s(T) e^2 + k_f(T) ep + k_d(T) p^2 \quad \text{dB/km}, \quad (5)$$

where  $e$  and  $p$  in kPa are partial pressures of water vapor and dry air, respectively. Pressure-broadening theory of the  $H_2O$  rotational spectrum predicts ( $e > 0.01$  kPa) a fixed ratio  $m$  between air- $(ep)$  and self- $(e^2)$  broadening; i.e.,

$$m = k_f/k_s. \quad (6)$$

An extensive series of controlled laboratory measurements was performed at 137.8 GHz to determine the  $k$ -coefficients of (5) and (6). Table 1 is a summary of over 2500 individual data points  $\alpha(T, e, p)$ .

At  $T = 303$  K, the foreign-gas broadener AIR ( $p$ ) was replaced by its principal constituents  $N_2$ ,  $O_2$ , and Ar. These results are listed in Table 2. The broadening efficiency  $m$  is useful to explain  $H_2O$  absorption processes that support (5) since  $\alpha = k_s e (e+mp)$ . Pure oxygen ( $O_2$ ) measurements for pressures up to 2.4 atm against Ar as the "loss-free" reference provided an estimate of  $k_d$  when multiplying the result by 0.21.

Data of Table 1 were further reduced to a reference temperature  $T_0 = 300$  K. Temperature dependence of the  $k_{s,f,d}$  coefficients was fitted to a power law,

$$k(T) = k\theta^x \quad \text{dB/km-kPa}^2, \quad (7)$$

where  $\theta = 300/T$  is an inverse  $T$ -parameter.

The results for moist air attenuation at 137.8 GHz, when expressed by (5) to (7), led to

Table 1. Comparison between Measured (X) and Model-Predicted (M-MPM, see Section 3) Coefficients  $k_{s,f}$  of (5). Experimental conditions:  $f = 137.8$  GHz,  $T = 282-316$  K,  $P = e_i + p$ ,  $p = 0-110$  kPa

	T	$e_i$ (RH)	Moist Air			Dry Air
			$k_s$	$k_f$	$m$	$k_d$
	K	kPa	dB/km-kPa <sup>2</sup> x10 <sup>-2</sup>		x10 <sup>-2</sup>	dB/km-kPa <sup>2</sup> x10 <sup>-6</sup>
X	315.5	7.49 (90%RH)	8.01	0.485	6.06	-
M			7.85	0.481	6.13	1.93
X	305.9	4.45 (90%RH)	10.9	0.540	4.95	-
M			10.81	0.530	4.90	2.10
X	303.2	3.80 (90%RH)	12.0	0.558	4.65	2.2
M			11.84	0.545	4.60	2.11
X	296.1	2.51 (90%RH)	15.0	0.59	3.9	-
M			15.08	0.589	3.91	2.29
X	286.7	1.39 (90%RH)	21.0	0.65	3.1	-
M			21.22	0.649	3.06	2.46
X	281.8	1.05 (94%RH)	25.7	0.68	2.65	-
M			25.49	0.687	2.70	2.64

Table 2. Attenuation Measurements of Water-Vapor/Air-Constituent Mixtures (f=137.8 GHz, T=303 K, E<sub>1</sub>=3.80 kPa) Expressed with k<sub>x</sub>-Coefficients of (5); and Corresponding Broadening Efficiencies m<sub>x</sub> (6). Included are Line-core Measurements m<sub>L</sub> and their Predictions m<sub>1</sub> and k<sub>1</sub> Transposed to 138 GHz

	FAR WING (303K)				LINE CORE (300K)		
	k <sub>x</sub>	k <sub>1</sub>	m <sub>x</sub>	m <sub>1</sub>	m <sub>L</sub>		
f(GHz)	137.8		137.8		22.2	183.3	
<u>Species</u>	dB/km-kPa <sup>2</sup> x10 <sup>-2</sup>		x10 <sup>-2</sup>		[16]	[16]	[11]
H <sub>2</sub> O	12.0	2.55	100	100	100	100	100
AIR	0.558		4.65	21.9*	20.8	22.7	22.1(θ <sup>-0.6</sup> )
N <sub>2</sub>	0.627		5.23	24.6	22.8	24.9	
O <sub>2</sub>	0.322		2.68	12.6	14.0	14.3	
Ar	0.222		1.85	8.7	11.4	10.3	
	Linewidth (MHz/kPa)				135.0	143.0	151.9(θ <sup>1.1</sup> )

\*Reference value (line-core average)

$$\begin{aligned}
k_s(T) &= 0.133(4)\theta^{10.3(3)}, \\
k_f(T) &= 5.68(5)10^{-3}\theta^{3.0(4)}, \\
k_d(T) &= 2.2(5)10^{-6}\theta^{2.8},
\end{aligned}
\tag{8}$$

and

$$m = 0.0427/\theta^{7.3}.$$

Digits in parentheses give the standard deviation from the mean in terms of the final listed digits. Typical examples of data plots  $\alpha_r(e)$  and  $\alpha_r(e_1 + p)$  are exhibited in Figure 6. All experimental results supported the formulation in (5). Model predictions of the experimental data are given in Figure 14 (Section 3.4).

### 3. ATMOSPHERIC PROPAGATION MODEL MPM

(see Appendix A and B for Details)

Dry air and atmospheric water vapor are major millimeter-wave absorbers; so are suspended droplets (haze, fog, cloud) and precipitating water drops that emanate from the vapor phase. A practical model (designated program code: MPM) was formulated that simulates the refractive index  $\underline{n} = n' - jn''$  of the atmospheric propagation medium for frequencies up to 1000 GHz [1] - [3]. Since the interaction with a neutral atmosphere is relatively weak, the refractive index is converted into a refractivity in units of parts per million,

$$\underline{N} = (\underline{n} - 1) 10^6 \text{ ppm.}$$

#### 3.1 Features of the Program

A user-friendly parametric program was developed that calculates the values of the complex refractivity  $\underline{N}$  for atmospheric conditions as a function of the variables  $f$ ,  $P$ ,  $T$ ,  $RH$ ,  $w_A$  (A/B/C/D),  $w$ , and  $R$ , as listed in Appendix A (Section A.1.1).

The output of MPM are three radio path-specific quantities:

- attenuation  $\alpha(f)$  dB/km
- refractive delay  $\beta_0$  ns/km
- dispersive delay  $\beta(f)$  ps/km



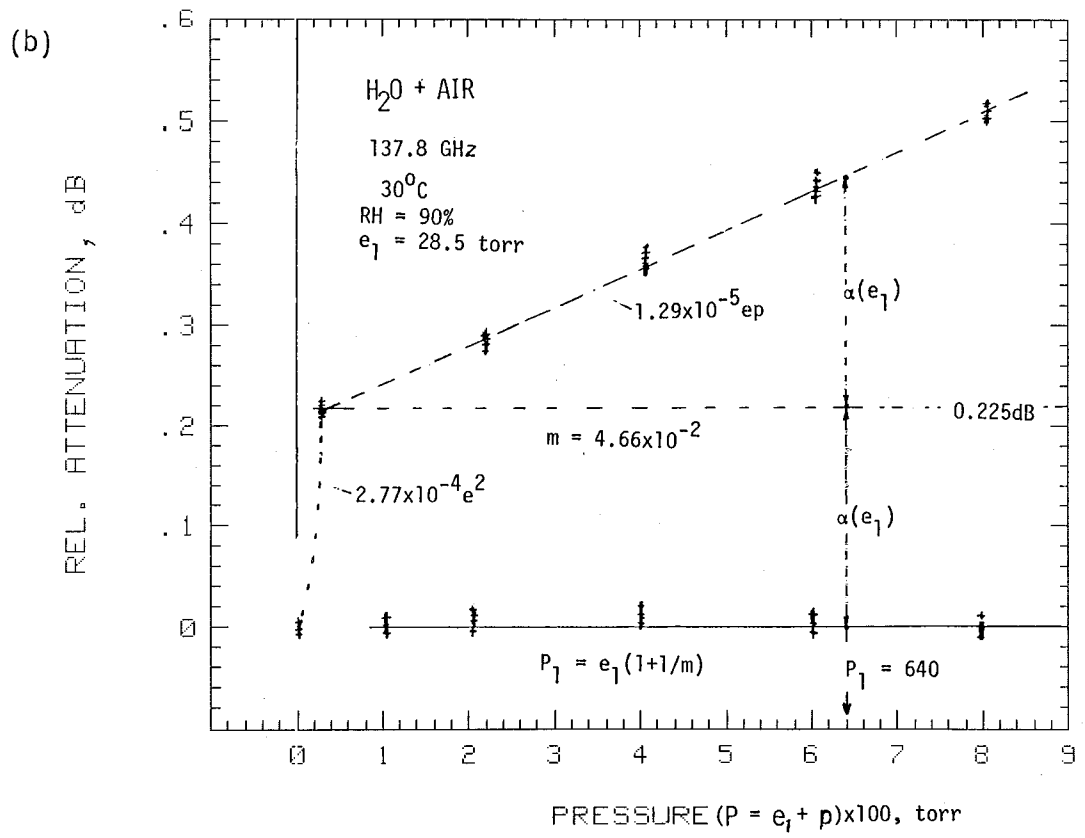
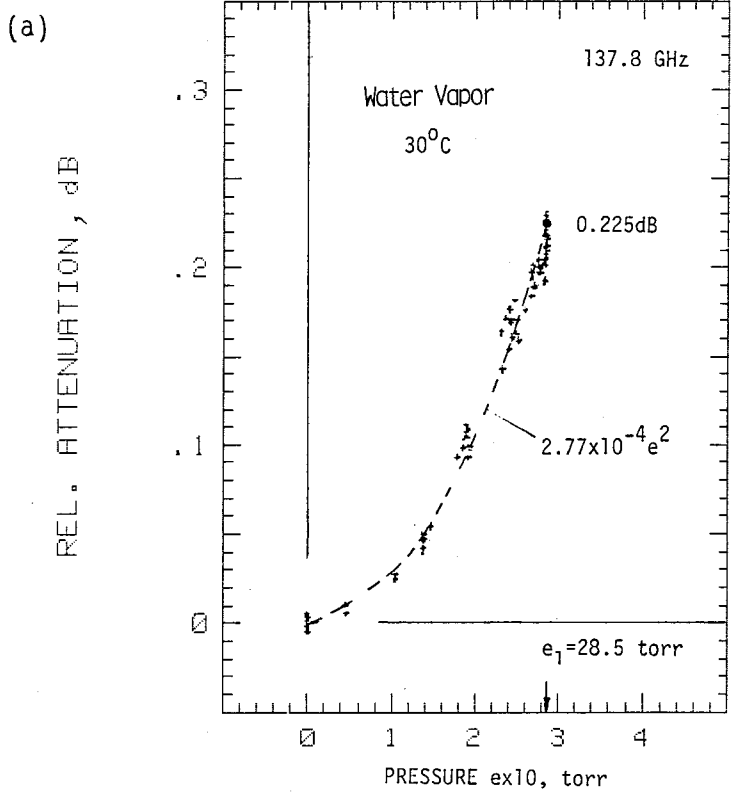


Figure 6. Typical raw data plots of relative attenuation  $\alpha(P)$  for pressure scans at 137.8 GHz introducing (a) water vapor,  $P = e$ , and (b) H<sub>2</sub>O + Air,  $P = e_1 + p$ .

The height range 30 to 100 km is treated approximately excluding the detailed  $O_2$ -Zeeman effect and trace gas spectra (e.g.,  $O_3$ , CO,  $N_2O$ , etc.). Program MPM is written with extensive comments to run on IBM-XT/AT + 8087 coprocessor, or equivalent, microcomputers.

Extensive revisions of the MPM code have been made recently. The latest version is described in Appendix A. Details include (a) a revised set of overlap coefficients  $a_5$  [(A-12)] in the dry air line table (see page 66) for the 60 GHz oxygen band based on a molecular fitting scheme reported by Rosenkranz [10]; (b) a relative humidity-driven growth model for hygroscopic aerosol addressing haze conditions for RH = 90 to 99.9% [(A-3)]; (c) a new double-Debye model describing the complex permittivity  $\underline{\epsilon}(f,T)$  of water for  $f = 0 - 1000$  GHz,  $T = -10$  to  $30^\circ C$  [(A-17)]; and (d) an improved fog/cloud model that includes a dispersive delay term [(A-16)].

A nonlinear least-squares fitting scheme was applied to dielectric data sets  $\underline{\epsilon}(f,T)$  reported below 1 THz. Various spectral functions (relaxation and resonance) were considered, and the double-Debye model provided the best fit [15]. The Rayleigh approximation of the fog/cloud model was tested with experimental results on fog attenuation at 50, 82, 141, and 246 GHz and on differential fog delay between 246/82 GHz. All measured data were found consistent with model predictions. Moist air effects and fog effects of  $\alpha$  and  $\beta$  were assumed to be additive [14].

### 3.2 MPM Calibration

Experimental results at 138 GHz, as described by (5) and (8), contain foremost contributions from water vapor continuum absorption. Equation (5) was used to "calibrate" the program MPM by enforcing the agreement between experimental and predicted data. The continuum, assuming an  $f^2$  dependence, is defined by (see (14a) of [1])

$$\alpha_c = 0.1820 f N_e''(f), \quad (9)$$

where the imaginary part of refractivity  $N$  is given by (Table 3)

$$N_e'' = f(3.57 e^{2\theta^{10.5}} + 0.113 e p \theta^3)10^{-5} \quad (10)$$

and  $f$  is in GHz. A comparison in Table 1 shows that at 138 GHz, within experimental uncertainties, a good fit was obtained.

In addition to (10), new width data [11] for the 183 GHz  $H_2O$  line ( $b_3$  listed in Table 1 of [1] was increased by 11.6%) were used to update the MPM program; also,  $b_3$  parameters of the 325 and 380 GHz  $H_2O$  lines were increased by 10 percent. Other MPM modifications were a change in the nonresonant line width  $\gamma_0$  of dry air from  $5.6 \times 10^{-3}$  to  $4.8 \times 10^{-3}$  [10], the elimination of the roll-off term  $1/[1 + (f/60)^2]$  (part of equation 13a in [1]), and the imposing of a high frequency cut-off  $F''(f) = 0$  [see Eq. (A-9)] for  $f \geq (\nu_0 + 40\gamma)$  [12].

### 3.3 Interpretation of $H_2O$ Continuum Absorption

Since MPM employs a limited ( $\leq 1$  THz)  $H_2O$  line base, it is of interest to find out which share of  $k_s$  and  $k_f$  (8) can be attributed to far-wing behavior of the rotational  $H_2O$  spectrum extending beyond 1 THz [6]. Results in Table 2 indicate broadening efficiency ratios  $\xi$  at 138 GHz; e.g.,

$$\xi = m(H_2O + N_2)/m(H_2O + Ar), \quad (11)$$

which are similar to those observed at cores of the 22 and 183 GHz lines. Consequently,  $k_f$  can be interpreted as a foreign-gas broadening effect whereby MPM lines account for about 30 percent of the rotational  $H_2O$  spectrum. Table 3 lists the assessment at 300 K ( $\theta = 1$ ). When the line core argument ( $m_L = 0.208/\theta^{0.5}$ ) is extended to  $k_s$ , then a substantial share,

Table 3. Summary Data of H<sub>2</sub>O line Spectrum and H<sub>2</sub>O Excess Attenuation at 137.8 GHz, T = 300 K

a) Experiment-versus-MPM Predictions								
	k <sub>S</sub>	x <sub>S</sub>	MOIST AIR				DRY AIR	
			k <sub>f</sub>	x <sub>f</sub>	m	x <sub>m</sub>	k <sub>d</sub>	x <sub>d</sub>
	x10 <sup>-2</sup>		x10 <sup>-2</sup>		x10 <sup>-2</sup>		x10 <sup>-6</sup>	
X	13.2	10.5	0.570	3.0	4.32	-7.5	2.2	-
M	13.15	10.51	0.5666	3.09	4.309	-7.42	2.10	2.35
b) Local H <sub>2</sub> O Lines in MPM (31% of c):								
M	0.802	3.5	0.175	3.8	21.8	0.3		
c) Complete H <sub>2</sub> O Line Spectrum (m = 0.22 assumed - see Table 2)								
	2.59	3.5	0.57	3.0	22	-0.5		
d) Excess H <sub>2</sub> O Absorption:								
Eq. (12)	10.3	12.5						

Table 4. Reported Data on (H<sub>2</sub>O)<sub>2</sub> Dimer Concentration e<sub>D</sub>/e over the Temperature Range for 300 to 386 K

T, kPa	300	358.4	367.1	375.9	386.4
e, kPa	2.80	58.27	81.47	111.9	159.3
e <sub>D</sub> , kPa	0.0024	0.44	0.76	1.28	2.27
e <sub>D</sub> /e, x10 <sup>-3</sup>	0.9	7.6	9.4	11.4	14.2
e <sub>D</sub> /e <sup>2</sup> , x10 <sup>-4</sup>	3.1	1.30	1.15	1.02	0.895
*Reference	[8]			[9]	

$$\alpha_i \approx 0.103 e^2 \theta^{12.5} \text{ dB/km} \quad (12)$$

where  $\alpha_i = (\alpha_x - \alpha_L)$  is not supported by the H<sub>2</sub>O monomer line spectrum ( $\theta^{12.5} \approx -4.3\%/K$ ).

At this point one might speculate about (H<sub>2</sub>O)<sub>2</sub> dimer absorption. An estimate of the partial dimer vapor pressure

$$e_D \approx 3.12 \times 10^{-4} e^2 \theta^5 \text{ kPa}, \quad (13)$$

was obtained by fitting data on physical dimer properties given in Table 4. A strong 138 GHz attenuation rate,

$$\alpha_i \approx 330 e_D \theta^{7.5} \text{ dB/km}, \quad (14)$$

results when (12) and (13) are combined ( $\theta^{7.5} \approx -2.5\%/K$ ).

### 3.4 MPM Predictions

Features of the user-friendly atmospheric propagation model MPM were discussed in Section 3.1. The microcomputer version is written in IBM Professional FORTRAN with extensive comments that guide the user to appropriate references for specific formulations. Three parametric presentations have been found useful in practical applications, which are addressed in separate subprograms:

Profiles	Variable	Parameters
A. Frequency	f	P, T, RH(v), w <sub>A</sub> , w, R.
B. Humidity	RH,v	f, P, T, w <sub>A</sub> , w.
C. Pressure	P	f, T, RH(e).

A copy of the line code for program MPM-N/A (frequency profiles) is shown in Appendix B. The detailed structure of MPM comes best to light in graphical examples. Typical sea level behavior of MPM-predicted rates,  $\alpha$  and  $\beta$ , is illustrated in Figures 7 to 13. Across the millimeter-wave spectrum (Figures 7 and 8) one recognizes more or less transparent window ranges (W1 to W5) separated by molecular resonance peaks. Calculations of total radio path

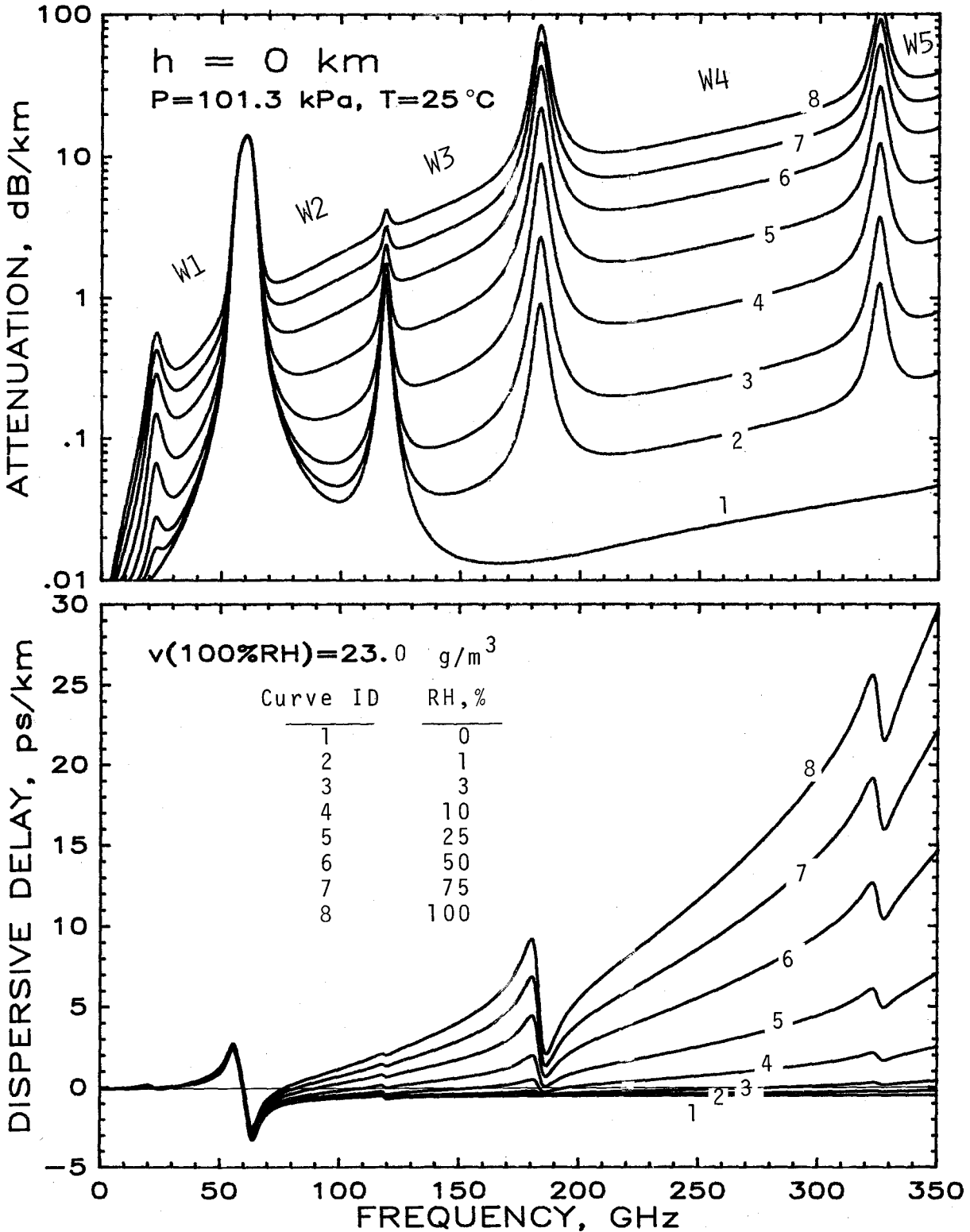


Figure 7. MPM-predicted specific values of attenuation  $\alpha$  and dispersive delay  $\beta$  at sea level height  $h=0 \text{ km}$  ( $P=101.3 \text{ kPa}$ ,  $T=25^\circ \text{C}$ ,  $RH=0$  to  $100\%$ ) over the frequency range,  $f=1$  to  $350 \text{ GHz}$ . Window ranges are marked W1 to W5.

attenuation  $A$  [dB], delay  $B$  [ps], and atmospheric noise temperature  $T_A$  [K] require distributions of  $P(x)$ ,  $T(x)$ ,  $RH(x)$  along the propagation direction  $x$  to be known [2].

Spectroscopic properties of the air-broadened water vapor line centered at 183 GHz are demonstrated in Figure 9. Accuracy of supporting line parameters (strength, width, shift) determines the reliability of predictions needed for remote sensing applications with respect to atmospheric humidity. With respect to line shape studies one observes that wing data from the delay spectrum  $\beta(f)$  are unaffected by dry air pressure  $p$ . Outside a line-center frequency range  $\nu_0 \pm 5\gamma$ , dispersion  $N'(f)$  is independent of a particular shape function  $F'(f)$  such as (A-9b).

A major concern for most MMW systems is their performance in rain. A simplified classification of rain events is given in Appendix A (A.1.1). When neglecting any statistical nature of rain within a radio path, the calculation scheme (A-18) provides an estimate on  $\alpha(f)$  and  $\beta(f)$ . Predictions (Figure 10) are based on adding to the known state of moist air (P-T-RH) only one additional parameter, namely the point rainfall rate  $R$ .

Of some importance is the fog/cloud prediction program in MPM. Systems operating in the MMW range offer an attractive alternative to electro-optical systems when operation has to be assured during periods of adverse weather (rain, cloud, fog, haze, high humidity). Current interest is focused on the frequency range 90 to 350 GHz where an optimum trade-off between atmospheric obscurations and angular resolution can be achieved. All atmospheric loss and delay effects have to be known accurately in order to analyze the potential for all-weather performance. The suspended water droplet (SWD) formulation (A-16) and (A-17) of MPM is an addition to the state of saturated air (P-T-RH=100%) as illustrated in Figure 11. Key parameters are SWD content  $w$  in  $\text{g}/\text{m}^3$  and temperature  $T$  in  $^\circ\text{C}$ .

Another atmospheric ingredient is the mass concentration  $w_A$  of hygroscopic aerosol (HAE). Solution droplets appear for  $RH > 80\%$ , and haze conditions develop as  $RH$  approaches 100 percent. These conditions can be modeled by assuming that at the reference humidity,  $RH = 80\%$ , the HAE concentration  $w_A(RH = 80\%)$  is known. The  $RH$  dependent swelling/shrinking  $w(RH)$  is described approximately up to  $RH = 99.9\%$  by a growth model (A-3).

Relative humidity  $RH$  is the variable that governs physical processes taking place in the atmosphere with respect to water vapor. Practical models

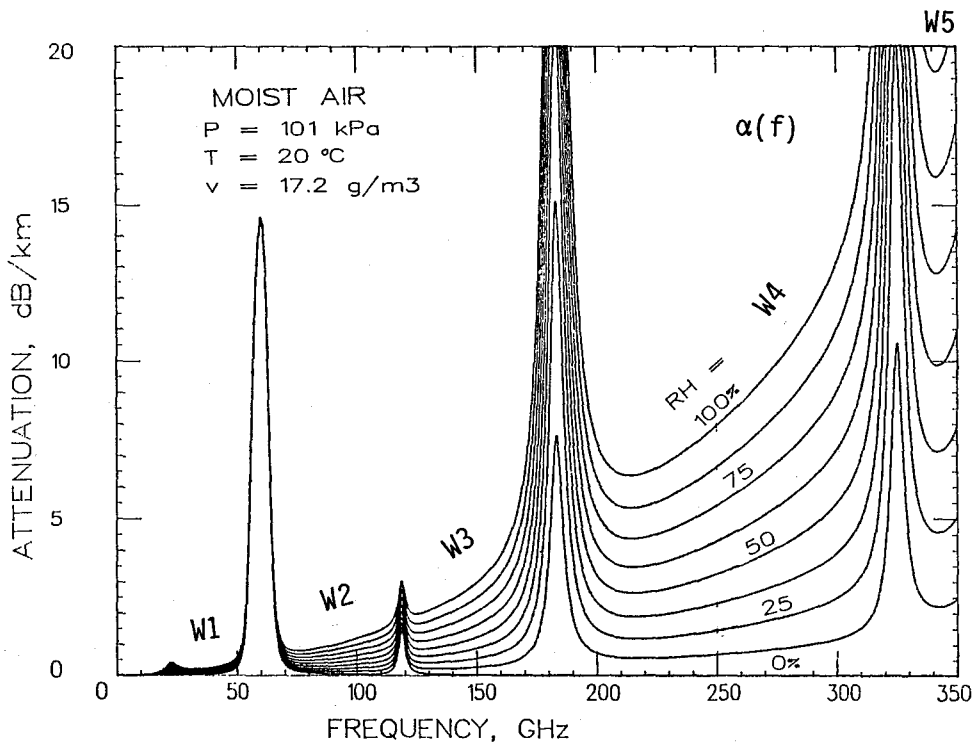


Figure 8. Water vapor absorption in window ranges for constant relative humidity increments ( $\Delta RH = 12.5\%$ ) at a sea level condition.

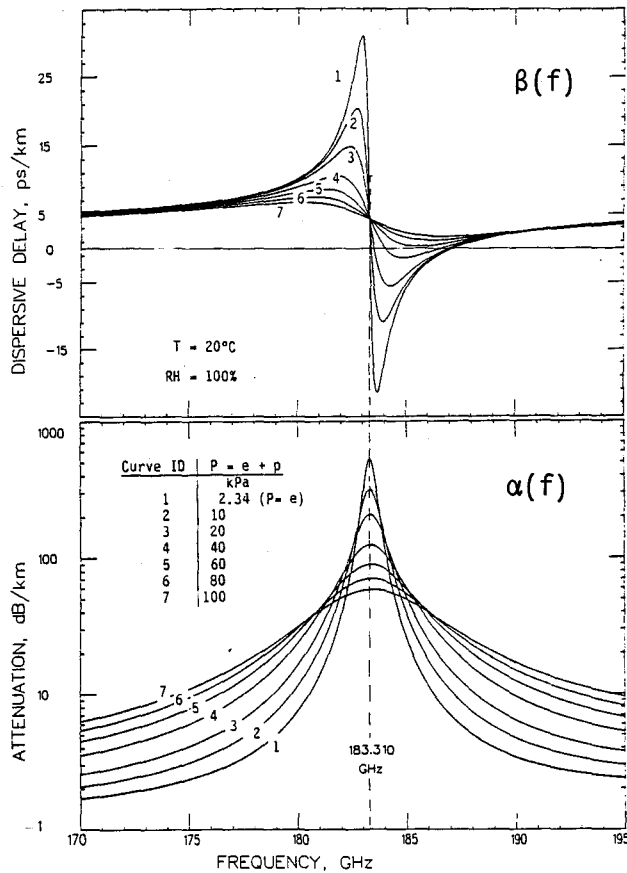


Figure 9. Pressure-broadening (AIR) example of the 183 GHz  $\text{H}_2\text{O}$  line.



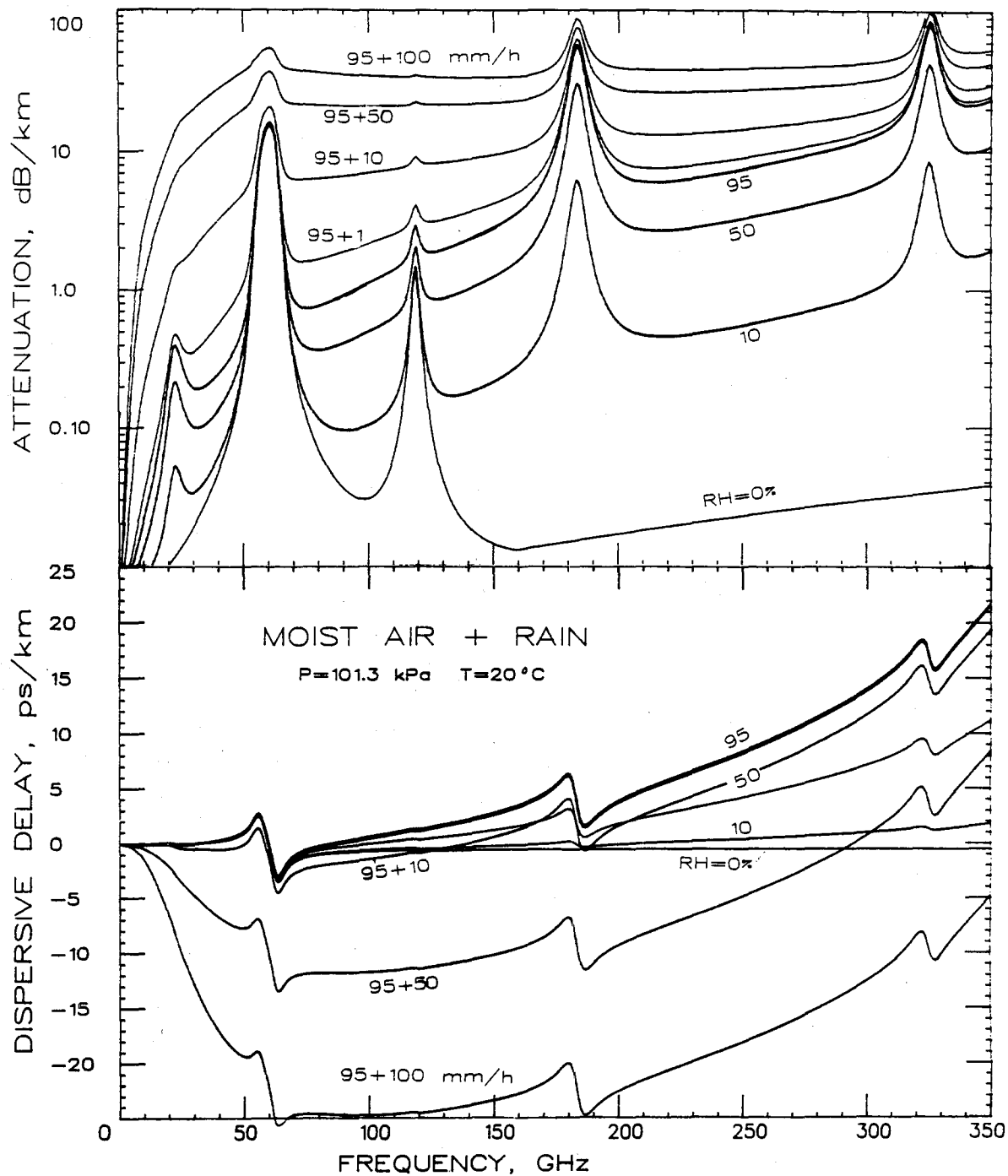


Figure 10. Attenuation  $\alpha$  and delay  $\beta$  rates for three rain events ( $R=10, 50,$  and  $100$  mm/h) added to a moist air ( $RH=95\%$ ) sea level condition. Also shown are dry air ( $0\%$  RH) and moist air ( $50\%$  RH) characteristics.

(a)

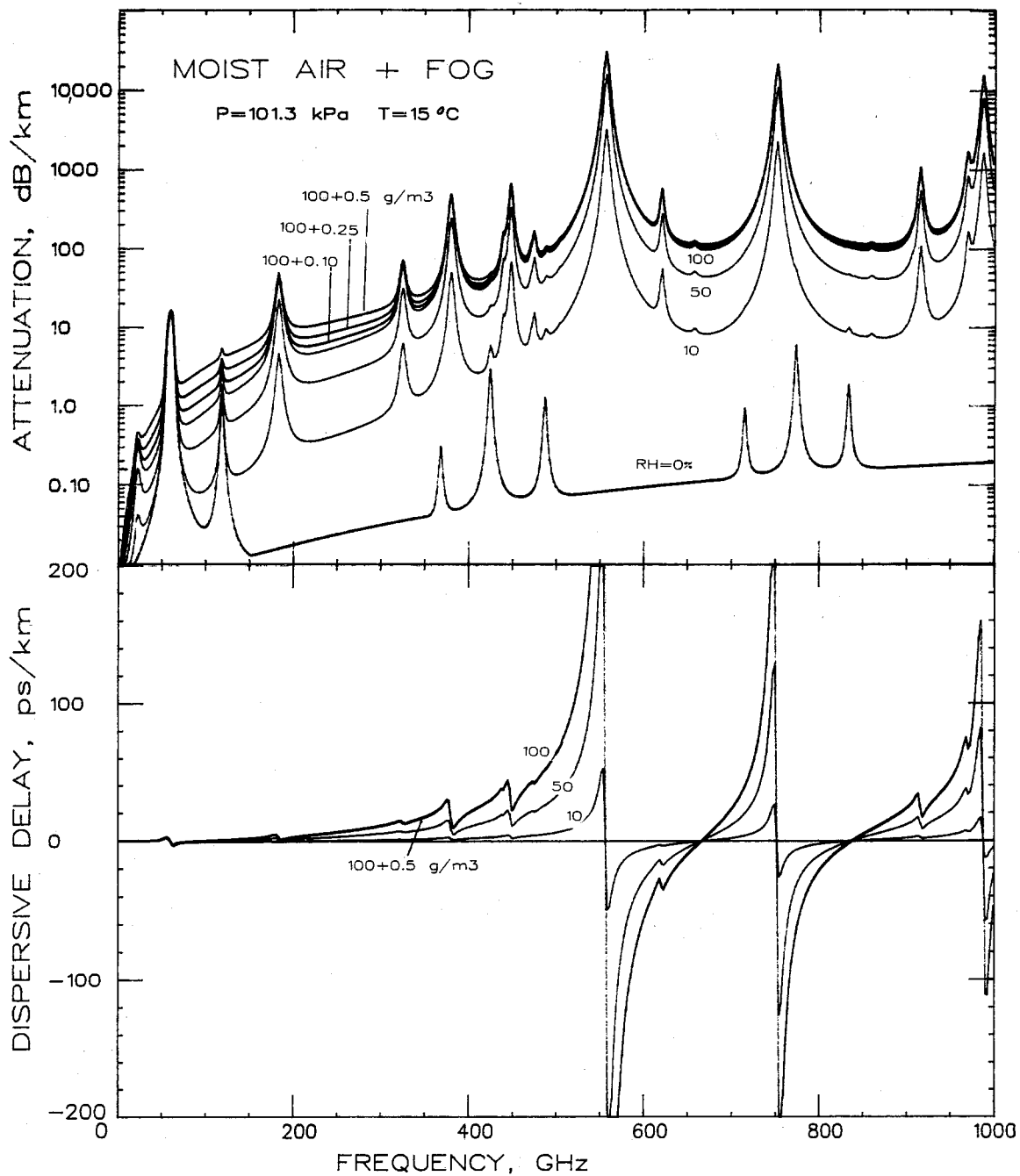


Figure 11. Attenuation  $\alpha$  and delay  $\beta$  rates for three fog events ( $w = 0.10, 0.25, \text{ and } 0.5 \text{ g/m}^3$ ) added to a saturated air (RH=100%) sea level condition. Also shown are dry air (0% RH) and moist air (50% RH) characteristics: (a)  $f = 1\text{-}1000 \text{ GHz}$ ,

(b)

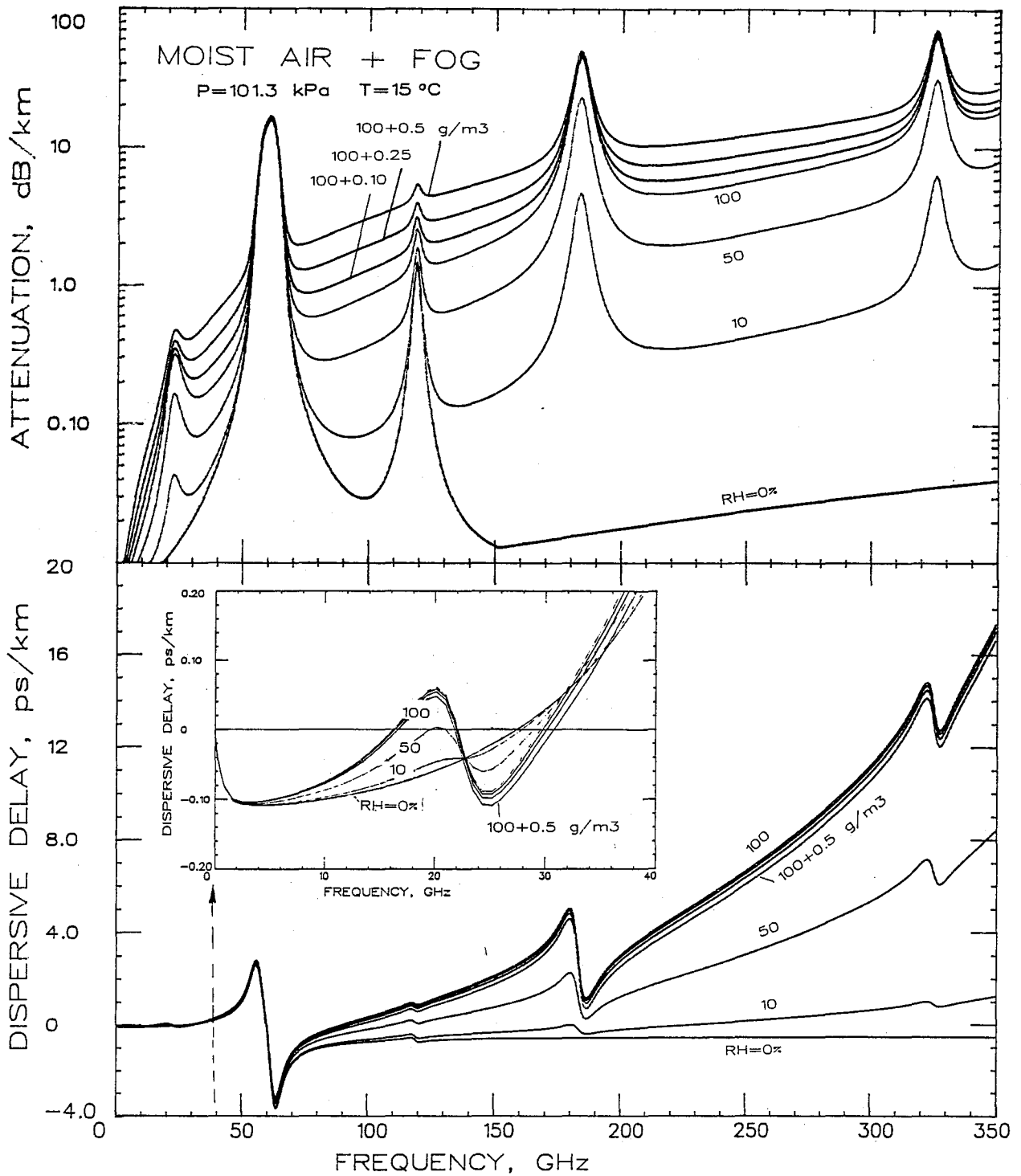


Figure 11. continued: (b)  $f = 1-350$  GHz and  $f = 0-40$  GHz (insert).

for RH parameterization exceeding saturation are not available. Both absolute humidity ( $v$ ) and suspended haze droplet concentration ( $w_A$ ) can be expressed in terms of RH variability. Absolute ( $v$ ) and relative (RH) humidity are inter-related through the ambient temperature  $T$ .

Sulfates are the major RH-active ingredient of both urban and rural aerosols; so is sodium chloride for maritime species. The atmosphere is never free from HAE, with greatest concentrations near the surface and scale heights on the order of 1 km. Above RH = 90%, suspended water droplets have developed carrying the HAE essence in solutions. Average values of  $w_A$  lie between 0.01 and 1 mg/m<sup>3</sup>. The humidity parameterization in MPM is demonstrated by the examples given in Figures 12 and 13.

Pressure variability comes into play when modeling height dependencies. Cumulative calculations of  $\alpha/\beta$  for a slanted radio path through the neutral atmosphere (e.g., ground-to-satellite) encounter pressures,  $P = 100$  to 0 kPa, which narrows the molecular absorption lines until they vanish altogether. Pressure-, Zeeman-, and Doppler-broadening [(A-11)] have to be considered over the height range 0 to 90 km. Another need for a formulation of pressure profiles arises from spectroscopic studies applying pressure-scanning techniques. A simulation of laboratory measurements discussed in Section 2.3 is exhibited in Figure 14.

#### 4. EXPERIMENTAL-VERSUS-MODEL (MPM) DATA

Corroborative experimental data of sufficient quality to scrutinize MPM predictions are scarce. Reliability, precision, and limited scope of supporting meteorological data often compromise the accuracy of results deduced from field observations. Generally, laboratory experiments are more accurate by simulating controlled electromagnetic and atmospheric conditions crucial to validate a specific model aspect. In this manner, contributions from water vapor lines (22 and 183 GHz) and from oxygen lines (48 to 70, 119 GHz) have been evaluated [1], [4], [10], [11], [16]. Theoretical refinements are motivated to improve the interpretation of empirical laboratory data by establishing a connection to the physics of the problem. For example, a set of our unpublished dispersion ( $N'$ ) results on dry air, taken during 1976 between 53.6 and 63.6 GHz, provided reference data for an elaborate reformulation of interference coefficients that describe the 60 GHz O<sub>2</sub> bandshape [10]. The new

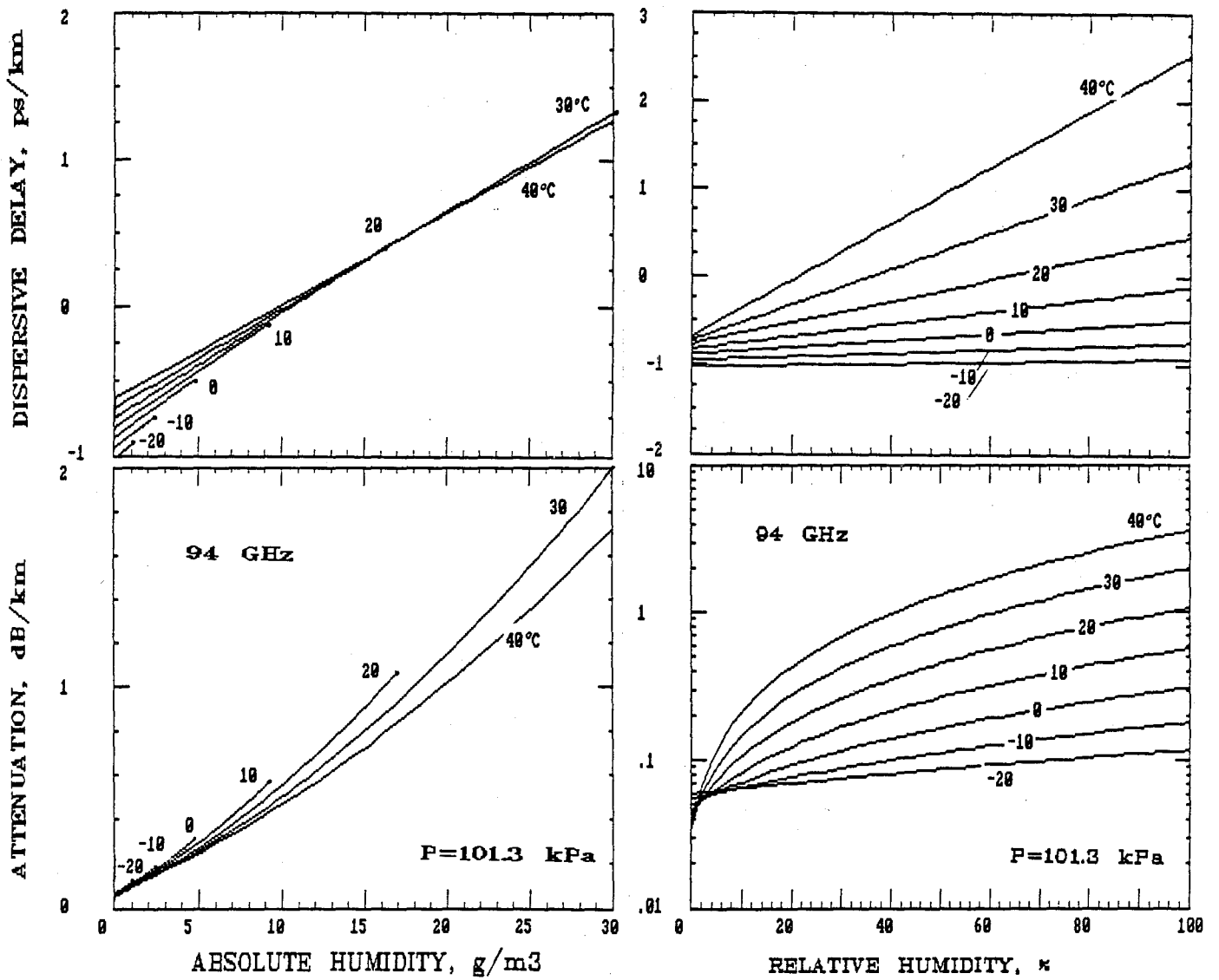


Figure 12. Absolute ( $\alpha$ ) and relative (RH) humidity dependence of attenuation  $\alpha$  and delay  $\beta$  at  $f = 94$  GHz for various sea level conditions ( $P = 101.3$  kPa and  $T = -20$  to  $40^\circ\text{C}$ ).

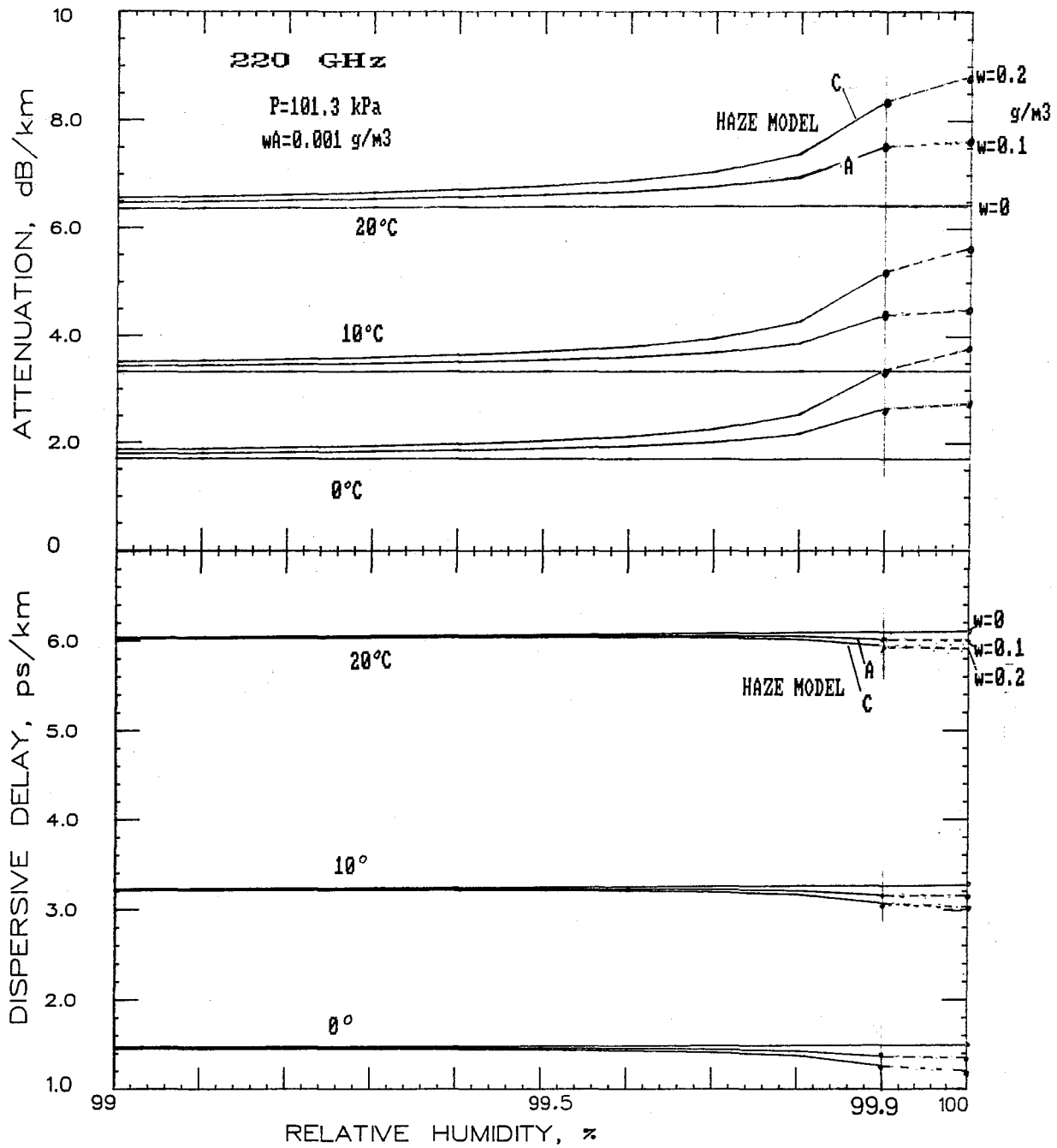


Figure 13. Two haze cases (A:1 mg/m<sup>3</sup> and C:1 mg/m<sup>3</sup>) for prefog (RH = 99-99.9%) and fog (w=0.1 and 0.2 g/m<sup>3</sup>) conditions at three temperatures (0, 10, 20°C) displaying the associated attenuation  $\alpha$  and delay  $\beta$  rates at  $f = 220 \text{ GHz}$ .

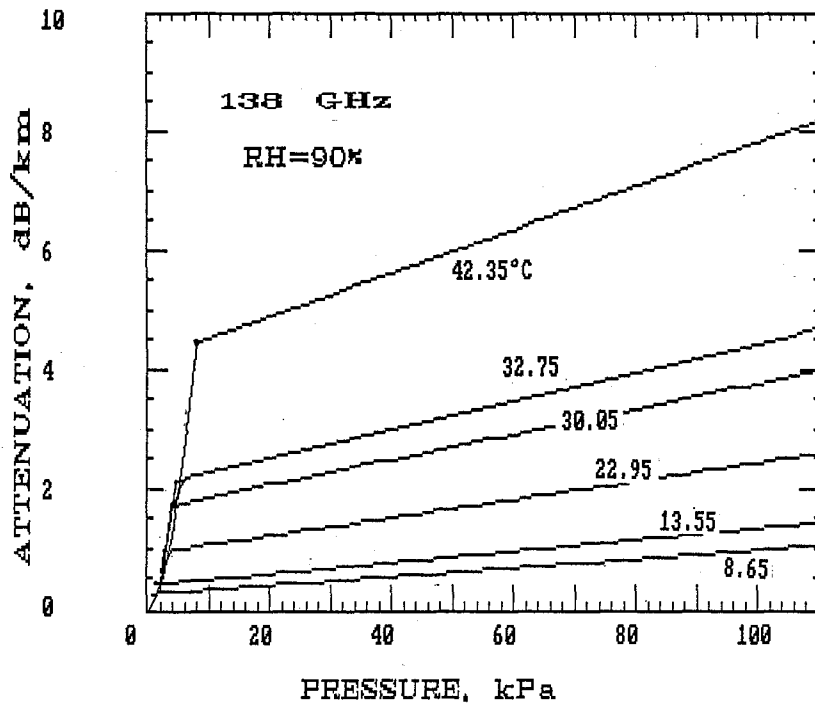
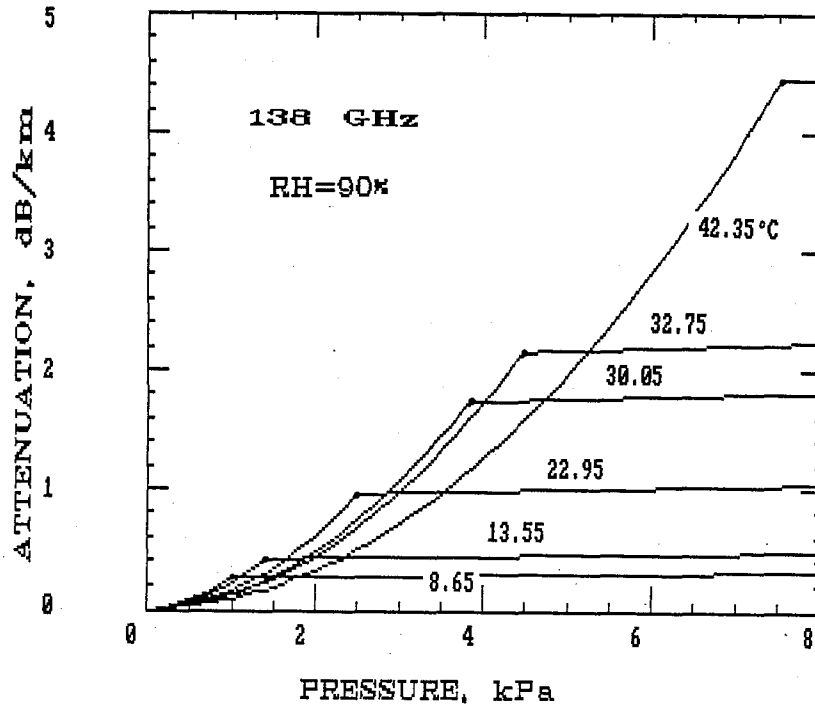


Figure 14. Pressure profiles at  $f = 138$  GHz simulating the laboratory attenuation measurements presented in Section 2.3.

coefficients  $a_5$  (see page 66) were adapted for MPM, and Table 5 demonstrates the degree of agreement.

#### 4.1 Laboratory Measurements

The results on moist air attenuation at 138 GHz [i.e., (5), (8)] provided clues to a formulation of an empirical MPM water vapor continuum. Data from other researchers were evaluated to check if the assumptions of (10) held up at different frequencies. Water vapor attenuation at frequencies between 330 and 430 GHz is compared with MPM predictions in Figure 15. The data were available in graphic form and had to be digitized by us. Considering the many difficulties that plague absolute calibrations, a comparison of model vs. experiment is encouraging. No anomalous absorption features have been uncovered.

Two laboratory studies of the 183-GHz water vapor line have been reported by a French group [11], [17]. We adapted the width results [11] for the line table of MPM. A detailed analysis of temperature-dependent wing data [17] is given in Table 6. Equation (5) was applied to reduce both experimental and MPM data for an intercomparison. At +1 GHz from the line center, the attenuation rate for pure water-vapor shows a discrepancy of 21 percent. The origin of such disagreement has to be attributed to the 183-GHz line broadening formulation but not to the rather small contribution from the continuum.

#### 4.2 Field Measurements

Ultimately, it is up to field experiments to garner realistic evidence in support of model predictions. When conducted with care at different locations under a variety of natural conditions, such experiments prove to be quite costly.

Data from ITS field studies on the propagation of millimeter waves were evaluated for water-vapor attenuation rates at 96.1 GHz [18], [19]. Clear air data and MPM predictions are in close agreement, allowing for the temperature dependence, as demonstrated in Figure 16. The mission of these experiments was to establish a data base for 11.4 to 96.1 GHz propagation in a humid climate (Huntsville, AL, April-August 1986). A similar comparison was not so favorable for a set of data displayed in Figure 17. The results were obtained over a 1.5 km line-of-sight path in the Soviet Union at subfreezing



Table 5. Measured (EXP) and Predicted (MPM) Dispersion in Dry Air at 300 K  
(Interference Coefficients from Rosenkranz [10])

Nearby Line	Frequency GHz	Dispersion $N'(f)$ EXP   MPM p = 53.3 kPa ppm		Frequency GHz	Dispersion $N'(f)$ EXP   MPM p = 80.0 kPa ppm	
		25-	53.588		0.30	0.300
23-	54.123	0.35	0.338	54.119	0.50	0.490
19-	55.214	0.40	0.407	55.210	0.58	0.576
17-	55.776	0.42	0.421	55.772	0.60	0.589
15-	56.356	0.41	0.398	56.352	0.59	0.565
13-	56.960	0.38	0.350	56.956	0.45	0.502
3+	58.439	0.19	0.174	58.435	0.26	0.253
7-	59.156	0.08	0.076	59.152	0.12	0.110
5+	59.583	0.03	0.027	59.579	0.03	0.032
5-	60.296	-0.075	-0.084	60.292	-0.11	-0.134
7+	60.425	-0.135	-0.122	60.421	-0.17	-0.170
9+	61.141	-0.275	-0.252	61.136	-0.383	-0.361
11+	61.790	-0.335	-0.342	61.785	-0.510	-0.522
13+	62.400	-0.480	-0.475	62.396	-0.685	-0.679
3-	62.475	-0.510	-0.495	62.471	-0.720	-0.705
15+	62.987	-0.590	-0.578	62.983	-0.80	-0.800
17+	63.558	-0.610	-0.589	63.554	-0.841	-0.831

Table 6. Comparison between MPM-Predicted and Experimental Attenuation for Water Vapor (e) and Moist Air (P = e<sub>1</sub> + p) in the Wing Region of the H<sub>2</sub>O Line Centered at  $\nu_0 = 183.310$  GHz

f, GHz		$\nu_0 + 3.0$			$\nu_0 + 1.0$			$\nu_0 + 0.4$		
<u>MPM - PREDICTIONS</u>										
	e <sub>1</sub>	1.766kPa (13.25 torr)			1.059kPa (7.94 torr)			0.529kPa (3.97 torr)		
	$\frac{T}{K}$	Lines	Cont.	Total	Lines	Cont.	Total	Lines	Cont.	Total
$\alpha$ , dB/km	310	3.66	0.53	4.19	11.35	0.19	11.54	17.37	0.05	17.41
	300	4.17	0.70	4.87	12.90	0.25	13.15	19.73	0.06	19.79
	290	4.76	0.95	5.71	14.17	0.33	15.05	22.49	0.08	22.58
	P	100kPa (750 torr)			100kPa (750 torr)			100kPa (750 torr)		
$\alpha$ , dB/km	310	21.52	1.83	23.52	21.39	0.95	22.52	11.66	0.43	12.27
	300	23.59	2.07	25.86	23.10	1.06	24.35	12.57	0.47	13.24
	290	25.92	2.40	28.53	25.00	1.19	26.41	13.58	0.51	14.31

DATA REDUCTION: MPM-vs-EXPERIMENT

		<u>MPM</u>	<u>EXP*</u>	$\frac{X}{M}$ %	<u>MPM</u>	<u>EXP*</u>	$\frac{X}{M}$ %	<u>MPM</u>	<u>EXP*</u>	$\frac{X}{M}$ %
k <sub>s</sub>	300	1.56	1.67	7.1	11.72	14.2	21.2	70.56	75.3	6.7
x <sub>s</sub>	-	4.56	4.1	-10.1	3.99	3.9	-2.3	3.88	3.5	-9.8
k <sub>f</sub>	300	0.121	0.136†	12.4	0.107	-			N.A.	
x <sub>f</sub>	-	2.48	2.7	8.9	1.96	-			N.A.	
m	300	0.0776	0.0814	4.9	0.0913	-			N.A.	

\*Reference [17],

†N<sub>2</sub>-result reduced by 0.907.

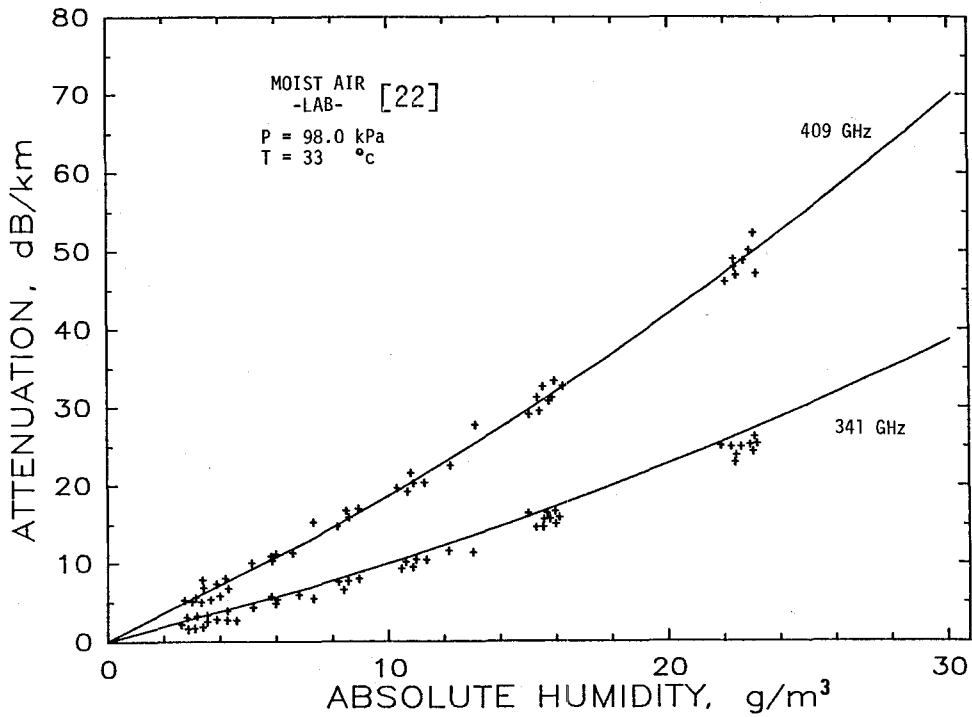
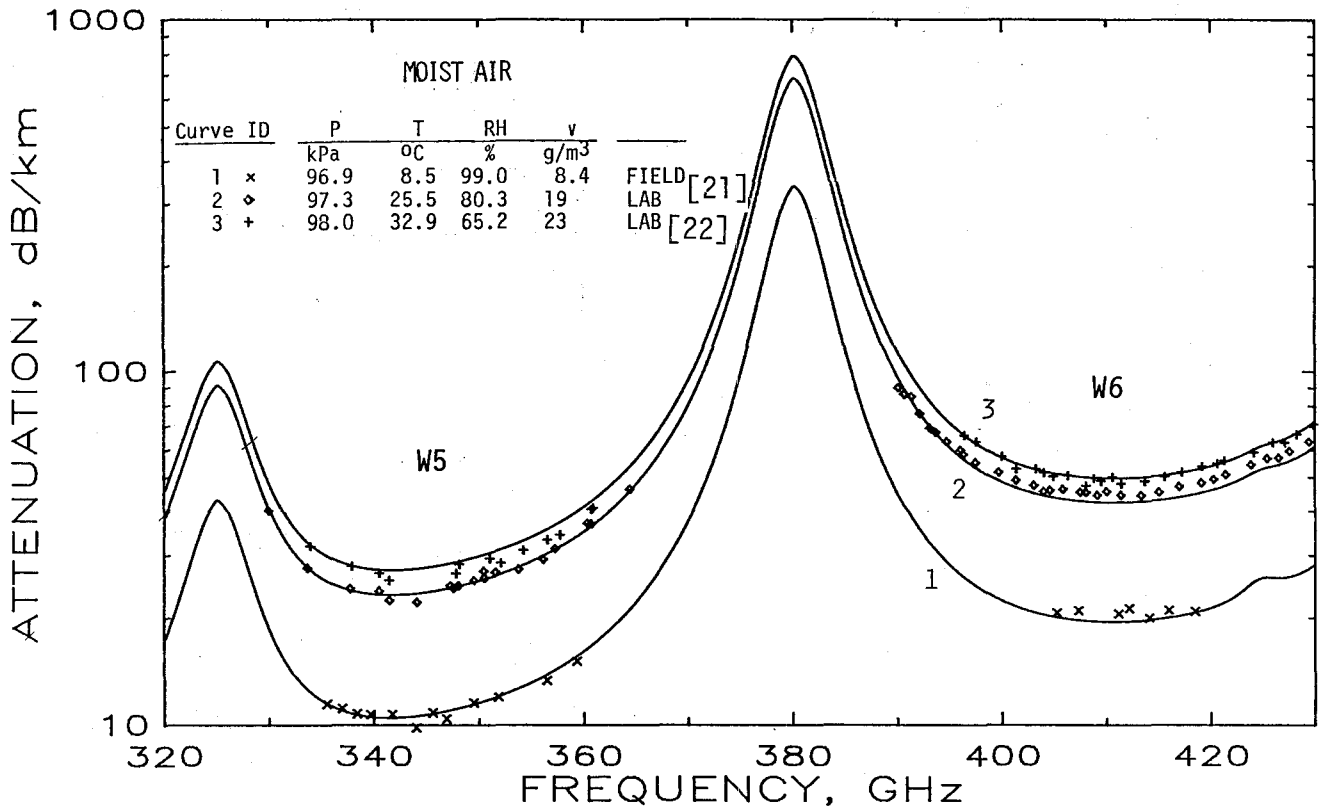


Figure 15. Moist air attenuation  $\alpha(f)$  across the atmospheric window ranges W5 and W6 (320 to 430 GHz) at temperatures 8.5, 25.5, and 32.9°C: data points [21], [22]; solid lines, MPM.

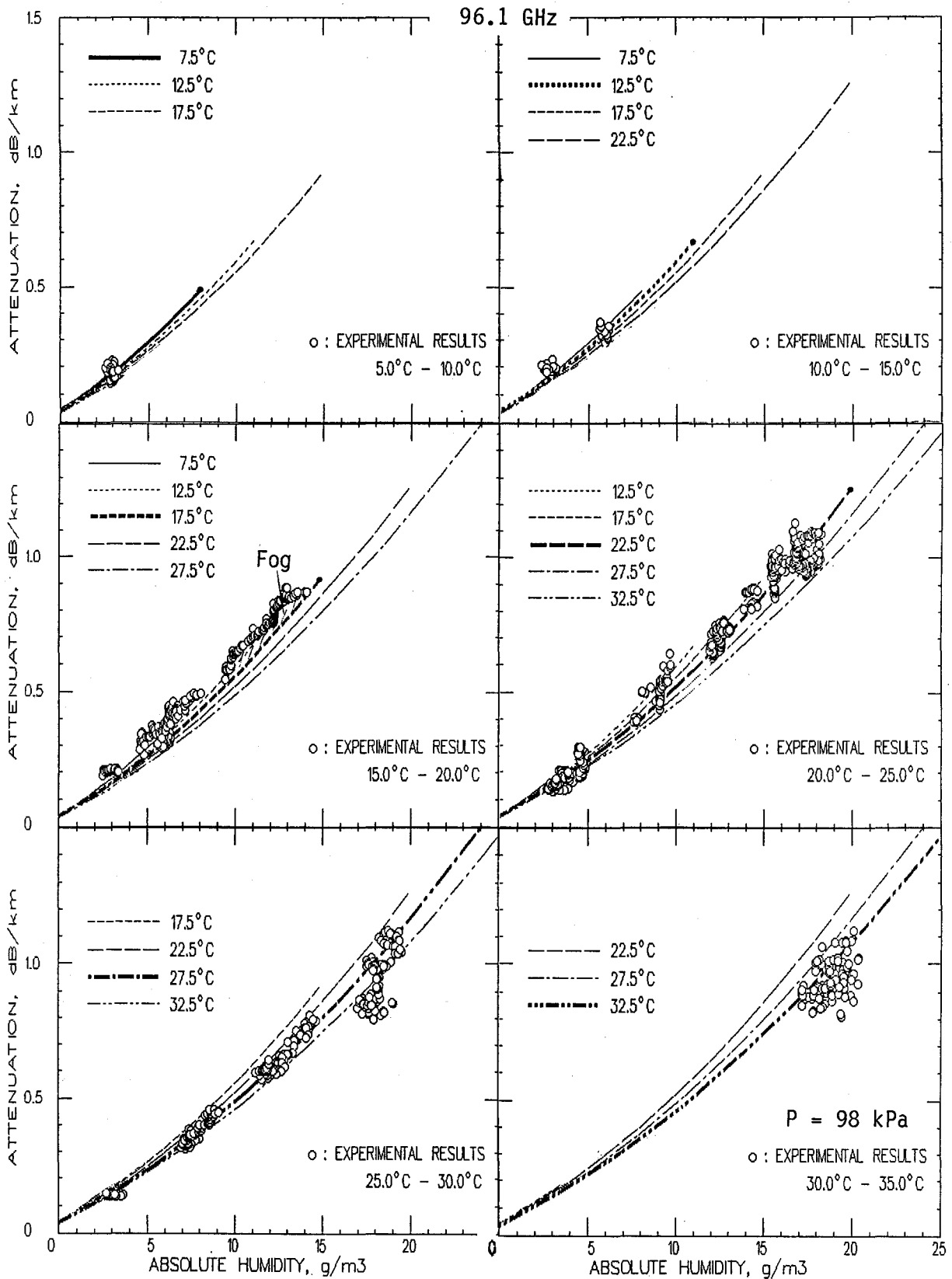


Figure 16. Moist air attenuation  $\alpha(v)$  measured at 96.1 GHz over a 21.4 km line-of-sight path located in Huntsville, AL ( $h \approx 0.3$  km) for six temperature groups between 2.5 and 37.5°C [19] data points are 5-min averages for 4.5 days (5/4-6, 8/15-16/1986); solid lines, MPM.

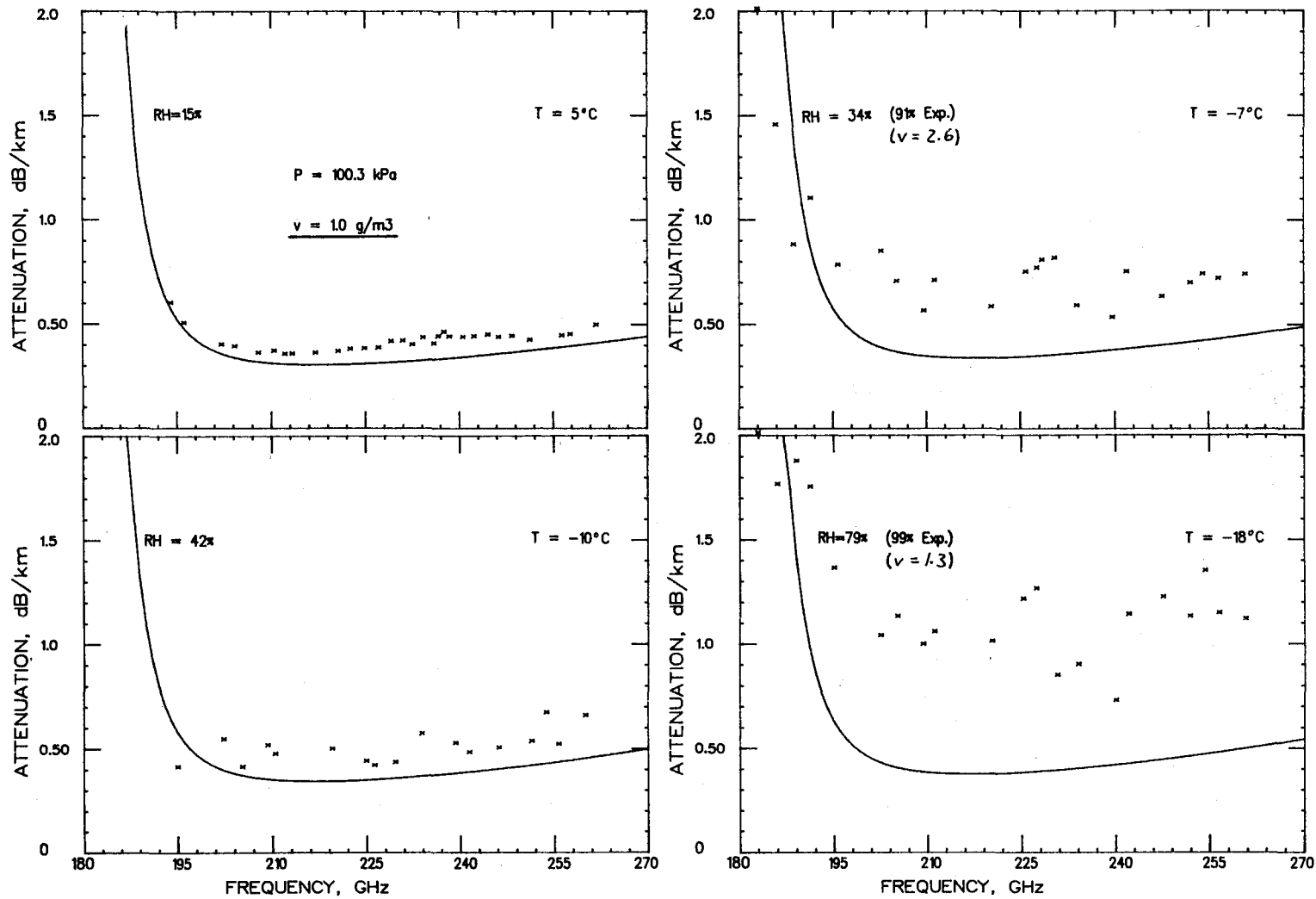


Figure 17. Water vapor attenuation rates  $\alpha(v)$  across the atmospheric window range W4 at four temperatures, 5, -7, -10, and  $-18^\circ\text{C}$ : data points [20]; solid lines, MPM.

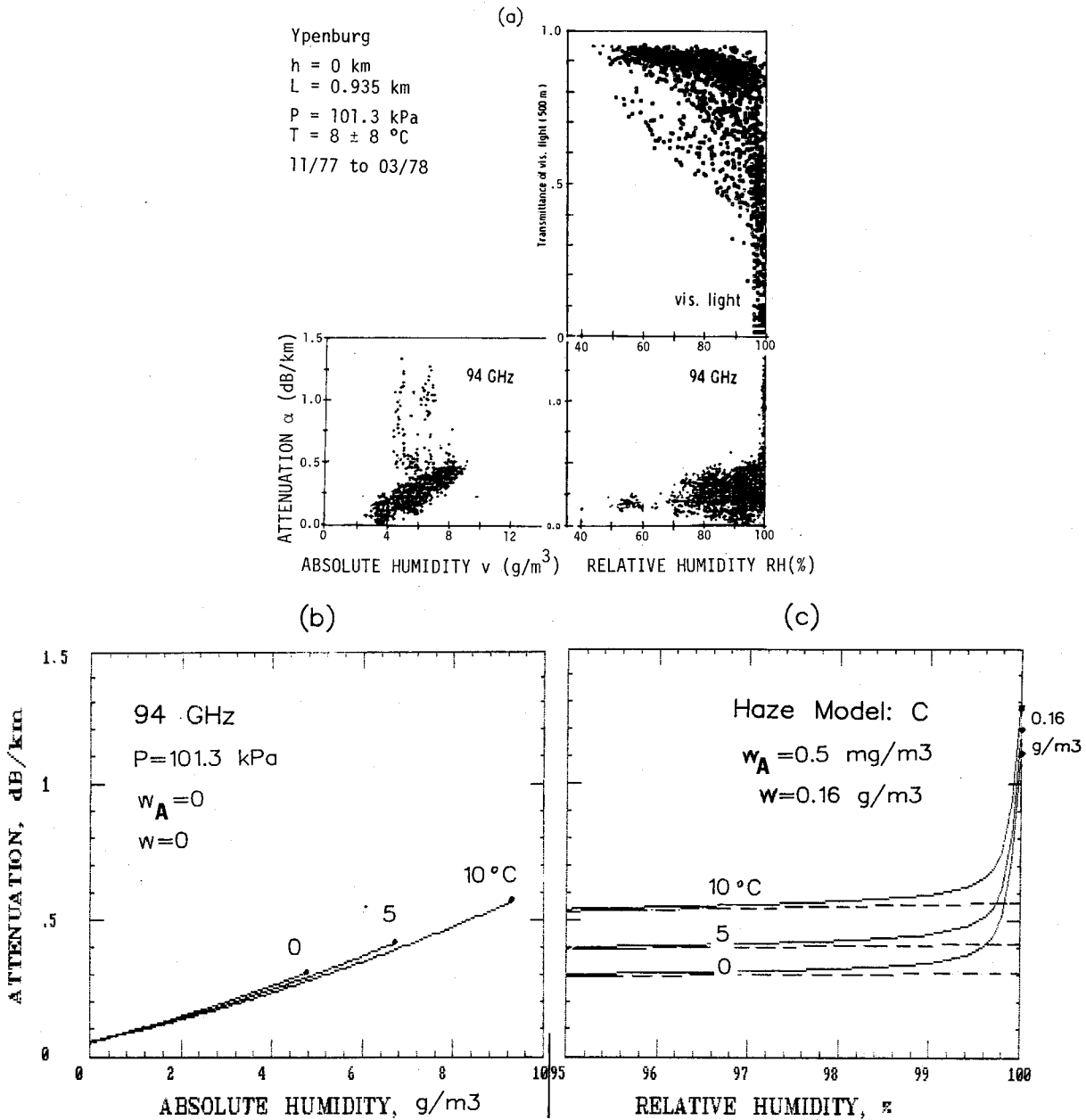


Figure 18. Terrestrial path attenuation at 94 GHz and  $0.65 \mu\text{m}$  (visible light) under nonprecipitating conditions as a function of absolute ( $v$ ) and relative (RH) humidity [3]: (a) data points, 5-min averages taken every 30 min during a period of 4 months [23]; (b) MPM simulation of (a) for absolute humidity; (c) MPM simulation of (a) over the range, RH = 95 to 100%, including haze model C.

temperatures for frequencies between 192 and 260 GHz [20]. Experimental uncertainties are not discussed, the extreme environmental conditions may have played a role. On the other hand, 335 - 420 GHz field data (included in Figure 15), that were reported by another group from the Soviet Union [21], [22] agree remarkably well with MPM predictions.

Attenuation data at 94 GHz have been recorded in a coastal region of the Netherlands [23]. Data, when presented in Figure 18 versus absolute humidity  $v$ , display significant random excess attenuation over MPM predictions. The same data plotted versus RH places all excess attenuation at  $RH > 98\%$ . Haze and fog conditions probably were present as evident from optical transmission data. The highest excess of 0.8 dB/km requires  $w \approx 0.16 \text{ g/m}^3$ , a value typical for heavy fog.

Figure 19 presents atmospheric noise temperatures measured against zenith at two different sites simultaneously at 10, 33, and 90 GHz [24]. Predictions with the MPM radio path program reproduce the frequency correlations quite correctly, which tends to confirm the  $f^2$  assumption made for  $\text{H}_2\text{O}$  continuum absorption (10). In addition, model data set a limit for total precipitable water vapor  $V[\text{mm}]$  carried by the air mass. Noise exceeding this limit probably originates from suspended droplets. Data trends stemming from differences in the  $f$ -dependence of moist air and SWD absorption support such assumption.

## 5. CONCLUSIONS

Radio properties of the atmosphere are both a barrier and a boon to applications in the 10-1000 GHz spectral range. The first part of this report gave a somewhat detailed description of a laboratory experiment that had to apply latest advances in digital electronics and cryogenic detection to derive at 138 GHz two attenuation coefficients,  $k_s$  and  $k_f$  (8). At first sight, these two quantities describe the attenuation rate of moist air over a rather inconspicuous range from 0.1 to 10 dB/km; however, a more detailed analysis revealed the  $k$ -formulation provides conclusive evidence on temperature and pressure dependence of the water vapor continuum. Attaching an  $f^2$  dependence to the 138-GHz results turned a frequency limited ( $< 1 \text{ THz}$ ) propagation model into a useful tool capable of operating in frequency, humidity, and pressure domains of the atmosphere.

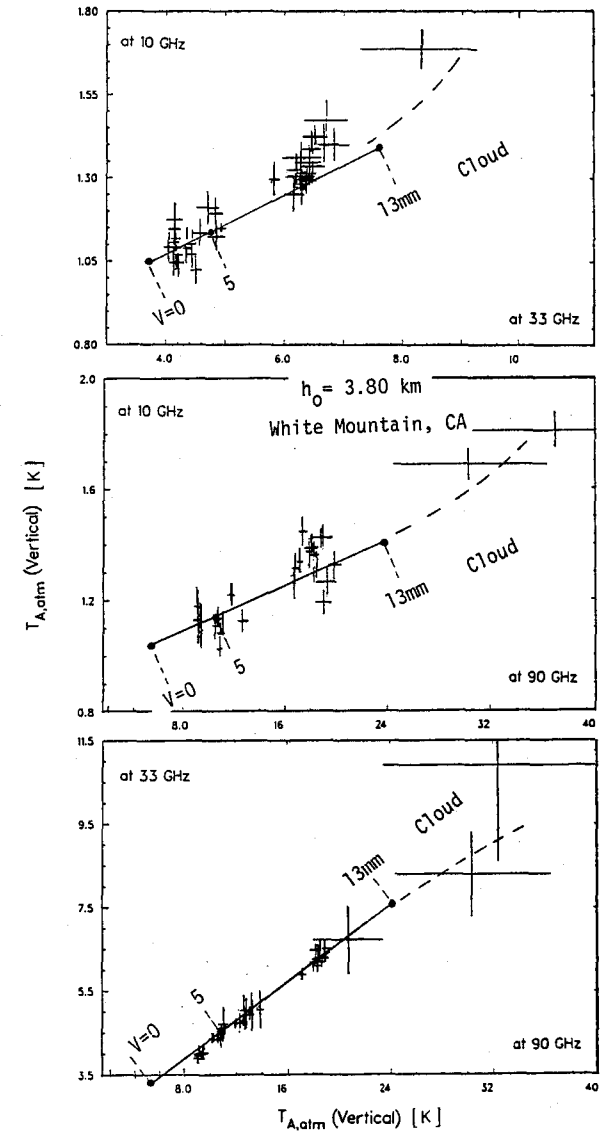
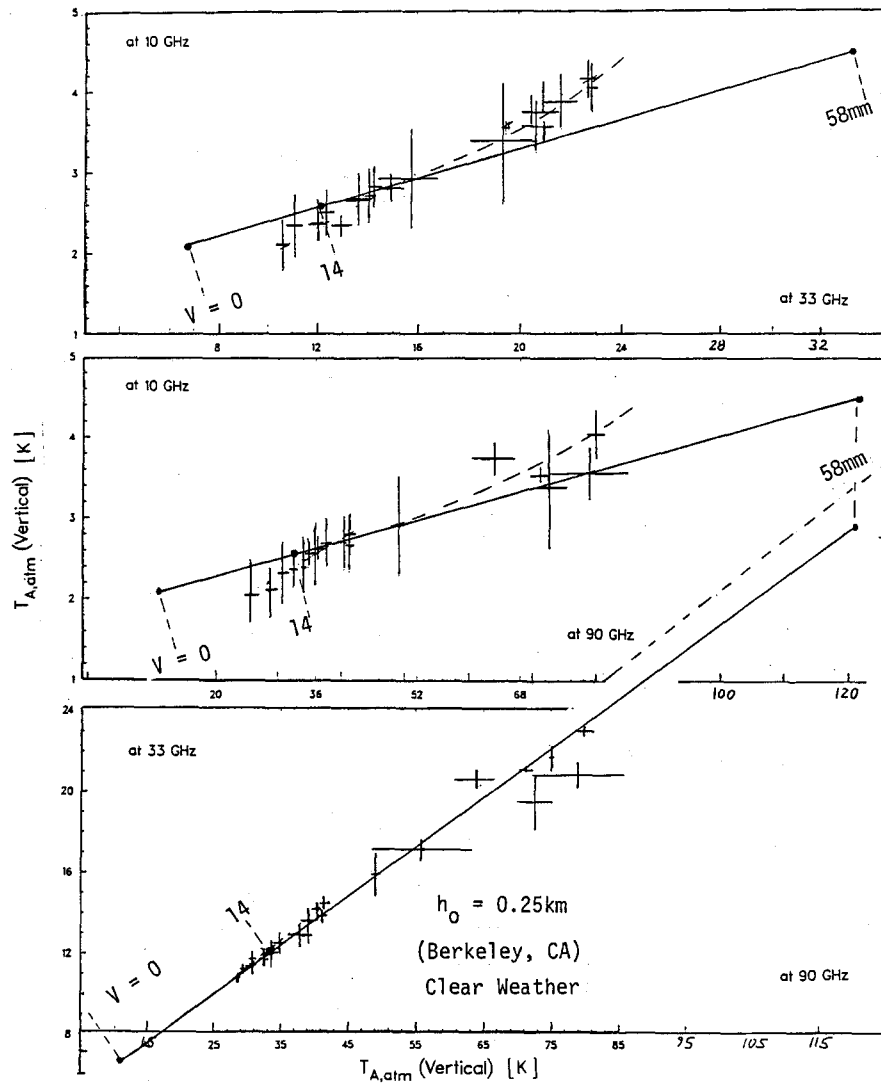


Figure 19. Correlated vertical atmospheric noise temperatures  $T_A$  at the frequency pairs 10/33, 10/90, and 33/90 GHz. Path-integrated water vapor is  $V = \int v dh$  mm. The measurements were conducted from two sites located at height levels  $h_0 = 0.25$  and  $3.30$  km: data points [24]; solid lines, MPM with a mean July height profile (0-30 km) of P, T, RH for San Francisco, CA [3].



The report discussed details of contributions to modeling atmospheric MMW properties, foremost the attenuation calibration of MPM employing new laboratory results on moist air. Water vapor continuum absorption and, above RH = 90%, droplet attenuation are both affected by relative humidity RH. For haze formation, the range up to RH = 99.9% was modeled. So far, in fog and cloud situations, when RH exceeds 100 percent, values for  $w$  cannot be model-generated from the atmospheric water vapor content.

The code MPM was readily accepted by radio scientists and engineers. About 90 requests for copies of MPM have been honored since January 1986. Quotes from received comments were encouraging: "MPM proved of considerable value," -- "documentation is about the best I have ever seen," -- "technical flow, model development and general visibility for application efforts is superior," etc. The Microwave Group of the International Radiation Commission largely adopted MPM as atmospheric transmission code [25].

Although MPM was found capable of predicting atmospheric NMMW propagation limitations, several shortcomings still exist. They are, for example, the missing confirmation for a physical basis of water vapor continuum absorption (e.g., [7], [13]) dominating transmission in atmospheric window ranges centered at 90, 140, 220, 340 GHz and higher; needed measurements of spectroscopic parameters (i.e., shape, strength, width and shift) for spectral lines of the main absorbers ( $O_2$  and  $H_2O$ ) over the full atmospheric temperature range (300-200 K); and a lack for reliable subfreezing transmission data to clarify the problems that are indicated by Figure 17. Further parametric (frequency, pressure, humidity, temperature, gas composition such as  $H_2O + AIR$ ) studies are proposed to realize the benefits obtainable from the high-humidity performance of the spectrometer that has been perfected to overcome a great deal of difficulties. Pressure-broadening of the 183-GHz line uniquely identifies monomer behavior (see Table 6). A comparative study of wing ( $f_0 \pm 6$  GHz) and far-wing (220 GHz) responses to  $T$  and  $v(RH)$  variations would allow an apportioning of local line (known) and continuum (unknown) contributions.

## 6. ACKNOWLEDGMENTS

The authors wish to thank J. P. Stricklen for his skillful programing efforts, and Dr. T. Manabe for a most beneficial cooperation.

The work was supported in part by the Naval Ocean Systems Center (Ref: RA35 G80), and the experimental portion (Section 2) by the U. S. Army Research Office under Contract ARO 107-86.

## 7. REFERENCES

- [1] Liebe, H. J. (1985), An updated model for millimeter wave propagation in moist air, *Radio Science* 20, no. 5, 1069-1089.
- [2] Hopponen, J. and H. Liebe (1986), A computational model for the simulation of millimeter-wave propagation through the clear atmosphere, NTIA Report 86-204, October, 32 pp. (NTIS Order No. PB 87-131173/AS).
- [3] Liebe, H. J. (1987), A contribution to modeling atmospheric millimeter-wave properties, *FREQUENZ (Telecom. J.)* 41, no. 1/2, pp. 31-36.
- [4] Read, W., K. Hillig II, E. Cohen, and H. Pickett (1987), The measurement of absolute absorption of millimeter radiation in gases: The absorption of CO and O<sub>2</sub>, *IEEE Transact. Ant. & Propagation*, submitted.
- [5] Liebe, H., V. Wolfe, and D. Howe (1984), Test of wall coatings for controlled moist air experiments, *Rev. Sci. Instr.* 55, no. 10, pp. 1702-1705.
- [6] Liebe, H. J. (1984), The atmospheric water vapor continuum below 300 GHz, *Int. J. Infrared & Millimeter Waves* 5, pp. 207-227.
- [7] Hinderling, J., M. Sigrist, and F. Kneubuehl (1987), Laser-photoacoustic spectroscopy of water-vapor continuum and line absorption in the 8 to 14  $\mu\text{m}$  atmospheric window, *Infrared Phys.* 27, no. 2, pp. 63-120.
- [8] Suck, S. H., A. E. Wetmore, T. S. Chen, and J. L. Kassner, Jr. (1982), Role of various water clusters in IR absorption in the 8-14- $\mu\text{m}$  window region, *Appl. Opt.* 21, no. 9, pp. 1610-1614.
- [9] Curtiss, L. A., D. J. Frurip, and M. Blander (1979), Studies of molecular association in H<sub>2</sub>O and D<sub>2</sub>O vapors by measurements of thermal conductivity, *J. Chem. Phys.* 71, no. 6, pp. 2703-2711.
- [10] Rosenkranz, P. W. (1987), Interference coefficients for overlapping oxygen lines in air, *J. Quant. Spectr. Radiat. Transfer*, in press.
- [11] Bauer, A., M. Godon, and B. Duterage (1985), Self- and air-broadened linewidth of the 183 GHz absorption in water vapor, *J. Quant. Spectr. Radiat. Transfer* 33, no. 2, pp. 167-175.
- [12] Hill, R. J. (1987), Absorption by the tails of the oxygen microwave resonances at atmospheric pressures, *IEEE Transact. Ant. & Propagation* AP-35, no. 2, pp. 198-204.
- [13] Rosenkranz, P. W. (1985, 1987), Pressure broadening of rotational bands. I. A statistical theory, *J. Chem. Phys.* 83, no. 12, pp. 6139-48; II. Water vapor from 300 to 1100  $\text{cm}^{-1}$ , *J. Chem. Phys.* 87, no. 1, pp. 163-170.
- [14] Liebe, H. J., T. Manabe, and J. P. Stricklen (1987), Millimeter-wave attenuation and delay for a fog event, *IEEE Digest: 12th Int. Conf. Infrared & Millimeter Waves*, Orlando, FL, December.

- [15] Manabe, T., H. J. Liebe, and G. A. Hufford (1987), Complex permittivity of water between 0 and 30 THz, IEEE Digest: 12th Int. Conf. Infrared & Millimeter Waves, Orlando, FL, December.
- [16] Liebe, H. J., and T. A. Dillon (1969), Accurate foreign-gas-broadening parameters of the 22-GHz H<sub>2</sub>O line from refraction spectroscopy, J. Chem. Phys. 50, no. 1, pp. 727-732.
- [17] Bauer, A., B. Duterage, and M. Godon (1986), Temperature dependence of water-vapor absorption in the wing of the 183 GHz line, J. Quant. Spectr. Radiat. Transfer 36, no. 4, pp. 307-318.
- [18] Liebe, H. J., K. Allen, G. Hand, R. Espeland, and E. Violette (1985), Millimeter-Wave Propagation in Moist Air: Model Versus Path Data, NTIA Report 85-171, March, 62 pp. (NTIS Order No. PB 85-208700).
- [19] Manabe, T., R. O. DeBolt, and H. J. Liebe (1987), Moist air attenuation at 96 GHz over a 21 km line-of-sight path, IEEE Digest: 12th Int. Conf. Infrared & Millimeter Waves, Orlando, FL, December.
- [20] Fedoseev, L. I., and L. M. Koukin (1984), Comparison of the results of summer and winter measurements of atmospheric water vapor absorption at wavelengths 1.5 to 1.55 mm, Int. J. Infrared and Millimeter Waves 5, no. 7, pp. 952-964.
- [21] Furashov, N. I., V. Y. Katkov, and V. Y. Ryadov (1984), On the anomalies of submillimeter absorption spectrum of atmospheric water vapor, Int. J. Infrared and Millimeter Waves 5, no. 7, pp. 971-981.
- [22] Furashov, N. I., and V. Y. Katkov (1985), Humidity dependence of the atmospheric absorption coefficient in the transparency windows centered and 0.88 and 0.73 mm, Int. J. Infrared and Millimeter Waves 6, no. 8, pp. 751-764.
- [23] Buys, J. H., and L. H. Janssen (1981), Comparison of simultaneous atmospheric attenuation measurements at visible light, mid-infrared (3-5 $\mu$ m) and millimeter waves (94 GHz), IEE Proc. 128, Pt. H., no. 3, pp. 131-136.
- [24] Costales, J. B., G. F. Smoot, C. Witebsky, G. DeAmici, and S. D. Friedman (1986), Simultaneous measurements of atmospheric emissions at 10, 33, and 90 GHz, Radio Science 21, no. 1, pp. 47-55.
- [25] Kuenzi, K. F., ed. (S. Clough, N. Grody, K. Kuenzi, H. Liebe, A. Neuendorffer, B. Read, P. Rosenkranz, and C. Warner; Contributors) (1987), Report of Microwave Group on ITRA-Intercomparison Campaign Workshop, University of Maryland, 86 pp., March.



## APPENDIX A

### THE REFRACTIVE INDEX OF THE NEUTRAL ATMOSPHERE FOR FREQUENCIES UP TO 1000 GHz

Hans J. Liebe

#### A.1. INTRODUCTION

Dry air and atmospheric water vapor are major millimeter-wave absorbers; so are suspended droplets (haze, fog, cloud) and precipitating water drops that emanate from the vapor phase. A practical model (designated program code: MPM) was formulated that simulates the refractive index  $\underline{n} = n' - jn''$  of the atmospheric propagation medium for frequencies up to 1000 GHz [1], [3]\*. The main purpose of the program is to express the electromagnetic properties of the neutral atmosphere in terms of available and/or measurable quantities.

The free propagation of a plane electromagnetic wave at frequency  $f$  and an initial field strength  $E_0$  in an isotropic gas medium over distance  $L$  is described by the complex transmission factor

$$\underline{\tau} \equiv E(L)/E_0 = \exp[-(2\pi f/c)(n'' + jn')L]$$

where  $n'(f)$  and  $n''(f)$  are frequency-dependent measures of delay and loss, and  $c$  is the speed of light in vacuum. Since the interaction with a neutral atmosphere is relatively weak, the refractive index is converted into a refractivity

$$\underline{N} = (\underline{n} - 1)10^6 \quad \text{ppm,}$$

in units of parts per million.

Refractivity  $N$  for moist air can be obtained, in principle, by a summation over all absorption features in a given volume element. In practice, various degrees of approximations are employed to reduce labor and computer time required, since the number of contributing spectral lines by the dominant absorbers (water vapor and oxygen) and by various trace gases (e.g.,  $O_3$ ) exceeds 10,000. The model MPM consists of local  $H_2O$  (30x) and  $O_2$  (48x) lines

---

\* [ ] See 7. REFERENCES in main text.

below 1 THz and an empirical approximation to the contributions by H<sub>2</sub>O lines above 1 THz. To complete the model, continuum spectra for dry air, suspended water droplets (haze, fog, cloud), and rain are added. The supporting spectroscopic data base contains more than 450 coefficients.

#### A.1.1 Features of Program MPM

A parametric program was developed (see Section A.2) that calculates the values of the complex refractivity

$$\underline{N} = N_0 + N'(f) - jN''(f) \quad \text{ppm}$$

or corresponding path-specific quantities of particular interest to radio engineering; i.e.,

refractive delay	$\beta_0$	ns/km,
dispersive delay	$\beta'(f)$	ps/km, and
attenuation	$\alpha(f)$	dB/km;

for atmospheric conditions as a function of the variables  $f$ ,  $P$ ,  $T$ ,  $RH$ ,  $w_A$  (A/B/C/D),  $w$ , and  $R$ , as listed in the scheme below:

Variable	Symbol	Validity Range	Medium
frequency	$f$	$\leq 1000$ GHz	
barometric pressure	$P$	120-0 kPa	Moist
temperature	$T$	- 50- + 50°C	Air
relative humidity	$RH$	0-100%	
haze model: code A, B, C, D (or combinations thereof) plus hygroscopic aerosol reference concentration	$w_A(80\%RH)$	$RH=80-99.9\%$ 0-1 mg/m <sup>3</sup>	Haze
suspended water droplet concentration	$w(100\%RH)$	0-10 g/m <sup>3</sup>	Fog, Cloud
rainfall rate	$R$	0-200 mm/h	Rain

The height range 30 to 100 km is treated approximately excluding the detailed O<sub>2</sub>-Zeeman effect and trace gas spectra (e.g., O<sub>3</sub>, CO, N<sub>2</sub>O, etc.).

### A.1.2 Physical Variables

The purpose of this section is to relate measurable variables to  $N$  model-specific variables, whereby the state of dry air is described by a partial air pressure  $p$  in kPa, a relative inverse temperature variable is  $\theta = 300/(273.15 + T)$  with  $T$  in °C, and relative humidity is given by

$$RH = (e/e_s)100 = (v/v_s)100 = 4.151 \times 10^{-9}(e/\theta^5)\exp(22.64\theta) \leq 100\%. \quad (A-1)$$

Equation (A-1) governs physical processes taking place in the atmosphere with respect to water vapor. Absolute ( $v$ ) and relative (RH) humidity are inter-related through

$$v = 1.739 \times 10^9 RH \cdot \theta^5 \exp(-22.64\theta) = 7.223 e \theta \text{ g/m}^3 \quad (A-2)$$

where  $e$  is the partial water vapor pressure in kPa as part of the total (barometric) pressure  $P = p + e$ .

Water vapor variability at sea level (e.g.,  $P = 101$  kPa,  $\theta = 1.016$  or  $22^\circ\text{C}$ ) is typically

	Dry	Normal	Humid	Saturated
$v$	1	10	17	$20\text{g/m}^3$
RH	5	50	85	100 %

Suspended hydrometeors are described by the liquid water concentration  $w$ , which relates approximately to optical ( $0.55 \mu\text{m}$ ) visibility  $U(\text{km})$ . A schematic categorization can be made by

	Haze	Fog	Stratus Cloud	Convective Cloud
$w \leq$	$10^{-2}$	$10^{-1}$	1	$5 \text{ g/m}^3$
$U \geq$	1.1	0.27	0.07	0.03 km

Another atmospheric ingredient is hygroscopic aerosol with a mass concentration  $w_A$  in  $\text{mg}/\text{m}^3$ . Solution droplets appear for  $\text{RH} > 80\%$ , and haze conditions develop as  $\text{RH}$  approaches 100 percent. The growing haze droplets can reach values ( $w < 0.1 \text{ g}/\text{m}^3$ ) sufficient to contribute to medium losses. Haze conditions are modeled by assuming that at the reference humidity,  $\text{RH} = 80\%$ , the concentration  $w_A(\text{RH}=80\%)$  is known. Any  $\text{RH}$ -dependent swelling/shrinking of  $w(\text{RH})$  up to  $\text{RH}=99.9\%$  is modeled by

$$w = w_A(C1-\text{RH})/C2(100-\text{RH}) = w_A g(\text{RH}), \quad (\text{A-3})$$

where  $g(\text{RH})$  is a growth function. The following values have been reported for  $C1, C2$ :

Case	Aerosol Species	C1	C2	$g(\text{RH}=99.9\%)$
A	Rural	117	1.87	91
B	Urban	128	2.41	117
C	Maritime	183	5.31	162
D	C + Strong Wind ( $>10 \text{ km}/\text{h}$ )	197	5.83	167

Average values of  $w_A$  for given stabilized climatic situations can be found in the literature. Typical values for  $w_A$  lie between  $0.01$  and  $0.5 \text{ mg}/\text{m}^3$  and the increase to  $w$  can be substantial as indicated by the maximum prefog values  $g(99.9\%)$ .

Precipitation originates as a statistical event within clouds suspended in saturated air. Its vertical distribution is separated into two regions by the height of the  $0^\circ\text{C}$  isotherm, which can vary between  $6 \text{ km}$  and ground level depending on season and latitude. The lower part is mostly liquid drops, and the upper region consists of frozen particles with occasional supercooled droplet loadings by strong updrafts.

Point rain rates  $R$  have proven useful in modeling rain-induced  $N$  effects. Rain rate can be related to percent time,  $t_R$ , a given value occurs over the period of an "average" year; to the effective rain cell extent  $L_R/L$ ; and to the instantaneous suspended liquid water concentration,

$$w_R = m R \quad \text{g}/\text{m}^3.$$

In terms of these variables, an hypothetical local rain may be classified as follows (horizontal path,  $L = 10 \text{ km}$ ):



	Drizzle	Steady	Heavy	Downpour	Cloudburst	
R	1	5	20	100	250	mm/h
$t_R$	2	0.5	0.07	0.001	0.0001	% per yr
$L_R/L$	1	1	0.7	0.35	0.2	
m	0.1	0.07	0.05	0.04	0.04	

These numbers may differ substantially for given locations.

The simple coefficient scheme reveals some fundamentals of rain. Changes in the factor m indicate rain rate-dependent characteristics of drop-size distributions. Widespread steady rain occurs more uniformly and favors small drop sizes ( $\leq 1$  mm diameter) that stay in the air longer. Heavy showers are more localized, favor larger drops, and occur less frequently.

#### A.2. MODEL FOR COMPLEX REFRACTIVITY

The complex refractivity in N units (i.e., ppm =  $10^{-6}$ )

$$\underline{N}(f; P/T/RH, w_A/w, R) = N_0 + N'(f) - jN''(f) \quad \text{ppm} \quad (\text{A-4})$$

is a macroscopic measure of interactions between radiation and absorbers. The refractivity consists of a frequency-independent term  $N_0$  plus various spectra of refractive dispersion  $N'(f)$  and absorption  $N''(f)$ .

In radio engineering it is customary to express the imaginary part of (A-4) as power attenuation  $\alpha$  and the real part as group delay  $\beta$  (with reference to vacuum) as follows:

$$\alpha = 0.1820 f N''(f) \quad \text{dB/km} \quad (\text{A-5a})$$

and

$$\beta = 3.336[N_0 + N'(f)] \quad \text{ps/km}, \quad (\text{A-5b})$$

where frequency  $f$  is in gigahertz (GHz) throughout.

Radio refractivity is defined to be  $\underline{N} = N_0$  at  $f = 0$  and consists of four terms; i.e.,

$$N_0 = N_p^0 + N_e^0 + N_w^0 + N_R^0.$$

The individual contributions are described for dry air by

$$N_p^0 = 2.588 p \theta, \quad (A-6)$$

for water vapor by

$$N_e^0 = 2.39 e \theta + 41.6 e \theta^2, \quad (A-7)$$

for the SWD term  $N_w^0$  by (A-16c), and for the rain term  $N_R^0$  by (A-18c). The results (A-6) and (A-7) have been determined experimentally at microwave frequencies where dispersive contributions  $N(f)$  are negligible.

A calculation of the spectrum  $\underline{N}(f)$  for frequencies up to 1000 GHz consists of several additive parts:

- resonance information of  $n_a=48$  oxygen lines and  $n_b=30$  water vapor lines
- nonresonant  $O_2$  and pressure-induced  $N_2$  absorption ( $\underline{N}_p$ )
- continuum absorption from far-wing contributions of strong  $H_2O$  lines falling in the frequency range 1-30 THz ( $\underline{N}_e$ )
- suspended water droplet SWD term ( $\underline{N}_w$ )
- rain-effect approximation ( $\underline{N}_R$ )

Absorption and dispersion spectra are obtained from line-by-line calculations plus various continuum spectra  $\underline{N}_{p,e,w,R}$  according to

$$N''(f) = \sum_{i=1}^{n_a} (SF'')_i + N_p'' + \sum_{i=1}^{n_b} (SF'')_i + N_e'' + N_w'' + N_R'' \quad (A-8a)$$

Dry Air      •Water Vapor      •SWD   •Rain

$$N'(f) = \sum_{i=1}^{n_a} (SF')_i + N_p' + \sum_{i=1}^{n_b} (SF')_i + N_e' + N_w' + N_R' \quad (A-8b)$$

where  $S$  is the line strength in kilohertz, and  $F'$  and  $F''$  are real and imaginary parts of a line shape function in  $\text{GHz}^{-1}$ .

### A.2.1 Local Line Absorption and Dispersion

The Van Vleck-Weisskopf function is modified to describe to first-order line overlap effects, which leads to local absorption and dispersion line profiles in the form

$$F''(f) = \left[ \frac{1}{X} + \frac{1}{Y} - \frac{\delta}{Y} \left( \frac{v_0 - f}{X} + \frac{v_0 + f}{Y} \right) \right] A \quad (\text{A-9a})$$

and

$$F'(f) = \frac{Z - f}{X} + \frac{Z + f}{Y} - \frac{2}{v_0} + \delta \left( \frac{1}{X} - \frac{1}{Y} \right) A \quad (\text{A-9b})$$

with the abbreviations  $A = \gamma f / v_0$ ,

$$X = (v_0 - f)^2 + \gamma^2, \quad Y = (v_0 + f)^2 + \gamma^2, \quad Z = (v_0^2 + \gamma^2) / v_0.$$

Standard line shapes  $F''(f)$ , including the modified Van Vleck-Weisskopf function (A-9), predict in frequency regions of local line dominance about the same results for  $N''(f)$  as long as  $F''(f)$  exceeds by 0.1% the peak value at  $f = v_0$ . Far-wing contributions of smaller magnitude depend very much upon the chosen shape function. For  $f \rightarrow \infty$ , the wing response of (A-9a) becomes non-physical and is cut off; i.e.,  $F'' = 0$  when  $f \geq (v_0 + 40\gamma)$ . So far, no line shape has been confirmed that predicts absorption intensities over ranges  $10^{-3}$  to  $< 10^{-6}$  of  $F''(v_0)$ . Far-wing contributions from strong infrared water vapor lines, where  $\alpha(v_0)$  can exceed  $10^6$  dB/km, are accounted for summarily by empirical correction [see (A-15a)].

The line parameters are calculated by the expressions below:

Symbol	$O_2$ Lines in Air	$H_2O$ Lines in Air	Eq.
$S$ , kHz	$a_1 p \theta^3 \exp[a_2(1-\theta)]$	$b_1 e \theta^{3.5} \exp[b_2(1-\theta)]$	(A-10)
$\gamma$ , GHz	$a_3(p\theta^{(0.8-a_4)} + 1.1e\theta)$	$b_3(p\theta^{0.6} + 4.80e\theta^{1.1})$	(A-11)
$\delta$	$a_5 p \theta^{a_6}$	0	(A-12)

Line center frequencies  $v_0$  and the spectroscopic coefficients  $a_1$  ( $\geq 10^{-7}$  Hz/Pa) to  $a_6$  and  $b_1$  ( $\geq 10^{-3}$  Hz/Pa) to  $b_3$  for strength  $S$ , width  $\gamma$ , and overlap correction  $\delta$  are listed in the Line Data File of MPM (see Appendix B).

For the  $O_2$  lines in air, (A-9) to (A-12) are valid for altitudes  $h \leq 35$  km ( $p > 0.7$  kPa), where lines are pressure-broadened. Higher up, Zeeman-splitting and Doppler-broadening of the Zeeman components must be taken into account (Liebe and Gimmestad, 1978). An estimate for  $h > 35$  km is made by

geometrically adding to the pressure proportional width  $\gamma_a$  in (A-11) a second term

$$\gamma_h = \left[ \gamma_a^2 + (25H)^2 \right]^{0.5} \quad \text{GHz} \quad (\text{A-11a})$$

where H is the scalar Earth magnetic field strength in Tesla, ranging from 0.2 to  $0.9 \times 10^{-4}$ . The  $O_2$  spectrum vanishes around  $H \approx 90$  km.

For the  $H_2O$  lines in air, Doppler-broadening has to be considered at altitudes above 60 km ( $p < 0.07$  kPa). An approximation is made by replacing the width  $\gamma_b$  in (A-11) with

$$\gamma_h = (\gamma_b^2 + \gamma_D^2)^{0.5} \quad \text{GHz} \quad (\text{A-11b})$$

where  $\gamma_D^2 = 2.14v_0^2 \times 10^{-12}/\theta$  is the squared Doppler width. In applications requiring the detailed mesospheric line shape it is necessary to apply the more correct Voigt line shape.

#### A.2.2 Continuum Spectra for Air

Continuum spectra in (A-8) identify dry air and water vapor terms  $\underline{N}_p + \underline{N}_e$  and must be added to the selected group of local (MPM)  $O_2$  and  $H_2O$  resonance lines described by (A-9). Continuum absorption increases monotonically with frequency.

The dry air continuum

$$N''_p(f) = f \left( 2a_0 \{ \gamma_0 [1 + (f/\gamma_0)^2] \}^{-1} + a_p p \theta^{1.5} \right) p \theta^2 \quad (\text{A-12a})$$

and

$$N'_p(f) = a_0 \{ [1 + (f/\gamma_0)^2]^{-1} - 1 \} p \theta^2 \quad (\text{A-12b})$$

make a small contribution at ground level pressures due to the nonresonant  $O_2$  spectrum below 10 GHz and a pressure-induced  $N_2$  spectrum that is effective above 100 GHz. A width parameter for the Debye spectrum of  $O_2$  is formulated in accordance with (A-11) to be  $\gamma_0 = 4.8 \times 10^{-3} (p + 1.1e) \theta^{0.8}$  (GHz) [10]. The continuum coefficients are  $a_0 = 3.07 \times 10^{-4}$  and  $a_p = 1.40(1 - 1.2f^{1.5} 10^{-5}) 10^{-10}$ .

Water vapor continuum absorption has been a major source of uncertainty in predicting millimeter-wave attenuation, especially in the window ranges. Moist-air attenuation  $\alpha$  at a frequency that falls within a window can be expressed by

$$\alpha = k_s(T)e^2 + k_f(T)e p + k_d(T)p^2 . \quad (\text{A-13})$$

A series of controlled laboratory measurements was performed at 137.8 GHz to determine the k-coefficients. Data  $\alpha(T,e,p)$  were taken covering the following range of parameters:

temperature	$T = 8$ to $43$ °C
vapor pressure	$e = 0$ to $e_1$ (RH $\leq$ 95%) and
total pressure	$P = e_1 + p$ , where $p = 0$ to 150 kPa.

Experimental data were reduced to a reference temperature  $T_0 = 26.85$  °C ( $\theta = 1$ ). The temperature dependence of each k-coefficient ( $k_{s,f,d}$ ) was fitted to a power law  $k(T) = k\theta^X$ . Moist-air attenuation at  $f_x = 137.8$  GHz behaved as follows:

$$k_s = 0.133(4)\theta^{10.3(3)}, \quad k_f = 5.68(5)10^{-3}\theta^{3.0(4)}, \quad k_d = 2(1)10^{-6}\theta^3. \quad (\text{A-14})$$

Values in parentheses give the standard deviation from the mean in terms of final listed digits. The experimental results (A-14) contain foremost contributions from water vapor continuum absorption and were used to "calibrate" MPM by enforcing agreement between experimental and predicted data; further, an  $f^2$  dependence was assumed.

The water vapor continuum is derived from fitting experimental data (A-14) in the case of

$$N_e''(f) = f(b_f p + b_e e) e \theta^3 \quad (\text{A-15a})$$

and based on theoretical data in the case of

$$N_e'(f) = f^2 b_0 e \theta^3, \quad (\text{A-15b})$$

where

$$\begin{aligned} b_f &= 1.13 \times 10^{-6}, \\ b_e &= 3.57 \times 10^{-5} \theta^{7.5}, \text{ and} \\ b_0 &= 6.47 \times 10^{-6}. \end{aligned}$$

In summary, (A-15) is needed to supplement local line (MPM) contributions, the coefficient  $b_f$  is valid only for the selected local line base treated with line shape (A-9), and the strong self-broadening component  $b_e e^2$  is nearly unaffected by (A-9). The coefficient  $b_0$  and both exponents in (A-15b) were obtained by fitting dispersion results of line-by-line calculations for the rotational  $H_2O$  spectrum above 1 THz.

### A.2.3 Suspended Water Droplet Continuum (Haze, Fog, Cloud)

Suspended water droplets (SWD) in haze, fog, or clouds are millimeter wave absorbers. Their size range of radii is below 50  $\mu m$ , which allows the Rayleigh approximation of Mie scattering theory to be used for calculating refractivity contributions  $\underline{N}_w$  to (A-8) in the form [14] (see p. 73)

$$N_w''(f) = (9/2)w/\epsilon''(1 + \eta^2), \quad (A-16a)$$

$$N_w'(f) = (9/2)w [1/(\epsilon_0 + 2) - \eta/\epsilon''(1 + \eta^2)], \quad (A-16b)$$

and

$$N_w^0 = (3/2)w [1 - 3/(\epsilon_0 + 2)], \quad (A-16c)$$

where  $\eta = (2 + \epsilon')/\epsilon''$ ;  $\epsilon'$ ,  $\epsilon''$  are real and imaginary, and  $\epsilon_0$  static parts of the permittivity for water. The contribution of (A-16c) is added to equation (A-6).

Values for the dielectric spectra  $\underline{\epsilon}(f)$  of water are calculated with a new double-Debye model [15]:

$$\epsilon'(f) = \epsilon_2 + (\epsilon_0 - \epsilon_1)/[1 + (f/f_D)^2] + (\epsilon_1 - \epsilon_2)/[1 + (f/f_S)^2], \quad (A-17a)$$

$$\epsilon''(f) = f(\epsilon_0 - \epsilon_1)/f_D[1 + (f/f_D)^2] + (\epsilon_1 - \epsilon_2)/f_S[1 + (f/f_S)^2], \quad (A-17b)$$

$$\epsilon_0 = 77.66 + 103.3(\theta - 1), \quad (A-17c)$$

where  $\epsilon_1 = 5.48$ ,  $\epsilon_2 = 3.51$ ,

$$f_D = 20.09 - 142(\theta - 1) + 294(\theta - 1)^2 \quad \text{GHz, and}$$

$$f_S = 590 - 1500(\theta - 1) \quad \text{GHz.}$$

Equation (A-17) is valid for frequencies up to 1000 GHz over a temperature range from -10 to +30 °C.

#### A.2.4 Rain Effects

The refractivity of rain is identified in (A-8) by  $\underline{N}_R = N_R' + jN_R''$ . Drop diameters (0.1 - 6 mm) and millimeter wavelengths are comparable, thus causing appreciable interactions due to Mie absorption and scattering. Bypassing elaborate, lengthy Mie calculations which require drop shape and size distributions as well as the complex dielectric properties of water (A-17), rain refractivity spectra are approximated via (see p. 73)

$$N_R''(f) = aR^b \quad (A-18a)$$

$$N_R'(f) = -N_R^0 [x^{2.5} / (1 + x^{2.5})] \quad (A-18b)$$

$$N_R^0 = R(3.68 - 0.012R)/f_R \quad (A-18c)$$

where  $f_R = 53 - R(370 - 1.5R)10^{-3}$  GHz and  $x = f/f_R$ .

Frequency-dependent coefficient  $a$  and exponent  $b$  were calculated using drop size spectra of Laws and Parsons and a temperature of  $T = 0$  °C. A regression fit to individual  $(a,b)$ -pairs over the frequency range from 1 to 1000 GHz resulted in the following calculation scheme:

$a = x_1 f^{x_2}$			$b = x_3 f^{x_4}$		
f	$x_1$	$x_2$	f	$x_3$	$x_4$
GHz			GHz		
1 to 2.9	$3.51 \times 10^{-4}$	1.03	1 to 8.5	0.851	0.158
2.9 to 54	$2.31 \times 10^{-4}$	1.42	8.5 to 25	1.41	-0.0779
54 to 180	0.225	-0.301	25 to 164	2.63	-0.272
180 to 1000	18.6	-1.151	164 to 1000	0.616	0.0126

### A.3. CONCLUSIONS

The parametric model MPM for atmospheric refractivity

$$\underline{N}(f, P/T/RH, w_A/w, R)$$

was developed for applications in areas such as telecommunications, remote sensing, and radio astronomy. Details of its structure and operation are explained in the extensive COMMENTS part of the code. The memory capacity required for MPM is 355 kbytes.

The format of the numerical print-out is demonstrated by the identical example given in Table A-1 for the N version and in Table A-2 for the  $\alpha/\beta$  version. A plotting system at the user's choice (e.g., HALO) can be added to include features such as auto or manual scaling, multiple cases (e.g., nine curves with up to 500 points each), special labels, etc. An example of a graphical presentation for a sea level condition of moist air ( $w_A = w = R = 0$ ) exhibits spectra at various relative humidities ( $RH = 0-100\%$ ) for the N version in Figure A-1 and for the identical case as  $\alpha/\beta$  version in Figure A-2.

### A.4. ADDITIONAL REFERENCE

Liebe, H. J. and G. G. Gimmestad (1978), Calculation of clear air refractivity, *Radio Science* 20, no. 2, pp. 245 - 251.



Table A-1.

FREQUENCY PROFILES OF ATMOSPHERIC COMPLEX REFRACTIVITY

INPUT Valid Parameter ranges indicated by [ ]):

CASE	PRES., P (kPa)	TEMP., T (C)	REL. HUM., RH (%)	HAZE MODEL (mg/m3)	SUSP. DROP., w (g/m3)	RAIN RATE, R (mm/hr)
[1-9]	[0 -110]	[+/-50]	[0-100]	[0-1]	[0-10]	[0-200]
1	101.3	15.0	100.0	: 0.00	1.000	10.0

Minimum Frequency F1 0.000 (GHz)  
 Maximum Frequency F2 [1000.]1000.000 (GHz)  
 Frequency Step [max 500] dF 100.000 (GHz)

-----  
 OUTPUT:

Case Number: 1 (No = 351.18 ppm)

FREQUENCY (GHz)	MOIST AIR (v= 12.81 g/m3)					= TOTAL
	DRY AIR	WATER VAPOR	HAZE, FOG CLOUD	HAZE, FOG CLOUD	RAIN	
0.000	+++++++	+++++++	+++++++	+++++++	+++++++	+++++++
	0.220E-09	-.317E-07	0.278E-08	0.431E-08	-.244E-07	
100.000	0.168E-02	0.454E-01	0.242E+00	0.317E+00	0.607E+00	
	-.219E+00	0.321E+00	-.139E+00	-.226E+00	-.264E+00	
200.000	0.476E-03	0.149E+00	0.288E+00	0.190E+00	0.629E+00	
	-.170E+00	0.107E+01	-.299E+00	-.266E+00	0.334E+00	
300.000	0.561E-03	0.174E+00	0.284E+00	0.120E+00	0.579E+00	
	-.162E+00	0.352E+01	-.391E+00	-.275E+00	0.269E+01	
400.000	0.807E-03	0.481E+00	0.276E+00	0.869E-01	0.845E+00	
	-.157E+00	0.619E+01	-.450E+00	-.278E+00	0.530E+01	
500.000	0.104E-02	0.118E+01	0.268E+00	0.675E-01	0.152E+01	
	-.162E+00	0.192E+02	-.495E+00	-.279E+00	0.183E+02	
600.000	0.846E-03	0.225E+01	0.260E+00	0.549E-01	0.257E+01	
	-.159E+00	-.172E+02	-.532E+00	-.280E+00	-.182E+02	
700.000	0.977E-03	0.101E+01	0.252E+00	0.461E-01	0.131E+01	
	-.157E+00	0.687E+01	-.563E+00	-.281E+00	0.587E+01	
800.000	0.117E-02	0.112E+01	0.242E+00	0.396E-01	0.140E+01	
	-.161E+00	-.635E+01	-.589E+00	-.281E+00	-.738E+01	
900.000	0.101E-02	0.795E+00	0.232E+00	0.347E-01	0.106E+01	
	-.159E+00	0.716E+01	-.611E+00	-.281E+00	0.611E+01	
1000.000	0.103E-02	0.603E+01	0.223E+00	0.308E-01	0.628E+01	
	-.159E+00	-.134E+02	-.629E+00	-.282E+00	-.145E+02	

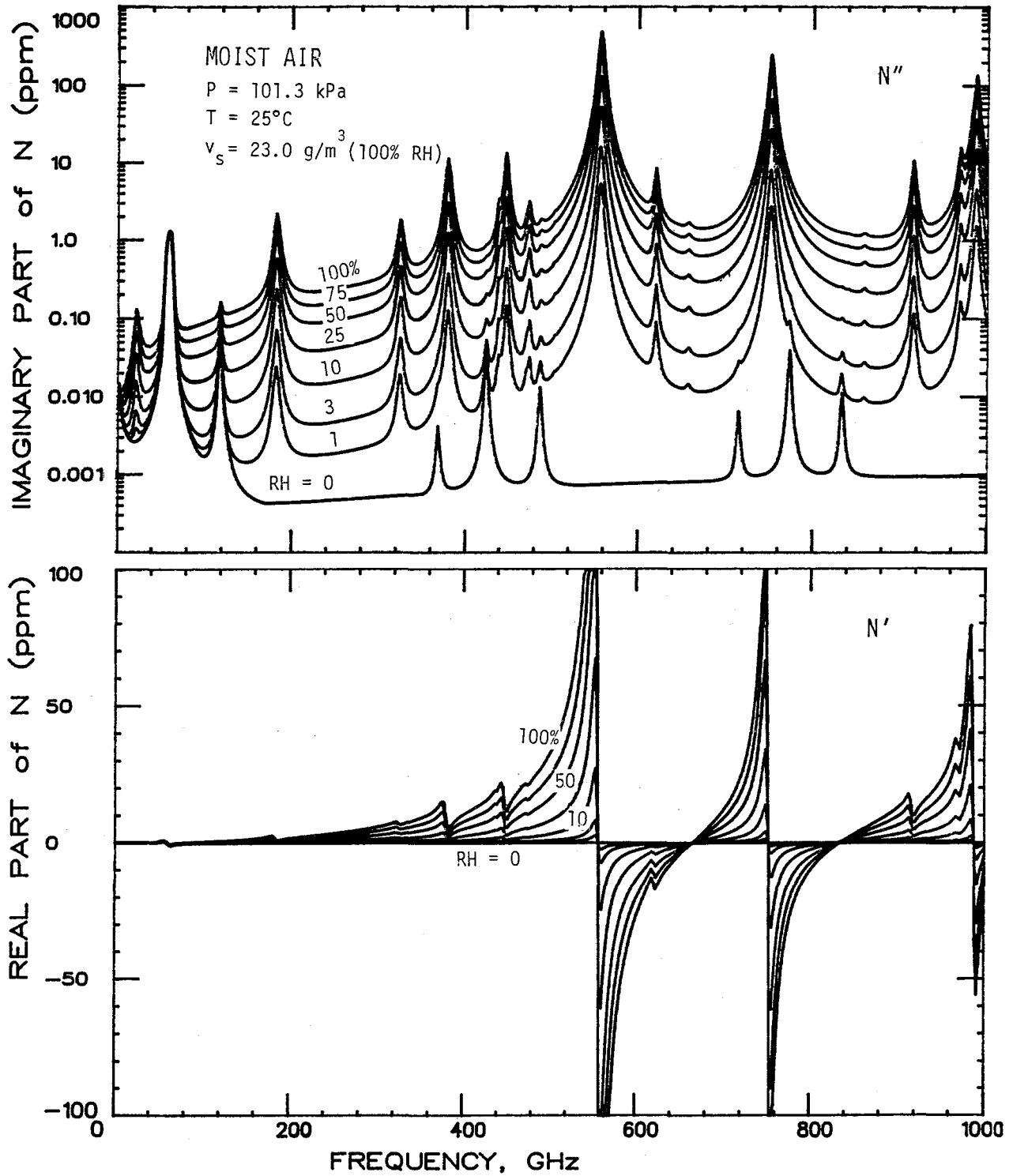


Figure A-1. Moist air refractivity  $\underline{N} = N' - jN''$  for sea level condition (P,T) and various relative humidities (RH) over the frequency range from 0 to 1000 GHz.

Table A-2.

FREQUENCY PROFILES OF ATTENUATION AND DELAY RATES

INPUT Valid Parameter ranges indicated by [ ]):

CASE	PRES.,P (kPa)	TEMP.,T (C)	REL. HUM.,RH (%)	HAZE MODEL (mg/m3)	SUSP. DROP.,w (g/m3)	RAIN RATE,R (mm/hr)
[1-9]	[0 -110]	[+/-50]	[0-100]	[0-1]	[0-10]	[0-200]
1	101.3	15.0	100.0	: 0.00	1.000	10.0

Minimum Frequency F1 0.000 (GHz)  
 Maximum Frequency F2 [1000.]1000.000 (GHz)  
 Frequency Step [max 500] dF 100.000 (GHz)

-----  
 OUTPUT:

Case Number: 1 (Refractive delay = 1171.5 ps/km)

-----  
 MOIST AIR (v= 12.81 g/m3)  
 DRY WATER HAZE, FOG  
 AIR + VAPOR + CLOUD + RAIN = TOTAL  
 -----

FREQUENCY (GHz)	$\alpha$ -ATTENUATION (dB/km)					$\beta$ -DISPERSIVE DELAY (ps/km)
	DRY AIR	WATER VAPOR	HAZE, FOG + CLOUD	HAZE	RAIN	
0.000	0.00	0.00	0.00	0.00	0.00	0.00
	0.00	0.00	0.00	0.00	0.00	0.00
100.000	0.03	0.83	4.41	5.78	11.05	
	-0.73	1.07	-0.46	-0.75	-0.88	
200.000	0.02	5.44	10.50	6.93	22.88	
	-0.57	3.56	-1.00	-0.89	1.11	
300.000	0.03	9.50	15.52	6.57	31.62	
	-0.54	11.75	-1.30	-0.92	8.99	
400.000	0.06	35.02	20.11	6.32	61.51	
	-0.52	20.64	-1.50	-0.93	17.68	
500.000	0.09	107.25	24.43	6.14	137.92	
	-0.54	64.18	-1.65	-0.93	61.06	
600.000	0.09	246.00	28.44	6.00	280.53	
	-0.53	-57.35	-1.77	-0.94	-60.59	
700.000	0.12	128.84	32.07	5.87	166.91	
	-0.52	22.92	-1.88	-0.94	19.58	
800.000	0.17	162.65	35.28	5.77	203.87	
	-0.54	-21.20	-1.96	-0.94	-24.63	
900.000	0.17	130.27	38.08	5.68	174.20	
	-0.53	23.88	-2.04	-0.94	20.37	
1000.000	0.19	1097.36	40.50	5.61	1143.65	
	-0.53	-44.84	-2.10	-0.94	-48.40	

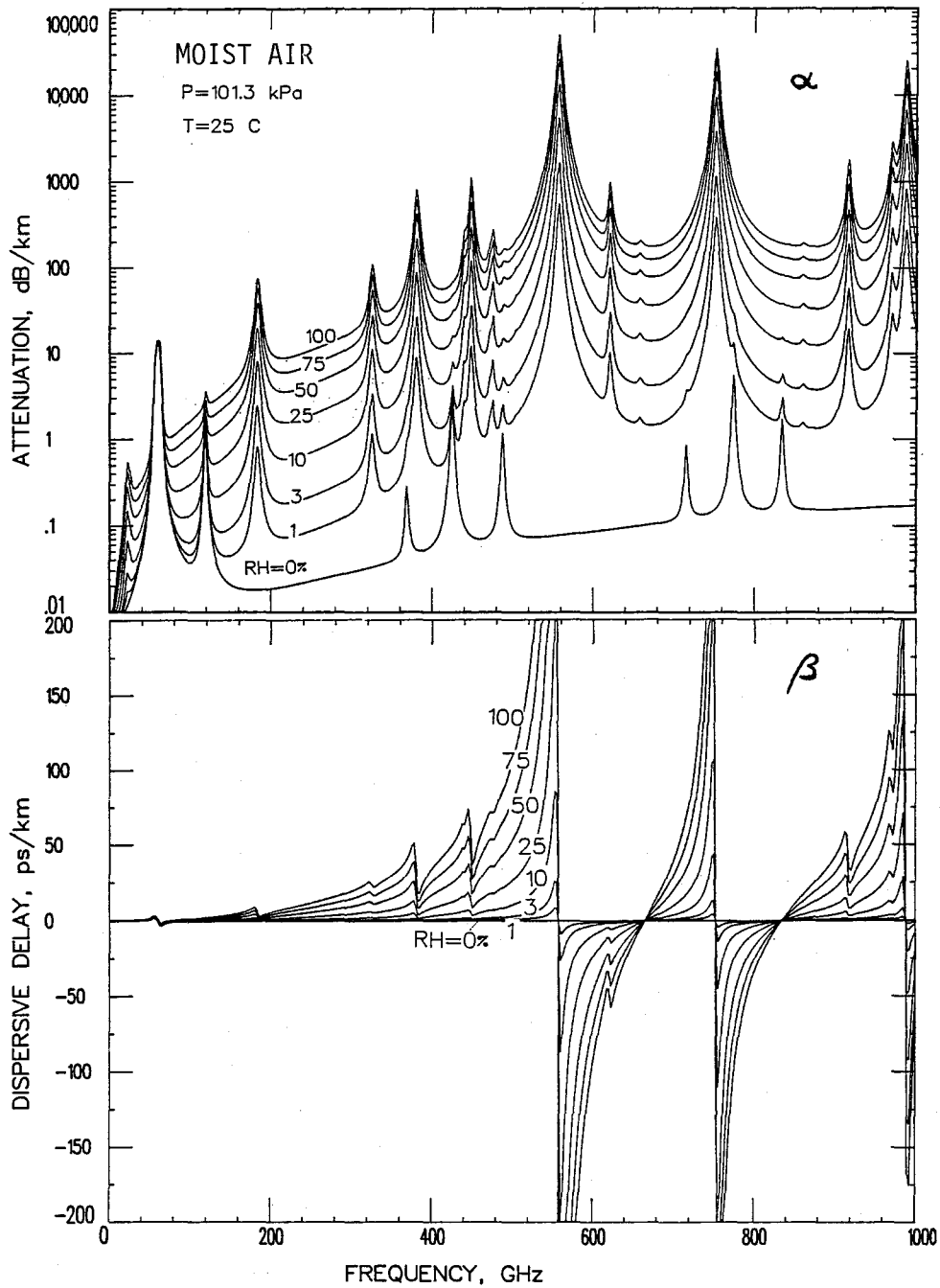


Figure A-2. Moist air attenuation ( $\alpha$ ) and delay ( $\beta$ ) rates for sea level condition (P,T) and various relative humidities (RH) over the frequency range from 1 to 1000 GHz.

## APPENDIX B

### PRINTOUT OF MPM-N PROGRAM FOR VERSION A (Frequency Profiles)

The computer program MPM-N is written in FORTRAN 77 with extensive comments to run on IBM-XT/AT + 8087/80287 coprocessor, or equivalent, microcomputers.

Program MPM-N is available on 5 1/4" diskettes, either in double (360 kbyte) or quadruple (1.2 Mbyte) density. Requests may be addressed to NTIA/ITS.S3, 325 Broadway, Boulder, CO 80303-3328 (ATTN: Dr. H. Liebe). Please provide the necessary disks.

ID for FORTRAN 77 (IBM Professional 8-bit compiler) version (disk No. 1):

MPM1	FOR	45675	7-16-87	-N/A Frequency Profiles
MPM2	FOR	29762	7-08-87	-N/B Humidity Profiles
MPM3	FOR	24564	6-11-87	-N/C Pressure Profiles
OXYGEN	DAT	3267	7-13-87	Line Data
WATER	DAT	<u>1166</u>	10-23-86	Tables
5 File(s)		254976 bytes free		

ID for EXECUTABLE version (disk No. 2):

MPM1	EXE	354565	7-08-87	-N/A Frequency Profiles
OXYGEN	DAT	3267	7-13-87	Line Data
WATER	DAT	<u>1166</u>	10-23-86	Tables
3 File(s)		1024 bytes free		

The executable code length for MPM2 and 3 is 402 and 356 kbyte, respectively.



C PROGRAM MPM-N  
C AUGUST 1987

C -----  
C COMPLEX RADIO REFRACTIVITY OF ATMOSPHERIC AIR (1 TO 1000 GHZ).  
C Hans J. Liebe  
C Institute for Telecommunication Sciences  
C NTIA/ITS.S3  
C 325 BROADWAY  
C Boulder, CO 80303

C Adapted for IBM-PC Professional FORTRAN by:  
C John Stricklen (1-303-497-3195, FTS 320-3195)

C Contents:  
C A. FREQUENCY PROFILES  
C B. HUMIDITY PROFILES  
C C. PRESSURES PROFILES OF MOIST AIR

C -----  
C A. FREQUENCY PROFILES  
C -----

C Program MPM-N/A calculates frequency profiles of the complex radio  
C refractivity N of ATMOSPHERIC AIR over a frequency range f=1 to  
C 1000 GHZ. The output is expressed in Real part of N and  
C Imaginary part of N and specific rates of power attenuation A  
C (Im. of N) and propagation delay B (Re. of N).

C OUTPUT:

C \* Real part of refractivity N' (f) in ppm  
C \* Imaginary part of refractivity N''(f) in ppm  
C \* Nondispersive Refractivity No in ppm  
C or  
C \* Attenuation A(f) in dB/km  
C \* Dispersive Delay B(f) in ps/km  
C \* Refractive Delay Bo in ps/km

C Frequency range, moist air, rain conditions (specified by five  
C meteorological variables P=p+e, T, RH, WA or w, RR), and haze model  
C code (A, B, C, or D) are the required input information to be  
C entered from the keyboard.

C INPUT:

C \* Frequency range f1, f2 in GHZ Valid Range:  
C and step size df in GHZ 1 to 1000  
C >= 1.E-05  
C (max. 500 freqs.)  
C \* Barometric pressure P in kPa 0.0 to 120  
C \* Temperature T in C -50 to 50  
C \* Relative humidity RH in % 0 to 100  
C [absolute humidity is calculated as v(RH,T) in g/m3  
C or e(RH,T) in kPa.]  
C \* Haze model (RH = 80 to 99.9%):  
C code A(rural), B(urban), C(maritime), and D(C +strong wind)  
C plus hygroscopic aerosol reference  
C concentration WA(80%RH) in mg/m3 0 to 1  
C \* Suspended water droplet  
C concentration w in g/m3 0 to 10  
C \* Rain Rate RR in mm/hr 0 to 200

C COMMENTS:

C The computation of attenuation A and delay B is described in  
C References [1] to [3].

C MOLECULAR effects due to oxygen, nitrogen, and water vapor  
C are considered as detailed in [1].

C This MPM version has been corrected for typesetting errors in [1]  
C and revised to include:

- C (a) an improved water vapor continuum spectrum and a haze model  
C reported in [2];  
C (b) an improved model for liquid water dielectric properties and  
C RAYLEIGH absorption and phase delay by suspended water droplets  
C (radii < 50 microns) such as haze, fog, and clouds [3];  
C (c) a rain attenuation model by Olsen, et.al. [4], as well as  
C dispersive delay due to rain approximated from results reported by  
C Zuffery [5];  
C (d) new line data for the 183 GHz water vapor line [6];  
C (e) a VW shape cutoff, setting F''=0 for f > (vo +40 x widths) [7];  
C (f) a new set of overlap correction coefficients A5 [8];  
C (g) an improved water vapor saturation pressure equation based on  
C degrees Celsius [9] (see comments in program);  
C (h) an approximation for Zeeman (O2) and Doppler (H2O) line broadening [10].

- C REFERENCES: [1] H.J. Liebe, "An updated model for millimeter wave  
C propagation in moist air", Radio Science, vol. 20  
C no. 5, pp. 1069-1089, 1985.  
C [2] H.J. Liebe, "A contribution to modeling atmospheric  
C mm-wave properties", FREQUENZ (J. Telecom.), vol.  
C 41, no. 1/2, pp. 31-36, 1987.  
C [3] H.J. Liebe, T. Manabe, and J.P. Stricklen,  
C "Millimeter-wave attenuation and delay for a fog event",  
C IEEE Digest: 12th Int. Conf. Infrared and Millimeter  
C Waves, Orlando, FL, December, 1987.  
C [4] R. L. Olsen, D. V. Rogers, and D. B. Hodge,  
C "The aRb relation in the calculation of rain  
C attenuation", IEEE Trans. Ant. Prop., vol. AP-26,  
C no. 2, pp. 318-329, 1978.  
C [5] C.H. Zuffery, "A study of rain effects on EM waves  
C in the 1-600 GHz range", MS-Thesis, Dept.  
C Electrical Eng., University of Colorado, Boulder,  
C CO 80309, Feb., 1972.  
C [6] A. Bauer, M. Godon, and B. Duterage, "Self- and  
C air-broadened linewidth of the 183 GHz absorption  
C in water vapor", J. Quant. Spectrosc. Radiat.  
C Transf., vol. 32, no. 2, pp. 167-175, 1985.  
C [7] R. J. Hill, "Absorption by the tails of the oxygen  
C microwave resonances at atmospheric pressures", IEEE  
C Trans. AP-35, no.2, pp. 198-204, 1987.  
C [8] P. W. Rosenkranz, "Interference coefficients for  
C overlapping oxygen lines in air", J. Quant. Spectr.  
C Rad. Transf., in review, 1987.  
C [9] W. Boegel, "Neue Naeherungsgleichungen fuer den  
C Saettigungsdruck des Wasserdampfes, DFVLR Bericht  
C DLR-FB 77-52, 1977.

```

C
C      [10] H. J. Liebe and G. B. Gimmetstad, "Calculation of
C      clear air EHF refractivity", Radio Sci., vol. 13,
C      no. 2, pp. 245-251, 1978.
C-----
C***** LIST OF VARIABLES *****
C      FMIN      Minimum Frequency
C      FMAX      Maximum frequency
C      STEP      Step Size between frequencies.
C      NF        No. of frequencies.
C      NCASE     No. of cases.
C      PBT(10)   Pressures
C      TCT(10)   Temperatures.
C      RHT(10)   Rel. Humidities
C      WT(10)    Droplet concentrations.
C      RR(10)    Rain Rate
C      HZ(10)    Haze growth models.
C*****
C      MAIN PROGRAM
C*****
C      COMMON /AIR/ NCASE,PBT(10),TCT(10),RHT(10),WT(10),R(10)
C      COMMON /FREQS/ FMIN,FMAX,STEP,NF
C      COMMON /RAIN/ RR(10),WA(10)
C      COMMON /ANS1/ D(12,501,10),ATT(501,10),DISP(501,10)
C      COMMON /ANS/  FREQA(501),No(10),Bo(10),EV(10)
C      COMMON /O2line/ F0O2(48),A(6,48)
C      COMMON /H2O/ F0water(30),B(3,30)
C      COMMON /HAZE/ HZ(10)
C      CHARACTER*1 HZ
C
C*****
C      WRITE(*,1101)
C      1101  FORMAT(//////////)
C      WRITE(*,2)
C      2     FORMAT(80(1H*),/,5X,' Executing PARAMETRIC ATTENUATION and ',
C      + 'DISPERSIVE DELAY Program',/,80(1H*))
C      WRITE(*,4)
C      4     FORMAT(///)
C
C***** INITIALIZE ALL DATA VALUES *****
C
C      OXYGEN LINE DATA
C      CALL OXYDA1
C      WATER VAPOR LINE DATA
C      CALL VAPDA1
C      NCASE=1
C      FMIN=10.
C      FMAX=100.
C      STEP=10.
C
C      STANDARD SEA LEVEL CONDITIONS FOR PRESSURE, TEMP., AND HUMIDITY
C      DO 3 I=1,10
C      PBT(I)=101.3
C      TCT(I)=15.0
C      RHT(I)=50.

```

```

HZ(I)=' '
3      CONTINUE
C
C*****
C      10     CALL MENU(IMENU)
C            IF (IMENU.EQ.1) THEN
C              CALL INSTR
C            ELSE IF (IMENU.EQ.2) THEN
C              CALL EDITSUMM(1)
C            ELSE IF (IMENU.EQ.3) THEN
C              CALL SAVETABL(2)
C            ELSE IF (IMENU.EQ.4) THEN
C              CALL COMPUTE(NCASE)
C            ELSE IF (IMENU.EQ.5) THEN
C              CALL SAVETABL(0)
C            ELSE IF (IMENU.EQ.6) THEN
C              CALL SAVETABL(1)
C            ELSE IF (IMENU.EQ.7) THEN
C              WRITE(*,*)'Quitting Program... Normal termination.'
C              GOTO 20
C            ELSE
C              WRITE(*,*)'NOT a valid menu option.'
C            ENDF
C            GOTO 10
C            STOP
C            END
C-----
C      SUBROUTINE INSTR
C      WRITE(*,1)
C      FORMAT(///)
C      1     WRITE(*,*)'The menu options are:'
C            WRITE(*,*)'1) Instructions'
C            WRITE(*,*)'2) Edit Data'
C            WRITE(*,*)'3) Summary of current data'
C            WRITE(*,*)'4) Process Data'
C            WRITE(*,*)'5) Print Results'
C            WRITE(*,*)'6) Save results to Disk'
C            WRITE(*,*)'7) Quit'
C            WRITE(*,*)
C            WRITE(*,*)'1) You have found the instruction set.'
C            WRITE(*,*)
C            WRITE(*,*)'2) The input data includes the frequency range and'
C            WRITE(*,*)'step, the parameter that you wish to vary, the'
C            WRITE(*,*)'number of cases and the values of pressure,'
C            WRITE(*,*)'temperature, relative humidity, and rain rate.'
C            WRITE(*,*)'For RH = 80 to 99.9%, a haze model predicts for'
C            WRITE(*,*)'four cases (A=rural, B=urban, C=maritime, and'
C            WRITE(*,*)'D=C+strong wind) the shrinking and swelling by'
C            WRITE(*,*)'hygroscopic aerosol concentrations specified at'
C            WRITE(*,*)'80% RH. At 100% RH a suspended water droplet'
C            WRITE(*,*)'concentration can be added to simulate fog or'
C            WRITE(*,*)'cloud conditions.'
C            WRITE(*,*)
C            WRITE(*,*)'The value that appears in parentheses () is the'
C            WRITE(*,*)'default value and will be used if you simply'
C            WRITE(*,*)'press the RETURN key. To enter a new value'
C            WRITE(*,*)'type the value and press the RETURN key.'
C            WRITE(*,*)
C            WRITE(*,*)'The computer will ask you which parameter you'

```



```

WRITE(*,*) wish to vary and you should type P, R, or T
WRITE(*,*) for Pressure, Relative humidity, or Temperature'
WRITE(*,*) respectively. The other two parameters will
WRITE(*,*) be fixed at the same value for every case'
WRITE(*,*) and you will be prompted for these values.'
WRITE(*,*) You will then be prompted for a value of your'
WRITE(*,*) selected parameter for each separate case.'
WRITE(*,*) For every case in which the relative humidity'
WRITE(*,*) is 100% you will be prompted to enter a value'
WRITE(*,*) for the suspended droplet concentration, and
WRITE(*,*) for cases in which the humidity is above 80%'
WRITE(*,*) you will be asked for a hygroscopic aerosol'
WRITE(*,*) content at 80%. This is used to calculate the'
WRITE(*,*) water droplet content using the haze growth'
WRITE(*,*) model of [2].
WRITE(*,*)
WRITE(*,*) The units on the parameters are:'
WRITE(*,*) Pressure in kPa.
WRITE(*,*) Relative Humidity in %
WRITE(*,*) Temperature in degrees C'
WRITE(*,*) Water Droplet concentration in grams/meter'
WRITE(*,*) cubed'
WRITE(*,*) Rain rate in millimeters per hour'
WRITE(*,*) These are given in the prompt'
WRITE(*,*)
WRITE(*,*) 3) This gives a summary of all the current input'
WRITE(*,*) data. It is a good idea to request a summary'
WRITE(*,*) after you edit the data to make sure that all'
WRITE(*,*) of the decimals are in the right place etc.'
WRITE(*,*)
WRITE(*,*) 4) This option causes the data to be used to
WRITE(*,*) generate a table of attenuation and dispersion.'
WRITE(*,*) This must be done every time you change the
WRITE(*,*) data to update the table.'
WRITE(*,*)
WRITE(*,*) 5) The table of attenuation and dispersion will be'
WRITE(*,*) printed to the console. To make a hard copy you'
WRITE(*,*) may use the CTRL-PRTS key or to make a disk'
WRITE(*,*) file you can use the menu option given next'
WRITE(*,*) and print the file. The output is in tabular'
WRITE(*,*) form with the components of the total'
WRITE(*,*) attenuation and dispersion shown in two lines'
WRITE(*,*) with the attenuation above the dispersion.'
WRITE(*,*)
WRITE(*,*) 6) This saves the results to a file you specify.'
WRITE(*,*)
WRITE(*,*) 7) This stops program execution.'
WRITE(*,*)
RETURN
END

```

---

SUBROUTINE MENU(IMENU)

```

C CHARACTER*1 IVAL
WRITE(*,1)
1 FORMAT(' Enter the number of the option you wish to choose.,',
+      /,' 1 - Instructions',
+      /,' 2 - Edit Data',
+      /,' 3 - Summary of current data',

```

```

+      /,' 4 - Process Data',
+      /,' 5 - Print Results ',
+      /,' 6 - Save output to Disk file',
+      /,' 7 - Quit',//)
C
100 WRITE(*,2)
2   FORMAT(' OPTION ? ')
   READ(*,3) IVAL
3   FORMAT(A1)
   IF((IVAL.EQ.'1').OR.(IVAL.EQ.'2')).OR.(IVAL.EQ.'3').OR.
+ (IVAL.EQ.'4').OR.(IVAL.EQ.'5').OR.(IVAL.EQ.'6').OR.(IVAL.EQ.'7'))
+ THEN
4   READ(IVAL,4,ERR=100) IMENU
   FORMAT(I1)
   ELSE
   WRITE(*,*)'Invalid option.'
   GOTO 100
   ENDIF
   RETURN
END
C-----
SUBROUTINE EDITSUMM(IFLAG)
C THIS ROUTINE PRINTS SUMMARY AND/OR EDITS THE DATA.
C
C IFLAG=1 IS FOR EDIT MODE--ANYTHING ELSE IS A SUMMARY.
C NFLAG IS INDEX FOR PARAMETER VARIATION
C
COMMON /AIR/ NCASE,PBT(10),TCT(10),RHT(10),WT(10),R(10)
COMMON /FREQS/ FMIN,FMAX,STEP,NF
COMMON /RAIN/ RR(10),WA(10)
COMMON /HAZE/ HZ(10)
CHARACTER*1 HZ
CHARACTER*8 IVAL
C*****
C
10   FORMAT(A8)
C
C ZERO OUT THE DROPLET CONCENTRATIONS
IF(IFLAG.EQ.1) THEN
DO 100 I=1,10
WT(I)=0.0
HZ(I)=' '
100  CONTINUE
ENDIF
200  CONTINUE
C ***** FREQUENCY DATA *****
300  WRITE(*,4) FMIN
4   FORMAT(' Minimum Frequency, GHz (' ,F7.2,') ')
IF(IFLAG.EQ.1) THEN
READ(*,10) IVAL
IF(IVAL.EQ.' ') THEN
GOTO 400
ELSE
READ(IVAL,8,ERR=300) FMIN
FORMAT(F8.0)
ENDIF
8   CHECK FOR VALID RANGE ON FMIN
IF((FMIN.GT.0.).AND.(FMIN.LE.1000.)) GOTO 400
WRITE(*,*)'Minimum Freq. must satisfy 0 < FMIN <= 1000.'
GOTO 300

```

C LINE DATA FILES (Table I in [1])  
 C (read as separate data files by MPM)  
 C

C Coefficients A5 after Rosenkranz [8], for 118.75 GHz line after Hill [7]

C	F0	A1	A2	A3	A4	A5	A6
C	49.452379	0.12	11.830	8.40	0	6.600	1.7
C	49.962257	0.34	10.720	8.50	0	6.600	1.7
C	50.474238	0.94	9.690	8.60	0	6.600	1.7
C	50.987748	2.46	8.690	8.70	0	6.600	1.7
C	51.503350	6.08	7.740	8.90	0	6.627	1.8
C	52.021409	14.14	6.840	9.20	0	6.347	1.8
C	52.542393	31.02	6.000	9.40	0	6.046	1.8
C	53.066906	64.10	5.220	9.70	0	5.719	1.9
C	53.595748	124.70	4.480	10.00	0	5.400	1.8
C	54.129999	228.00	3.810	10.20	0	5.157	2.0
C	54.671157	391.80	3.190	10.50	0	4.783	1.9
C	55.221365	631.60	2.620	10.79	0	4.339	2.1
C	55.783800	953.50	2.115	11.10	0	4.011	2.1
C	56.264777	548.90	0.010	16.46	0	2.772	0.9
C	56.363387	1344.00	1.655	11.44	0	3.922	2.3
C	56.968180	1763.00	1.255	11.81	0	3.398	2.5
C	57.612481	2141.00	0.910	12.21	0	1.145	3.2
C	58.323874	2386.00	0.621	12.66	0	0.317	-2.5
C	58.446589	1457.00	0.079	14.49	0	6.270	0.8
C	59.164204	2404.00	0.386	13.19	0	-4.119	0.1
C	59.590982	2112.00	0.207	13.60	0	6.766	0.5
C	60.306057	2124.00	0.207	13.82	0	-6.183	0.7
C	60.434775	2461.00	0.386	12.97	0	3.290	-0.4
C	61.150558	2504.00	0.621	12.48	0	-1.591	3.5
C	61.800152	2298.00	0.910	12.07	0	-2.068	2.9
C	62.411212	1933.00	1.255	11.71	0	-4.158	2.3
C	62.486253	1517.00	0.078	14.68	0	-4.068	0.9
C	62.997974	1503.00	1.660	11.39	0	-4.482	2.2
C	63.568515	1087.00	2.110	11.08	0	-4.442	2.0
C	64.127764	733.50	2.620	10.78	0	-4.687	2.0
C	64.678900	463.50	3.190	10.50	0	-5.074	1.8
C	65.224067	274.80	3.810	10.20	0	-5.403	1.9
C	65.764769	153.00	4.480	10.00	0	-5.610	1.8
C	66.302088	80.09	5.220	9.70	0	-5.896	1.8
C	66.836827	39.46	6.000	9.40	0	-6.194	1.7
C	67.369595	18.32	6.840	9.20	0	-6.468	1.8
C	67.900862	8.01	7.740	8.90	0	-6.718	1.7
C	68.431001	3.30	8.690	8.70	0	-6.70	1.7
C	68.960306	1.28	9.690	8.60	0	-6.60	1.7
C	69.489021	0.47	10.720	8.50	0	-6.60	1.7
C	70.017342	0.16	11.830	8.40	0	-6.60	1.7
C	118.750341	945.00	0.000	16.30	0	-0.134	0.8
C	368.498350	67.90	0.020	19.20	0.6	0	1
C	424.763120	638.00	0.011	19.16	0.6	0	1
C	487.249370	235.00	0.011	19.20	0.6	0	1
C	715.393150	99.60	0.089	18.10	0.6	0	1
C	773.838730	671.00	0.079	18.10	0.6	0	1
C	834.145330	180.00	0.079	18.10	0.6	0	1

C C Width B3 of 183, 325, and 380 GHz lines increased by 10% [6]

C	F0	B1	B2	B3
C	22.235080	0.1090	2.143	27.84
C	67.813960	0.0011	8.730	27.60
C	119.995940	0.0007	8.347	27.00
C	183.310117	2.3000	0.653	31.64
C	321.225644	0.0464	6.156	21.40
C	325.152919	1.5400	1.515	29.70
C	336.187000	0.0010	9.802	26.50
C	380.197372	11.9000	1.018	30.36
C	390.134508	0.0044	7.318	19.00
C	437.346667	0.0637	5.015	13.70
C	439.150812	0.9210	3.561	16.40
C	443.018295	0.1940	5.015	14.40
C	448.001075	10.6000	1.370	23.80
C	470.888947	0.3300	3.561	18.20
C	474.689127	1.2800	2.342	19.80
C	488.491133	0.2530	2.814	24.90
C	503.568532	0.0374	6.693	11.50
C	504.482692	0.0125	6.693	11.90
C	556.936002	510.0000	0.114	30.00
C	620.700807	5.0900	2.150	22.30
C	658.006500	0.2740	7.767	30.00
C	752.033227	250.0000	0.336	28.60
C	841.073593	0.0130	8.113	14.10
C	859.865000	0.1330	7.989	28.60
C	899.407000	0.0550	7.845	28.60
C	902.555000	0.0380	8.360	26.40
C	906.205524	0.1830	5.039	23.40
C	916.171582	8.5600	1.369	25.30
C	970.315022	9.1600	1.842	24.00
C	987.926764	138.0000	0.178	28.60

C  
 C\*\*\*\*\*  
 C EXAMPLE FOR A.  
 C\*\*\*\*\*

C FREQUENCY PROFILES OF ATTENUATION AND DELAY RATES

C INPUT Valid Parameter ranges indicated by [ ]):

C  
 C CASE PRES.,P TEMP.,T REL. HUM.,RH HAZE MODEL SUSP. DROP.,w RAIN RATE,R  
 C (kPa) (C) (%) (mg/m3) (g/m3) (mm/hr)  
 C [1-9] [0.0-110] [+/-50] [0-100] [0-1] [0-10] [0-200] MOIST AIR  
 C +  
 C 1 101.3 15.0 99.5 C: 1.00 0.033 0.0 HAZE  
 C 2 101.3 15.0 100.0 : 0.00 1.000 10.0 FOG, RAIN  
 C  
 C Minimum Frequency F1 0.000 (GHz)  
 C Maximum Frequency F2 [1000.]1000.000 (GHz)  
 C Frequency Step [max 500] dF 100.000 (GHz)

C-----  
 C OUTPUT:

C Case Number: 1 (Refractive delay = 1164.49 ps/km)

-----  
 C MOIST AIR (v= 12.74 g/m3)  
 C DRY WATER HAZE, FOG  
 C AIR + VAPOR + CLOUD + RAIN = TOTAL  
 C-----

FREQUENCY (GHz)	ATTENUATION (dB/km)						DISPERSIVE DELAY (ps/km)					
	DRY AIR	WATER VAPOR	HAZE, FOG	CLOUD	HAZE, FOG	RAIN	DRY AIR	WATER VAPOR	HAZE, FOG	CLOUD	HAZE, FOG	RAIN
0.000	0.00	0.00	0.00	0.00	0.00	0.00	0.00	0.00	0.00	0.00	0.00	0.00
100.000	0.03	0.82	0.14	0.00	0.00	0.99	0.03	1.06	-0.02	0.00	0.32	0.00
200.000	0.02	5.40	0.34	0.00	0.00	5.76	-0.57	3.55	-0.03	0.00	2.95	0.00
300.000	0.03	9.44	0.51	0.00	0.00	9.98	-0.54	11.69	-0.04	0.00	11.11	0.00
400.000	0.06	34.82	0.65	0.00	0.00	35.53	-0.52	20.53	-0.05	0.00	19.96	0.00
500.000	0.09	106.65	0.80	0.00	0.00	107.54	-0.54	63.86	-0.05	0.00	63.27	0.00
600.000	0.09	244.65	0.93	0.00	0.00	245.67	-0.53	-57.07	-0.06	0.00	-57.65	0.00
700.000	0.12	128.10	1.04	0.00	0.00	129.27	-0.52	22.80	-0.06	0.00	22.22	0.00
800.000	0.17	161.71	1.15	0.00	0.00	163.03	-0.54	-21.09	-0.06	0.00	-21.69	0.00
900.000	0.17	129.49	1.24	0.00	0.00	130.89	-0.53	23.76	-0.07	0.00	23.16	0.00
1000.000	0.19	1091.46	1.32	0.00	0.00	1092.96	-0.53	-44.61	-0.07	0.00	-45.21	0.00

C Case Number: 2 (Refractive delay = 1169.10 ps/km)

-----  
 C MOIST AIR (v= 12.81 g/m3)  
 C DRY WATER HAZE, FOG  
 C AIR + VAPOR + CLOUD + RAIN = TOTAL  
 C-----

FREQUENCY (GHz)	ATTENUATION (dB/km)						DISPERSIVE DELAY (ps/km)					
	DRY AIR	WATER VAPOR	HAZE, FOG	CLOUD	HAZE, FOG	RAIN	DRY AIR	WATER VAPOR	HAZE, FOG	CLOUD	HAZE, FOG	RAIN
0.000	0.00	0.00	0.00	0.00	0.00	0.00	0.00	0.00	0.00	0.00	0.00	0.00
100.000	0.03	0.83	4.41	5.77	0.00	11.04	-0.73	1.07	-0.46	0.00	-0.12	0.00
200.000	0.02	5.44	10.50	6.92	0.00	22.87	-0.57	3.56	-1.00	0.00	2.00	0.00
300.000	0.03	9.50	15.52	6.56	0.00	31.61	-0.54	11.75	-1.30	0.00	9.90	0.00
400.000	0.06	35.02	20.11	6.31	0.00	61.50	-0.52	20.64	-1.50	0.00	18.61	0.00
500.000	0.09	107.25	24.43	6.13	0.00	137.91	-0.54	64.18	-1.65	0.00	61.99	0.00
600.000	0.09	246.00	28.44	5.99	0.00	280.52	-0.53	-57.35	-1.77	0.00	-59.66	0.00
700.000	0.12	128.84	32.07	5.87	0.00	166.90	-0.52	22.92	-1.88	0.00	20.52	0.00
800.000	0.17	162.65	35.28	5.76	0.00	203.86	-0.54	-21.20	-1.96	0.00	-23.70	0.00
900.000	0.17	130.27	38.08	5.67	0.00	174.19	-0.53	23.88	-2.04	0.00	21.31	0.00
1000.000	0.19	1097.36	40.50	5.60	0.00	1143.64	-0.53	-44.84	-2.10	0.00	-47.46	0.00

C\*\*\*\*\*  
 C

```

ENDIF
400 WRITE(*,5) FMAX
5  FORMAT(' Maximum Frequency, GHz (' ,F7.2,' ) ')
   IF(IFLAG.EQ.1)THEN
     READ(*,10) IVAL
     IF(IVAL.EQ.' ')THEN
       GOTO 500
     ELSE
       READ(IVAL,8,ERR=400) FMAX
     ENDIF
C CHECK FOR VALID RANGE ON FMAX
  IF((FMAX.GE.FMIN).AND.(FMAX.LE.1000.)) GOTO 500
  WRITE(*,*)'Maximum Freq. must satisfy FMIN <= FMAX <= 1000.'
  GOTO 400
ENDIF
500 WRITE(*,6) STEP
6  FORMAT(' Frequency Step, GHz (' ,F7.2,' ) ')
   IF(IFLAG.EQ.1)THEN
     READ(*,10) IVAL
     IF(IVAL.EQ.' ')THEN
       GOTO 600
     ELSE
       READ(IVAL,8,ERR=500) STEP
       IF(STEP.EQ.0.) THEN
         IF(FMAX-FMIN.EQ.0) THEN
           STEP=1.
           GOTO 511
         ENDIF
         WRITE(*,*)' STEP must be greater than 0'
         GOTO 500
       ENDIF
     ENDIF
C CHECK FOR VALID # OF FREQS. (MAX=501)
511 FF=(FMAX-FMIN)/STEP+1
   IF(FF.GT.501) THEN
     WRITE(*,7) (FMAX-FMIN)/502
7  FORMAT(' Minimum STEP for given freq. range is ',F7.2)
   GOTO 500
ENDIF
NF=INT(FF)
ENDIF
C ***** PARAMETER VARIATION *****
600 CONTINUE
   IF(IFLAG.NE.1) GOTO 700
   WRITE(*,*)'Which param. would you like to vary (P, R, T) ? '
   READ(*,10)IVAL
   IF(IVAL.EQ.'P'.OR.IVAL.EQ.'p') THEN
     NFLAG=1
     GOTO 700
   ELSEIF(IVAL.EQ.'R'.OR.IVAL.EQ.'r')THEN
     NFLAG=2
     GOTO 700
   ELSEIF(IVAL.EQ.'T'.OR.IVAL.EQ.'t')THEN
     NFLAG=3
     GOTO 700
   ELSE
     GOTO 600
   ENDIF
C ***** NUMBER OF CASES *****
700 CONTINUE

```

```

P=PBT(1)
RH=RHT(1)
T=TCT(1)
11 WRITE(*,11) NCASE
   FORMAT(' No. of Cases (' ,I2,' ) ')
   IF(IFLAG.NE.1)GOTO 800
   READ(*,10)IVAL
   IF(IVAL.EQ.' ')THEN
     GOTO 800
   ELSE
     READ(IVAL,12,ERR=700) NCASE
12  FORMAT(I1)
     IF(NCASE.GE.10) THEN
       WRITE(*,*)'NO. of Cases must be less than 10.'
       GOTO 700
     ENDIF
   ENDIF
C ***** PRESSURE, TEMPS, RH, DROP CONC. *****
800 CONTINUE
   IF(IFLAG.EQ.1) THEN
     IF(NFLAG.NE.1) THEN
       WRITE(*,9) P
9      FORMAT(' Pressure for all cases (kPa) (' ,F7.2,' ) ')
       READ(*,10) IVAL
       IF(IVAL.EQ.' ') GOTO 830
       READ(IVAL,8,ERR=800) P
       DO 831 I=1,10
831    PBT(I)=P
       GOTO 830
     ENDIF
830  IF(NFLAG.NE.2)THEN
       WRITE(*,19) RH
19  FORMAT(' Rel. Humidity for all cases (%) (' ,F7.2,' ) ')
       READ(*,10) IVAL
       IF(IVAL.EQ.' ') GOTO 840
       READ(IVAL,8,ERR=800) RH
       DO 832 I=1,10
832    RHT(I)=RH
       GOTO 840
     ENDIF
840  IF(NFLAG.NE.3)THEN
       WRITE(*,20) T
20  FORMAT(' Temperature for all cases (C) (' ,F7.2,' ) ')
       READ(*,10) IVAL
       IF(IVAL.EQ.' ') GOTO 850
       READ(IVAL,8,ERR=800) T
       DO 833 I=1,10
833    TCT(I)=T
       GOTO 850
     ENDIF
850  CONTINUE
C***** PRESSURE *****
   IF(NFLAG.EQ.1)THEN
     DO 801 I=1,NCASE
821    WRITE(*,13)I,PBT(I)
13    FORMAT(' Pressure for case # ',I1,' (kPa) (' ,F7.2,' ) ')
       READ(*,10) IVAL
       IF(IVAL.EQ.' ') GOTO 801
       READ(IVAL,8,ERR=821) PBT(I)
801  CONTINUE

```

```

      ENDIF
C***** TEMPERATURE *****
      IF(NFLAG.EQ.3) THEN
        DO 802 I=1,NCASE
822      WRITE(*,14)I,TCT(I)
14      FORMAT(' Temperature for case # ',I1,' (C) ('F7.2,') ')
        READ(*,10) IVAL
        IF(IVAL.EQ.' ') GOTO 802
        READ(IVAL,8,ERR=822) TCT(I)
802      CONTINUE
      ENDIF
C***** HUMIDITY *****
      IF(NFLAG.EQ.2)THEN
        DO 803 I=1,NCASE
823      WRITE(*,15)I,RHT(I)
15      FORMAT(' Rel. Hum. for case # ',I1,' (%) ('F6.2,') ')
        READ(*,10) IVAL
        IF(IVAL.EQ.' ') GOTO 803
        READ(IVAL,8,ERR=823) RHT(I)
803      CONTINUE
      ENDIF
      ENDIF
C***** DROP. CONC. *****
      IF(IFLAG.EQ.1)THEN
        DO 804 I=1,NCASE
834      WRITE(*,22)I,WT(I)
22      FORMAT(' Drop. Conc. for case # ',I1,' (g/m3) ('F6.2,') ')
        READ(*,10)IVAL
        IF(IVAL.EQ.' ')GOTO 804
        READ(IVAL,8,ERR=834) WT(I)
        GOTO 804
      ENDIF
C
C***** HAZE MODEL [2] *****
      IF(RHT(I).LT.80.) GOTO 804
844      WRITE(*,23)I,WA(I)
23      FORMAT(' Aerosol conc. at 80% RH for case # ',
+      I1,' (mg/m3) ('f6.2,') ')
        READ(*,10)IVAL
        IF(IVAL.EQ.' ')GOTO 824
        READ(IVAL,8,ERR=844) WA(I)
C
824      IF(WA(I).EQ.0.) GOTO 804
        WRITE(*,16)I,HZ(I)
16      FORMAT(' Haze Model for case # ',I1,/,
+      ' (A-RURAL,B-Urban,C-Maritime,D-C+strong Wind) ('A1,') ')
        READ(*,10)IVAL
        IF(IVAL.EQ.' ') THEN
          HZ(I)=HZ(I)
        ELSEIF((IVAL.EQ.'A').OR.(IVAL.EQ.'B').OR.(IVAL.EQ.'C')).OR.
+      (IVAL.EQ.'D')) THEN
          HZ(I)=IVAL
        ELSE
          GOTO 824
        ENDIF
        IF(HZ(I).EQ.'A') THEN
          C1=117.
          C2=1.87
        ELSEIF(HZ(I).EQ.'B')THEN

```

```

          C1=128.
          C2=2.41
        ELSEIF(HZ(I).EQ.'C')THEN
          C1=183.
          C2=5.13
        ELSEIF(HZ(I).EQ.'D')THEN
          C1=197.
          C2=5.83
        ELSE
          GOTO 824
        ENDIF
        WT(I)=WA(I)*((C1-RHT(I))/(C2*(100.-RHT(I))))*(1.E-3)
804      CONTINUE
      ELSE
        WRITE(*,17)
17      FORMAT(' CASE ',3X,' PRES. ',3X,' TEMP. ',3X,' HUM. ',5X,
+      ' DROP. ',,' RAIN ')
        DO 805 I=1,NCASE
          WRITE(*,18) I, PBT(I),TCT(I),RHT(I),WT(I),RR(I)
18      FORMAT(3X,I2,2X,5(3X,F7.2))
805      CONTINUE
      ENDIF
900      CONTINUE
C***** RAIN RATE *****
      IF(IFLAG.EQ.1)THEN
        DO 902 I=1,NCASE
922      WRITE(*,21)I,RR(I)
21      FORMAT(' Rain Rate for case # ',I1,' (mm/hr) ('F7.2,') ')
        READ(*,10)IVAL
        IF(IVAL.EQ.' ') GOTO 902
        READ(IVAL,8,ERR=922) RR(I)
902      CONTINUE
      ENDIF
1000     CONTINUE
      RETURN
      END
-----
      SUBROUTINE SAVETABL(IFLAG)
      COMMON /ANSI/ D(12,501,10),ATT(501,10),DISP(501,10)
      REAL No,Bo
      COMMON /ANS/ FREQA(501),No(10),Bo(10),EV(10)
      COMMON /AIR/ NCASE,PBT(10),Tct(10),Rht(10),Wt(10),R(10)
      COMMON /RAIN/ RR(10),WA(10)
      COMMON /HAZE/ HZ(10)
      COMMON /FREQS/ FMIN,FMAX,STEP,NF
      CHARACTER*1 HZ,IVAL
      CHARACTER*20 SAVE
      INTEGER*2 DFLAG,HFLAG
C
C IFLAG = 0 MEANS PRINT TO CONSOLE
C IFLAG = 1 FILE
C IFLAG = 2 PRINT SUMMARY TO CONSOLE
C
      DFLAG=0
      HFLAG=0
      IF(IFLAG.EQ.2)THEN
        OPEN(1,FILE='CON')
        GOTO 110
      ENDIF
C

```

```

WRITE(*,*)'Press C for Complex Refractivity output '
WRITE(*,*)'or ENTER for normal output '
READ(*,101)IVAL
IF((IVAL.EQ.'C').OR.(IVAL.EQ.'c'))THEN
  FFLAG=1
ELSE
  FFLAG=0
ENDIF
C
WRITE(*,*)'Press D to suppress dispersion data '
WRITE(*,*)'Press H to print only the input information'
WRITE(*,*)'Press ENTER for a normal printout'
WRITE(*,*)
READ(*,101)IVAL
101  FORMAT(A1)
IF((IVAL.EQ.'D').OR.(IVAL.EQ.'d'))THEN
  DFLAG=1
ELSEIF((IVAL.EQ.'H').OR.(IVAL.EQ.'h'))THEN
  HFLAG=1
ELSE
  DFLAG=0
  HFLAG=0
ENDIF
C
IF (FFLAG.EQ.1)THEN
  CALL SAVREF(IFLAG,DFLAG,HFLAG)
  RETURN
ENDIF
C
110  CONTINUE
C
IF (IFLAG.EQ.1)THEN
WRITE(*,*)'Enter a DOS filename (PRN for a printout): '
READ(*,12) SAVE
12  FORMAT(A20)
IF(SAVE.EQ.'PRN')THEN
OPEN(1,FILE=SAVE,ERR=900)
ELSE
OPEN(1,FILE=SAVE,STATUS='NEW',ERR=900)
ENDIF
ELSEIF(IFLAG.EQ.0)THEN
OPEN(1,FILE='CON')
ELSE
ENDIF
C
1  FORMAT(//)
C
WRITE(1,175)
175  FORMAT(8X,'FREQUENCY PROFILES OF ATTENUATION AND DELAY RATES')
WRITE(1,*)
WRITE(1,*)'INPUT ',
+ ' Valid Parameter ranges indicated by [ ]):'
WRITE(1,*)
C
WRITE(1,6)
6  FORMAT
+('
WRITE(1,7)
7  FORMAT
+(' CASE  PRES.,P  TEMP.,T  HUM.,RH  MODEL  DROP.,w  RATE',

```

```

+ ',R')
WRITE(1,75)
75  FORMAT
+('          (kPa)          (C)          (%)',
+ '          (mg/m3)   (g/m3)   (mm/hr)')
WRITE(1,76)
76  FORMAT
+(' [1-9] [0.0-110] [ +/-50] [0-100] [0-1]',
+ ' [0-10] [0-200]')
C
WRITE(1,*)
DO 10 LP=1,NCASE
WRITE(1,8)LP,PBT(LP),TCT(LP),RHT(LP),HZ(LP),WA(LP),
+ WT(LP),RR(LP)
8  FORMAT(I3,3(3X,F7.1),7X,A1,' : ',F4.2,1X,F7.3,1X,F7.1)
10  CONTINUE
WRITE(1,*)
WRITE(1,2) FMIN
2  FORMAT(' Minimum Frequency F1          ',F8.3,' (GHz)')
WRITE(1,3) FMAX
3  FORMAT(' Maximum Frequency F2 [1000.]',F8.3,' (GHz)')
WRITE(1,4) STEP
4  FORMAT(' Frequency Step [max 500] dF ',F8.3,' (GHz)')
WRITE(1,*)
WRITE(1,*)
C
IF(IFLAG.EQ.2)RETURN .
IF(HFLAG.EQ.1)RETURN
C
WRITE(1,45)
45  FORMAT(62(1H-))
WRITE(1,*)'OUTPUT:'
C
DO 200 LP=1,NCASE
WRITE(1,9) LP,No(LP)*3.336
9  FORMAT(' Case Number: ',I2,' (Refractive delay = '
+ ',F7.2,' ps/km)')
C
WRITE(1,16)
16  FORMAT(11X,51(1H-))
WRITE(1,17)R(LP)
17  FORMAT(15X,'MOIST AIR (v= ',F5.2,' g/m3)')
WRITE(1,18)
18  FORMAT(13X,'DRY WATER HAZE, FOG')
WRITE(1,19)
19  FORMAT(13X,'AIR + VAPOR + CLOUD + RAIN ',
+ ' = TOTAL ')
WRITE(1,16)
WRITE(1,14)
14  FORMAT(' FREQUENCY ',17X,'ATTENUATION (dB/km)')
IF(DFLAG.EQ.0)THEN
WRITE(1,15)
15  FORMAT(' ',24X,'DISPERSIVE DELAY (ps/km)')
ENDIF
WRITE(1,*)' (GHz)'
DO 100 IF=1,NF
SM1=D(1,IF,LP)+D(2,IF,LP)
SM2=D(3,IF,LP)+D(4,IF,LP)
WRITE(1,11)FREQA(IF),SM1,SM2,D(5,IF,LP),D(11,IF,LP),

```

```

+      ATT(IF,LP)
11  FORMAT(F9.3,2X,F8.2,3(1X,F8.2),2X,F8.2)
    IF(DFLAG.EQ.0)THEN
      WRITE(1,30)D(6,IF,LP)+D(7,IF,LP),D(8,IF,LP)+D(9,IF,LP),
+      D(10,IF,LP),D(12,IF,LP),DISP(IF,LP)
30  FORMAT(12X,F8.2,4(2X,F8.2))
    ENDIF
100  CONTINUE
    WRITE(1,*)
200  CONTINUE
    CLOSE(1)
    RETURN
900  WRITE(*,13) SAVE
13   FORMAT(' ERROR Opening file: ',A20)
    RETURN
    END
-----C-----
SUBROUTINE SAVREF(IFLAG,DFLAG,HFLAG)
COMMON /ANS1/ D(12,501,10),ATT(501,10),DISP(501,10)
REAL No,Bo
COMMON /ANS/ FREQA(501),No(10),Bo(10),EV(10)
COMMON /AIR/ NCASE,PBT(10),Tct(10),Rht(10),Wt(10),R(10)
COMMON /RAIN/ RR(10),WA(10)
COMMON /HAZE/ HZ(10)
COMMON /FREQS/ FMIN,FMAX,STEP,NF
CHARACTER*1 HZ,IVAL
CHARACTER*20 SAVE
INTEGER*2 DFLAG,HFLAG
C
IF (IFLAG.EQ.1)THEN
  WRITE(*,*)'Enter a DOS filename (PRN for a printout): '
  READ(*,12) SAVE
12  FORMAT(A20)
  IF(SAVE.EQ.'PRN')THEN
    OPEN(1,FILE=SAVE,ERR=900)
  ELSE
    OPEN(1,FILE=SAVE,STATUS='NEW',ERR=900)
  ENDIF
  ELSEIF(IFLAG.EQ.0)THEN
    OPEN(1,FILE='CON')
  ELSE
    ENDIF
C
1   FORMAT(//)
C
  WRITE(1,175)
175  FORMAT(8X,'FREQUENCY PROFILES OF ATMOSPHERIC COMPLEX',
+ ' REFRACTIVITY')
  WRITE(1,*)
  WRITE(1,*)'INPUT ',
+ ' Valid Parameter ranges indicated by [ ]):'
  WRITE(1,*)
C
  WRITE(1,6)
6   FORMAT
+ ('
  WRITE(1,7)
7   FORMAT
+ (' CASE PRES.,P TEMP.,T HUM.,RH MODEL DROP.,w RATE',
+ ',R')

```

```

75  WRITE(1,75)
    FORMAT
+ ('      (kPa)      (C)      (%)',
+ '      (mg/m3) (g/m3) (mm/hr)')
76  WRITE(1,76)
    FORMAT
+ (' [1-9] [0.0-110] [ +/-50] [0-100] [0-1]',
+ ' [0-10] [0-200]')
C
  WRITE(1,*)
  DO 10 LP=1,NCASE
    WRITE(1,8)LP,PBT(LP),TCT(LP),RHT(LP),HZ(LP),WA(LP),
+ WT(LP),RR(LP)
8   FORMAT(13,3(3X,F7.1),7X,A1,' : ',F4.2,1X,F7.3,1X,F7.1)
10  CONTINUE
    WRITE(1,*)
    WRITE(1,2) FMIN
2   FORMAT(' Minimum Frequency F1 ',F8.3,' (GHz)')
    WRITE(1,3) FMAX
3   FORMAT(' Maximum Frequency F2 [1000.]',F8.3,' (GHz)')
    WRITE(1,4) STEP
4   FORMAT(' Frequency Step [max 500] dF ',F8.3,' (GHz)')
    WRITE(1,*)
    WRITE(1,*)
C
  IF(IFLAG.EQ.2)RETURN
  IF(HFLAG.EQ.1)RETURN
C
  WRITE(1,45)
45  FORMAT(62(1H-))
    WRITE(1,*)'OUTPUT:'
C
  DO 200 LP=1,NCASE
    WRITE(1,9) LP,No(LP)
9   FORMAT(' Case Number: ',I2,' (No = ',F7.2,' ppm)')
C
  WRITE(1,16)
16  FORMAT(11X,66(1H-))
    WRITE(1,17)R(LP)
17  FORMAT(15X,' MOIST AIR (v= ',F5.2,' g/m3)')
    WRITE(1,18)
18  FORMAT(13X,' DRY WATER HAZE, FOG')
    WRITE(1,19)
19  FORMAT(13X,' AIR + VAPOR + CLOUD + RAIN ',
+ '= TOTAL ')
    WRITE(1,16)
    WRITE(1,14)
14  FORMAT(' FREQUENCY ',22X,'IMAGINARY PART (ppm)')
    IF(DFLAG.EQ.0)THEN
      WRITE(1,15)
15  FORMAT(' ',31X,'REAL PART (ppm)')
    ENDIF
    WRITE(1,*)' (GHz)'
    DO 100 IF=1,NF
      SM1=(D(1,IF,LP)+D(2,IF,LP))/(.182*FREQA(IF))
      SM2=(D(3,IF,LP)+D(4,IF,LP))/(.182*FREQA(IF))
      SM3=D(5,IF,LP)/(.182*FREQA(IF))
      SM4=D(11,IF,LP)/(.182*FREQA(IF))
      WRITE(1,11)FREQA(IF),SM1,SM2,SM3,SM4,

```

```

+      ATT(IF,LP)/(.182*FREQA(IF))
11  FORMAT(F9.3,5(3X,E9.3))
    IF(DFLAG.EQ.0)THEN
      SM1=(D(6,IF,LP)+D(7,IF,LP))/3.336
      SM2=(D(8,IF,LP)+D(9,IF,LP))/3.336
      WRITE(1,30)SM1,SM2,D(10,IF,LP)/3.336,D(12,IF,LP)/3.336,
+      DISP(IF,LP)/3.336
30  FORMAT(12X,5(3X,E9.3))
    ENDIF
100  CONTINUE
    WRITE(1,*)
200  CONTINUE
    CLOSE(1)
    RETURN
900  WRITE(*,13) SAVE
13  FORMAT(' ERROR Opening file: ',A20)
    RETURN
    END

```

```

-----
C-----
SUBROUTINE COMPUTE(LOOP)
C*****
C THIS SUBROUTINE COMPUTES THE ATTENUATION & DISPERSIVE DELAY RATES
C*****
COMMON /ANS1/ D(12,501,10),ATT(501,10),DISP(501,10)
COMMON /ANS/ FREQA(501),No(10),Bo(10),EV(10)
COMMON /AIR/ NCASE,PBt(10),Tct(10),Rht(10),Wt(10),R(10)
COMMON /RAIN/ RR(10),WA(10)
COMMON /FREQS/ FMIN,FMAX,STEP,NF
REAL No,Bo
DIMENSION AD(12)

C      NF=(FMAX-FMIN)/STEP +1.5
C      NUMBER OF FREQUENCIES
C      DO 800 LP=1,LOOP
C*****
      Pbi=PBt(LP)
      Tci=Tct(LP)
      Rhi=Rht(LP)
      Wi=Wt(LP)
      RRi=RR(LP)
C*****
C      DO 55 IF=1,NF
C      DO 55 I=1,8
55  D(I,IF,LP)=0.
      WRITE(*,56) LP,LOOP
56  FORMAT(' Computing for ***** Case',I3,' of ',I3,' *****')
C
60  DO 100 IF=1,NF
C      FREQUENCY LOOP
      F=FMIN + (IF-1)*STEP
      FREQA(IF)=F
      IF(F.EQ.0.)F=1.E-6
C      SAVE FREQUENCY
      CALL Gas1(F,IF,Ad,Pbi,Rhi,Tci,Wi,RRi,V,Es,E,P,Tau,Nwv,Eps,fr)
85  DO 95 I=1,12
      D(I,IF,LP)=Ad(I)
95  CONTINUE
D      WRITE(*,*)'D(12)= ',D(12,IF,LP)

```

```

100  CONTINUE
C
      R(LP)=7.223*E*V
C      NONDISPERSIVE REFRACTIVITY No in ppm and DELAY Bo in ps/km [1].
      No(LP)=(2.588*P+(41.6*V+2.39)*E)*V+Nwv
      Bo(LP)=3.336*No(LP)
C      COMPUTE No,Bo
      DO 510 IF=1,NF
C      ADD TOTAL ATTENUATION AND DISPERSION
      ATT(IF,LP)=D(1,IF,LP)+D(2,IF,LP)+D(3,IF,LP)+D(4,IF,LP)+
+      D(5,IF,LP)+D(11,IF,LP)
      DISP(IF,LP)=D(6,IF,LP)+D(7,IF,LP)+D(8,IF,LP)+
+      D(9,IF,LP)+D(10,IF,LP)+D(12,IF,LP)
510  CONTINUE
800  CONTINUE
    RETURN
    END

```

```

-----
C-----
SUBROUTINE Gas1(F,Mt,Ad,Pb,Rh,Tc,W,RR,V,Es,E,P,Tau,Nwv,Eps,fr)
C*****
C COMPUTES SPECIFIC ATTENUATION & DISPERSIVE DELAY RATES
C USING LINE DATA
C*****
COMMON /O2line/ FOO2(48),A(6,48)
C      OXYGEN LINES
COMMON /H2O/ FOWater(30),B(3,30)
C      WATER VAPOR LINES
DIMENSION AD(12),GAMD2(30)
DIMENSION S(48),GAMMA(48),DELTA(48),SH(30),GAMH(30),DELH(30)
REAL NIPP,NDPP,NOXPP,NVPP,NWPP,Noxp,Ndp,Nip,Nrp,NS,NU

C      IF(Mt.GT.1) GO TO 40
C      ONLY CALC THESE FOR 1st FREQUENCY
C
      V=300./(Tc+273.15)
C      RELATIVE INVERSE TEMPERATURE
C      COMPUTE WATER VAPOR PARTIAL PRESSURE E in kPa
C      Eqn. (1) [1] -- CORRECTED!
C      Es=2.409*V**5*10**((10.-9.834*V)
      Es=0.61078*(EXP(((18.61-Tc)/240.7)*Tc)/(256.1+Tc)))
C      New Es [9] -- either version may be used.
      E=Es*Rh/100.
      P=Pb-E
      IF(P.LT.0)THEN
        P=0.
        Pb=E
      ENDIF
C
C      COMPUTE LINE FACTORS S,Gamma,Delta
      DO 10 I=1,48
C      For OXYGEN
      S(I)=A(1,I)*P*V**3*EXP(A(2,I)*(1.-V))*1.E-6
      GAMMA(I)=A(3,I)*(P*V**(.8-A(4,I)) + 1.1*E*V)*1.E-3
      IF(Pb.LT.0.7)THEN
        GAMMA(I)=(GAMMA(I)**2+(25*0.6E-4)**2)**0.5
C      Zeeman approximation for .6 Gauss, [10]
      ENDIF
10  DELTA(I)=A(5,I)*P*V**A(6,I)*1.E-3
      DO 20 I=1,30
C      For WATER VAPOR

```



```

SH(I)=B(1,I)*E*V**3.5*EXP(B(2,I)*(1.-V))
c Slightly different temperature dependence for width, following [6].
  GAMH(I)=B(3,I)*(P*V**6 + 4.8*E*V**1.1)*1.E-3
  IF(Pb.LT.0.7)THEN
    GAMD2(I)=(2.14*FOWATER(I)**2)*1E-12/V
    GAMH(I)=(GAMH(I)**2+GAMD2(I))**0.5
C Doppler approximation [10]
  ENDF
20 DELH(I)=0.
C
C WATER VAPOR CONTINUUM
C Eqn. (14) [1]; was revised in [2], Eqn. (10)
40 Bf=1.13E-6
  Bs=3.57E-5
  Nipp=(Bf*E*P*V**3.0 + Bs*E**2*V**10.8)*F
  Bo=6.47E-6
  Nip=E*Bo*F**2.05*V**2.4
C
C DRY AIR CONTINUUM
C Eqn. (13) [1] -- CORRECTED!
  Ao=6.14E-4
  An=1.40E-10 *(1.-1.2E-5*F**1.5)
  GAMMAo=4.8E-3*(P+1.1*E)*V**0.8
C FAC=1./(1.+F**2/3600.)
C Nonresonant rolloff FAC taken out.
  FAC=1.
  Ndp=(Ao*P*V**2*GAMMAo*FAC/(F*F + GAMMAo**2) + An*P*V**3.5)*F
  Ndp =P*Ao/2.*V**2*(1./(1.+(F/GAMMAo)**2)-1.)
C
C MOLECULAR OXYGEN LINES
  S1=0
  S2=0
  DO 60 I=1,48
    CALL FPPFP(F,FOO2(I),GAMMA(I),DELTA(I),FPP,FP,0)
  S1=S1+S(I)*Fpp
60 S2=S2+S(I)*Fp
  Noxpp=S1
C N' FROM OXYGEN
  Dox=S2 + Ndp
  Ad(6)=3.336*S2
  Ad(7)=3.336*Ndp
C D FROM OXYGEN
C
C WATER VAPOR LINES
  S1=0
  S2=0
  DO 70 I=1,30
    CALL FPPFP(F,FOWATER(I),GAMH(I),DELH(I),FPP,FP,1)
  S1=S1+SH(I)*Fpp
70 S2=S2+SH(I)*Fp
  Nvpp=S1
C N' FROM WATER VAPOR
  Dv=S2 + Nip
  Ad(8)=3.336*S2
  Ad(9)=3.336*Nip
C D FROM WATER VAPOR
C
C LIQUID WATER DIELECTRIC CONSTANT AND
C FOG/CLOUD RAYLEIGH TERMS [3]
  fD=20.09-142*(V-1)+294*(V-1)**2

```

```

  NU=(F/fD)
  fs=590.-1500*(V-1)
  NS=F/fs
  Epinf=5.48
  Eopt=3.51
C EPSILON SUB INFINITY
  Eps=103.3*(V-1)+77.66
C EPSILON SUB S
  Epp=Eopt+(Eps-Epinf)/(1+NU**2)+(Epinf-Eopt)/(1+NS**2)
C EPSILON'
  Eppp=((Eps-Epinf)*NU)/(1+NU**2)+((Epinf-Eopt)*NS)/(1+NS**2)
C EPSILON''
  Ep=(2.+Epp)/Eppp
C SUSPENDED WATER DROPLET EXTINCTION
  Nwpp=(4.50*W/(Eppp*(1.+Ep**2)))
C N' FROM WATER DROPLETS
  Dw=-4.5**W*(Ep/(Eppp*(1.+Ep*Ep)))+4.5*W/(Eps+2.)
  Nwv=1.5**W*(1.-(3./(Eps+2.)))
C
C ATTENUATION DUE TO RAIN [4]
C
  ARAIN=0.
  BRAIN=0.
  ATRAN=0.
  Nrp=0.
  IF (RR.EQ.0.) GOTO 501
C ALPHA CALCULATION
  IF(F.GE.2.9) GOTO 300
  GA=6.39E-5
  EA=2.03
  GOTO 330
300 CONTINUE
  IF(F.GE.54.) GOTO 310
  GA=4.21E-5
  EA=2.42
  GOTO 330
310 IF(F.GE.180.) GOTO 320
  GA=4.09E-2
  EA=0.699
  GOTO 330
320 GA=3.38
  EA=-0.151
330 ARAIN=GA*(F**(EA))
C
C BETA CALCULATION
  IF(F.GE.8.5) GOTO 340
  GB=0.851
  EB=0.158
  GOTO 370
340 IF(F.GE.25.) GOTO 350
  GB=1.41
  EB= -0.0779
  GOTO 370
350 IF(F.GE.164.)GOTO 360
  GB=2.63
  EB= -0.272
  GOTO 370
360 GB=0.616
  EB=0.0126
370 BRAIN=GB*(F**(EB))

```

```

      ATRAN=ARAIN*RR**(BRAIN)
C
C RAIN DELAY approximated after ZUFFEREY [5] who
C used MARSHALL-PALMER drop size spectra and 20 deg. C
      fr=53.-0.37*RR+1.5E-3*RR**2
      Nro=(RR*(3.68-0.012*RR))/fr
      X=F/fr
      Nrp=-Nro*(X**2.5/(1+X**2.5))
501  CONTINUE
C
C CALC ABSORPTION
      Ad(1)=.182*F*Noxpp
C OXYGEN LINE ABSORPTION
      IF(Ad(1).LT.0.) Ad(1)=0.
C Cannot be less than 0.
      Ad(2)=.182*F*Ndpp
C NONRESONANT DRY AIR ABSORPTION
      Ad(3)=.182*F*Nvpp
C WATER VAPOR LINE ABSORPTION
      Ad(4)=.182*F*Nipp
C WATER VAPOR CONTINUUM ABSORPTION
      Ad(5)=.182*F*Nwpp
C SUSPENDED WATER DROPLET EXTINCTION
      Ad(6)=3.336*S2
C OXYGEN LINE DISPERSIVE DELAY (SEE ABOVE)
      Ad(7)=3.336*Ndp
C OXYGEN NON-RESONANT DISP. DELAY (SEE ABOVE)
      Ad(8)=3.336*S2
C WATER VAPOR CONTINUUM DISPERSIVE DELAY (SEE ABOVE)
      Ad(9)=3.336*Nip
C WATER VAPOR LINE DISPERSIVE DELAY (SEE ABOVE)
      Ad(10)=3.336*Dw
C WATER DROPLET DISPERSIVE DELAY
      Ad(11)=ATRAIN
C ATTENUATION DUE TO RAIN
      Ad(12)=3.336*Nrp
D      WRITE(*,*)'Ad(12)= ',Ad(12)
C RAIN DELAY
      RETURN
      END
-----
      SUBROUTINE FPPFP(F,Vo,GAMMA,DELTA,Fpp,Fp,FLAG)
C*****
C CALC Fpp & Fp -- VW line shape functions
C*****
      G2=GAMMA*GAMMA
      VMF=Vo-F
      VPF=Vo+F
      CUTOFF=40.
      Fpp=F/Vo*((GAMMA-VMF*DELTA)/(VMF**2+G2) +
+ (GAMMA-VPF*DELTA)/(VPF**2+G2))
      IF(FLAG.EQ.1)THEN
      IF(F.GT.(Vo+CUTOFF*GAMMA)) Fpp=0.
C SET ABSORPTION TO ZERO IF F IS > NU+40*GAMMA
C High-frequency wing problem of VW shape function for H2O lines [7]!
C Intensities <(approx. 7.5 E-4 Fpp) are neglected.
      ENDIF
      Fp=(VMF + GAMMA*(GAMMA+F*DELTA)/Vo)/(VMF**2+G2) +
+ (VPF + GAMMA*(GAMMA-F*DELTA)/Vo)/(VPF**2+G2) - 2./Vo
      RETURN

```

```

      END
-----
      SUBROUTINE Oxyda1
      COMMON /O2line/ F0O2(48),A(6,48)
C PUT MOLECULAR OXYGEN LINE DATA OF [1] IN A(1:6,1:48)
      OPEN (2,FILE='OXYGEN.DAT',ERR=900)
C DUMMY READ TO ALLOW FOR COMMENT.
      READ(2,*)
      READ(2,*)
      READ (2,*,ERR=910) (F0O2(I),(A(J,I),J=1,6),I=1,48)
      CLOSE (2)
      RETURN
900  WRITE(*,901) IOS
901  FORMAT('Could not OPEN OXYGEN.DAT file, error=',I6)
      WRITE(*,*)'Check that OXYGEN.DAT is in the current directory.'
      STOP 'Could not OPEN OXYGEN file.'
910  STOP 'ERROR READING OXYGEN file.'
      END
-----
      SUBROUTINE Vapda1
      COMMON /H2O/ F0water(30),B(3,30)
C PUTS WATER VAPOR LINE DATA OF [1] IN B(1:3,1:30)
      OPEN (2,FILE='WATER.DAT',ERR=900)
C DUMMY READ TO ALLOW FOR COMMENTS.
      READ(2,*)
      READ(2,*)
      READ (2,*,ERR=910) (F0water(I),(B(J,I),J=1,3),I=1,30)
      CLOSE (2)
      RETURN
900  WRITE(1,901) IOS
901  FORMAT('Could not OPEN WATER file, error=',I6)
      WRITE(*,*)'Check that WATER.DAT is in the current directory.'
      STOP 'Could not OPEN WATER file.'
910  STOP 'ERROR READING WATER file.'
      END

```

BIBLIOGRAPHIC DATA SHEET

1. PUBLICATION NO. NTIA Report 87-224		2. Gov't Accession No.	3. Recipient's Accession No.
4. TITLE AND SUBTITLE Millimeter-Wave Properties of the Atmosphere: Laboratory Studies and Propagation Modeling		5. Publication Date October 1987	
7. AUTHOR(S)		6. Performing Organization Code NTIA/ITS.S3	
8. PERFORMING ORGANIZATION NAME AND ADDRESS U.S. Dept. of Commerce/Nat'l Telecomm. and Information Administration Institute for Telecommunication Sciences 325 Broadway, Boulder, CO 80303 3328		9. Project/Task/Work Unit No. 910 7108/910 5398	
11. Sponsoring Organization Name and Address U.S. Dept. of Commerce National Telecommunications and Information Administration Herbert C. Hoover Building 14th & Constitution Ave. NW Washington, D.C. 20230		10. Contract/Grant No.	
14. SUPPLEMENTARY NOTES		12. Type of Report and Period Covered	
15. ABSTRACT (A 200-word or less factual summary of most significant information. If document includes a significant bibliography or literature survey, mention it here.) Laboratory measurements have been performed at 138 GHz of water vapor attenuation $\alpha$ for pure vapor ( $H_2O$ ) and its mixtures with air, nitrogen ( $N_2$ ), oxygen ( $O_2$ ), and Argon(Ar). A computer-controlled resonance spectrometer was employed. The results are interpreted in terms of underlying absorption mechanisms. A substantial amount of the self-broadening term proportional to the square of vapor pressure is left unaccounted. The negative temperature coefficient of the excess absorption is consistent with a dimer ( $H_2O_2$ ) model. An empirical formulation of the experimental findings is incorporated into the parametric propagation model MPM that utilizes a local ( $30x H_2O$ , $48x O_2$ ) line base to address frequencies up to 1000 GHz. Details of MPM are given in two Appendices. Predictions of moist air attenuation and delay by means of the revised MPM program generally compare favorably with reported (10 - 430GHz) data from both field and laboratory measurements.		13.	
16. Key Words (Alphabetical order, separated by semicolons) atmospheric attenuation and delay; laboratory studies of moist air attenuation; millimeter/submillimeter-wave spectral range; propagation program MPM; terrestrial radio path data			
17. AVAILABILITY STATEMENT <input checked="" type="checkbox"/> UNLIMITED. <input type="checkbox"/> FOR OFFICIAL DISTRIBUTION.		18. Security Class. (This report) unclassified	20. Number of pages 80
		19. Security Class. (This page) unclassified	21. Price.

